Ames

IN-22081

NASA CONTRACTOR REPORT 177403

Development of a ROT22 - DATAMAP Interface

K. R. Shenoy
T. Waak
J. T. Brieger

CONTRACT NAS2-10331
April 1986

NASA

NASA CONTRACTOR REPORT 177403

Development of a ROT22 - DATAMAP Interface

K. R. Shenoy
T. Waak
J. T. Brieger
Bell Helicopter Textron Inc.
Fort Worth, Texas

Prepared for
Ames Research Center
under Contract NAS2-10331
April 1986

National Aeronautics and
Space Administration

Ames Research Center
Moffett Field, California 94035

TABLE OF CONTENTS

LIST OF FIGURES

LIST OF FIGURES (Continued)

LIST OF FIGURES (Continued)

LIST OF FIGURES (Continued)

LIST OF FIGURES (Concluded)

LIST OF TABLES

LIST OF SYMBOLS

a	local speed of sound
a_∞	speed of sound in the ambient
a_o, a_1, a_2	Fourier components of flapping angle (Equation 7)
A_1	longitudinal cyclic
b_1, b_2	Fourier components of flapping angle (Equation 7)
B_1	lateral cyclic
C	blade chord
C_N	normal force coefficient
C_p	pressure coefficient (Equations 1, 3, and 4)
GW	gross weight of the helicopter
M	local Mach number
M_r	Freestream Mach number at given radial station, r
N	blade rotational speed in revolutions per minute
p_a	absolute pressure
p_∞	ambient pressure
r	radial location
R	blade radius
v_i	induced velocity
V_F	helicopter flight speed
α_r	angle of attack at radial station r
α_s	shaft tilt angle, positive aft
α_{TPP}	tip path plane tilt, positive aft
β	flapping angle

$\dot{\beta}$	first derivative of β with respect to azimuth
$\sqrt{}$	ratio of specific heats (=1.4 for perfect gas)
δ_3	pitch flap coupling angle
λ	inflow ratio
ρ	air density
θ_o	collective angle
θ_{T_r}	twist at radial station r
ϕ	inflow angle (Equation 11)
ψ	azimuth angle
Ω	angular velocity of the rotor (in radians/sec)

INTRODUCTION

This report, prepared under Contract NAS2-10331 (MOD 10), outlines the development and validation of an interface between the three-dimensional transonic analysis program ROT22 (Reference 1) and the DATAMAP (Reference 2) program.

Following the section describing the development of the interface, the validation is carried out as follows. First, the DATAMAP program is used to analyze the instrumented AH-1G flight test data (Reference 3). Specifically, records 2872 and 2873 are analyzed at an azimuth of 90°, and Record 2806 is analyzed at 60°. Trim conditions for these flight conditions are then calculated using the Bell performance prediction program ARAM45 (Reference 4). Equivalent shaft, pitch, and twist angles are calculated from ARAM45 results and used as input to the ROT22 program. The interface uses the ROT22 results and creates DATAMAP information files from which the surface pressure contours and sectional pressure coefficients are plotted. Twist angles input to ROT22 program are then iteratively modified in the tip region until the computed pressure coefficients closely match the measurements.

The results of this match are discussed. Conclusions derived from this work are then summarized.

DEVELOPMENT OF THE INTERFACE

ROT22 was modified to pass its results to DATAMAP. The appropriate ROT22 results at different station and chord values are interpolated to a rectangular grid usable to DATAMAP. The interpolated values are then written to a file in a format appropriate for DATAMAP to process. Variable identification, plot identification, plot titles, and the grid definition are also written to the file. DATAMAP then processes the file and stores the information for further analysis and plotting.

Program ARSA05 is the result of the above development. A user's guide to this program is contained in the appendix which details the program's function, input information, and output description.

OUTLINE OF THE INTERFACE

ROT22 has been modified to write Data Transfer Files (DTFs) in the format specified in USAAVRADCOM-TR-80-D-30B. Now that a connection to DATAMAP through a DTF is established, DATAMAP is able to produce the required plots. However, several analytic and procedural abilities (in addition to writing DTFs) were added to ROT22 to produce the data required by DATAMAP. These include (see Figures 1A through 1C):

a. Conversion of static pressure coefficient to local absolute pressure.

b. Chordwise and spanwise interpolation of blade thickness, local Mach numbers and local absolute pressure.

c. Conversion of local absolute pressure to static pressure coefficient.

d. Data extension to obtain pseudo rotor cycles.

First, DATAMAP cannot compute backwards from the static pressure coefficient (C_p) to absolute pressure so this analysis was added to ROT22. Thus, ROT22 writes negative C_p, local absolute pressure and incidentally local Mach number on the DTF. Second, ROT22 computes values at station (z direction) and chord (y direction) values that are, in general, different from the values desired in DATAMAP. ROT22 will not provide values at a user specified grid via two-way interpolation. Third, the local C_p is computed from the interpolated local absolute pressure since C_p cannot be meaningfully interpolated. Fourth, ROT22 computes values for one azimuth during a run. To enable DATAMAP to use azimuth for computations and displays, ROT22 provides constant-valued time histories for each of the three quantities at each chord (y) and span (z) position that includes one complete rotor cycle. The time histories will be correct only at the specified azimuth for which ROT22 computations were actually performed. However, the simulation of a complete rotor cycle allows DATAMAP to use azimuth in computations and displays of the data.

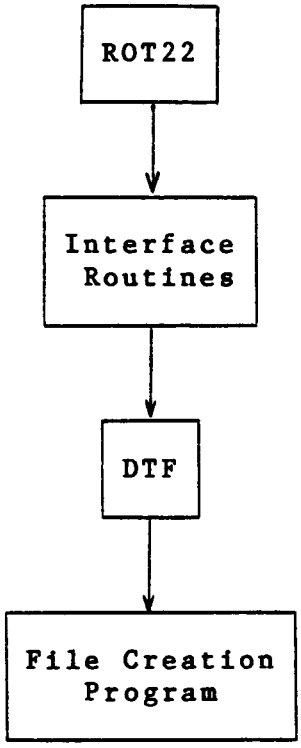

Figure 1A. Information flow chart.

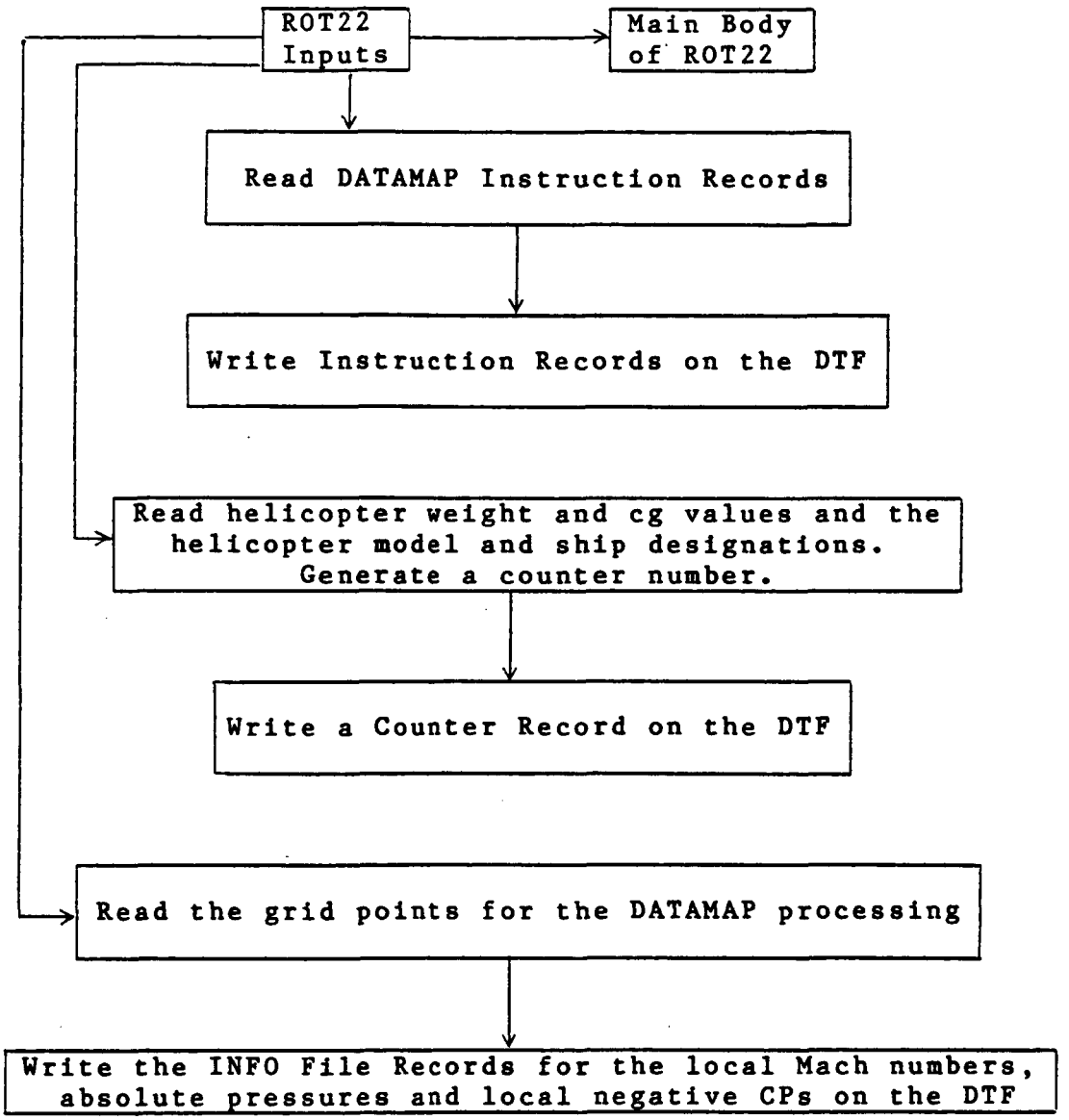

Figure 1B. Information flow chart - initialize the DTF.

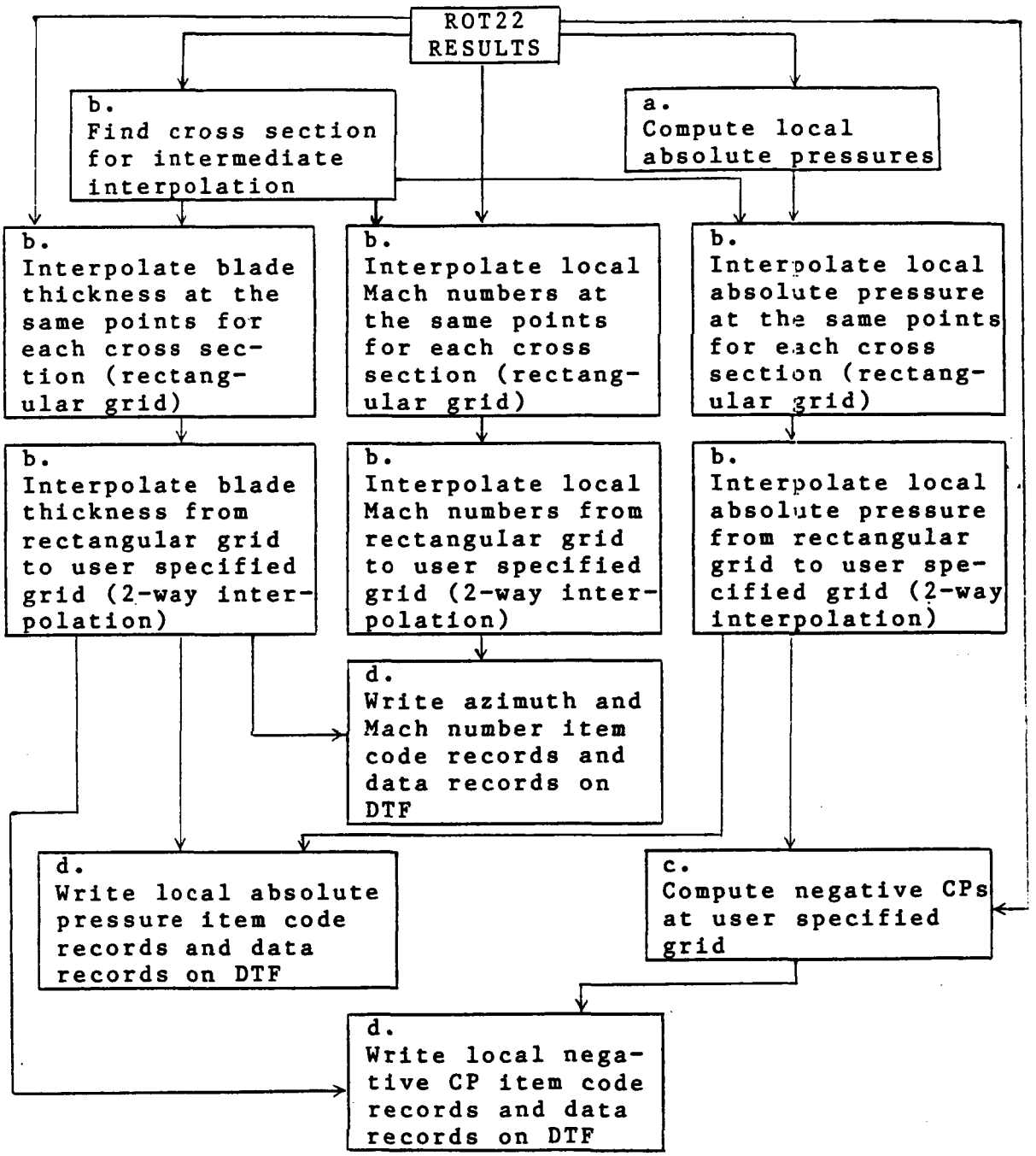

Figure 1C. Information flow chart - ROT22 results
(see text for explanation of a-d)

ROT22 writes five record types to the DTF. Three of the five record types are written in the input routines. These are Instruction Records, a Counter Record, and Info File Records. After ROT22 is otherwise finished, the other two record types are written. These are Item Code Records and Data Records.

The ROT22 results to be transferred to DATAMAP are the values on the blade surface. The quantities of interest are the station (z) and chord (x) values used in the ROT22 analysis, the station Mach numbers, local Mach numbers, local C_ps and blade surface (y) at each point (measured from reference line). The C_ps are converted to local absolute pressures by the relation

$$\text{local absolute pressure} = [1+0.7*C_p*(\text{station Mach number})^2]* \text{ambient air pressure}$$

A rectangular grid is generated by chordwise interpolation of the surface (y), local Mach number and local absolute pressures. These values are then converted to the user specified grid via a two-way interpolation on the station and chord values. If, during the above interpolations, a point is extrapolated, a warning message is written. The local C_ps are computed from the local absolute pressures by the relation

$$C_p = [(\text{local absolute pressure}/\text{ambient pressure}) - 1]/[.7*(\text{station Mach number})^2]$$

The negative of C_p is passed to DATAMAP.

After all the interpolations are finished, the Item Code Records and Data Records are written to the DTF. The azimuth and Mach numbers are written to the DTF. Five of these Data Records are written with the only difference being the azimuth position (0°, 90°, 180°, 270°, 360°). This generates the pseudo time history. Next the local absolute pressures are written to the DTF five times. Finally, the local negative C_ps are written to the DTF five times.

THEORETICAL CONSIDERATIONS

Various equations used to calculate pressure coefficients are provided in this section. In addition, equations used for calculating the equivalent shaft angle, pitch angle, and twist angles are also developed here.

Pressure Relationships

$$C_p = \frac{p_a - p_\infty}{\frac{1}{2}\rho U_r^2} \tag{1}$$

where C_p is coefficient of pressure, p_a is absolute pressure, p_∞ is ambient pressure, ρ is air density, U_r is sectional free stream velocity defined as

$$U_r = \Omega r + V_F \sin \psi \tag{2}$$

where Ω is angular velocity of the blade, r is the radial location, V_F is flight velocity, and ψ is blade azimuth.

From gasdynamic relations equation (1) can also be written as

$$C_p = \frac{2}{\gamma M_r^2} \frac{p_a}{p_\infty} - 1 \tag{3}$$

or

$$C_p = \frac{2}{\gamma M_r^2} \left(\frac{a}{a_\infty}\right)^{\frac{\gamma}{\gamma-1}+1} - 1 \tag{4}$$

where M_r is the sectional free-stream Mach number, γ is the ratio of specific heats, a_∞ is speed of sound in the ambient, and a is the local speed of sound in the flow.

In DATAMAP program, Eq. 1 is used where the ambient pressure and density are input. On the other hand, Eq. 4 is used in ROT22 program where the ambient speed of sound is input. In any event, Equations 1, 3, and 4 are identical when perfect gas assumptions are made.

Flight Condition Simulations

Changes in the blade sectional angles of attack due to flapping, pitch-flap coupling, and blade cyclic are not represented in ROT22 analysis. However, by equating the relationship for the effective angle of attack in ROT22 with that in a performance analysis such as ARAM45 program, one can readily obtain relationships for equivalent twist and pitch angles.

Similarly, one can obtain an equivalent shaft tilt angle. In ROT22 program,

$$\alpha_{TPP} = \alpha_s \tag{5}$$

In ARAM45 program,

$$\alpha_{TPP} = \alpha - a_1 \tag{6}$$

where α_{TPP} is tip path plane tilt with respect to flight velocity vector, α_s is the shaft tilt angle, and a_1 is Fourier coefficient from blade flapping angle written as

$$\beta = a_o + a_1 \cos \psi + b_1 \sin \psi + a_2 \cos 2\psi + b_2 \sin 2\psi \tag{7}$$

In the present analysis, shaft tilt aft is defined to be positive.

Upon equating equations 5 and 6,

$$(\alpha_s)_{Eq.} = (\alpha_s - a_1)_{ARAM45} \tag{8}$$

Both α_s and a_1 on the right-hand side of Eq. 8 can be obtained from ARAM45 results.

Equivalent pitch and twist:

Blade element angle of attack relationship in ROT22 can be written as,

$$a_r = \theta_o + \theta_{T_r} + \tan^{-1} \frac{\lambda \Omega R}{\Omega r + V_F \sin \psi} \tag{9}$$

The same relationship in ARAM45 analysis is,

$$\alpha_r = \theta_o + \theta_{T_r} - B_1 \sin \psi - A_1 \cos \psi - \beta \tan \delta_3 + \phi \tag{10}$$

where θ_o is collective pitch, $\theta_{T\,r}$ is geometric twist at radius r, B_1, and A_1 are cyclic pitch coefficients, δ_3 is pitch flap coupling, λ is inflow ratio, and ϕ is inflow angle defined as

$$\tan \phi = \frac{-r \dot{\beta} \sin \psi - V_F \cos \alpha_s \cos \psi \sin \beta + (V_F \sin \alpha_s - v_i) \cos \beta}{\Omega r + V_F \sin \psi} \tag{11}$$

where $\dot{\beta}$ is first azimuthal derivative of blade flapping motion and v_i is induced velocity. Since ARAM45 program calculates ϕ, one need not use Eq. 11. On the other hand, ROT22 program does not explicitly solve for the inflow ratio. Instead, it solves finite difference flow field equations to calculate local velocity components. Though one can use these to calculate an effective inflow ratio, it is a very time consuming and computationally demanding task. Here it is assumed that

$$\lambda_{ARAM45} = \lambda_{ROT22} \tag{12}$$

Now Eq. 9 can be equated with Eq. 10 to get

$$\theta_{o_{Eq}} = \theta_o - B_1 \sin \psi - A_1 \cos \psi - \beta \tan \delta_3 \tag{13}$$

$$\theta_{T_{r_{Eq}}} = \theta_{T_r} + \phi - \tan^{-1} \frac{\lambda \Omega R}{\Omega r + V_F \sin \psi} \qquad (14)$$

where

ψ = azimuth angle

$\theta_{o_{Eq}}$ = the equivalent pitch angle

$\theta_{T_{r_{Eq}}}$ = the equivalent twist at station r

ANALYSIS

In this report, the ROT22 - DATAMAP interface is validated by using three level flight records acquired by NASA-ARC of the instrumented AH-1G helicopter. This instrumented helicopter has a two-bladed main rotor with rectangular planform blades of 28.63 inch chord. The airfoil section used on this blade is a symmetrical section of 9.3% thickness. Airfoil coordinates for this blade are provided in Table 1.

Flight conditions representing records 2806, 2873, and 2872 are provided in Table 2. The ARAM45 results, equivalent shaft angle, equivalent pitch angle, and equivalent twist angles, are provided in Table 3.

These equivalent angles are input to ROT22 program to calculate blade surface pressure distribution for each of the records selected.

The normal force coefficients computed for these records are compared in Figures 2 to 4 with the normal force coefficients derived from flight tests. In these figures, the flight test data is shown by a solid line and the ROT22 data by a broken line. Initial plans called for approximately matching these normal force coefficients by modifying the tip region twist. However, a careful examination has revealed that the combination of test data scatter and the linear interpolation/extrapolation scheme used in DATAMAP program makes the normal force calculations unreliable. Consequently, tip region twist is modified to approximately match the pressure coefficients rather than the normal force coefficients. It will be shown later that the agreement between the normal coefficients worsens when the agreement between the pressure coefficients is improved. Since we already discussed that the normal coefficients calculated from test data are unreliable, we may not have to be concerned with this discrepancy.

TABLE 1. AIRFOIL COORDINATES

0.0	0.0
0.00453	0.01163
0.00862	0.01569
0.01250	0.01857
0.01628	0.02087
0.02366	0.02453
0.03092	0.02743
0.03810	0.02986
0.04524	0.03195
0.05590	0.03463
0.06652	0.03689
0.08064	0.03939
0.09121	0.04098
0.10177	0.04235
0.11231	0.04353
0.12285	0.04455
0.13339	0.04543
0.15093	0.04660
0.17548	0.04773
0.20001	0.04836
0.21402	0.04851
0.22102	0.04855
0.22452	0.04855
0.23503	0.04851
0.25253	0.04832
0.28053	0.04767
0.30152	0.04696
0.32950	0.04572
0.35048	0.04461
0.38544	0.04244
0.42036	0.04015
0.45528	0.03785
0.49020	0.03556
0.52512	0.03326
0.56003	0.03097
0.59495	0.02867
0.62987	0.02638
0.66479	0.02408
0.69970	0.02179
0.73462	0.01949
0.76954	0.01720
0.80446	0.01490
0.83938	0.01261
0.87430	0.01031
0.90921	0.00801
0.94413	0.00572
0.97905	0.00342
1.00000	0.00205

TABLE 2. FLIGHT CONDITIONS

Rec #	2872	2873	2806
V_F, KTAS	150.2	143.7	123.7
N, rpm	301	315.5	316
ψ	90°	90°	60°
GW	8150	8050	8100
OAT °F	68.9	63.5	69.1
P_o, psi	11.98	11.56	13.17
θ_o	18.594°	16.796°	14.92
A_1, B_1	0°, 6.405°	0°, 4.8839°	0, 2.808
a_o	2.75°	2.75°	2.75
a_1, b_1	-2.385°, -1.61°	-1.6108°, -1.1737°	-1.743, -0.975
a_2, b_2	0°, 0°	0°, 0°	0, 0
δ_3	0°	0°	0°
α_s	-6.7144°	-6.365	-5.87
λ	-0.052378°	-0.0467	-0.03902

TABLE 3. CALCULATED EQUIVALENT CONDITIONS

Rec #	2872			2873			2806		
$\alpha_{s_{Eq}}$	-4.3294			-4.755			-4.13		
$\theta_{o_{Eq}}$	12.185°			11.91°			12.488		
r/R =	θ_{T_r}°	ϕ°	$(\theta_{T_r})°_{Eq}$	θ_{T_r}	ϕ°	$(\theta_{T_r})_{Eq}$	θ_{T_r}	ϕ	$(\theta_{T_r})_{Eq}$
0.15	-1.5	-6.6	-2.25	-1.5	-6.1	-2.05		-6.5	-2.36
0.3	-3.0	-5.65	-4.11	-3	-5	-3.75		-4.95	-3.85
0.5	-5.0	-4.9	-6.4	-5	-4.2	-5.97		-3.9	-5.89
0.75	-7.5	-4.35	-9.14	-7.5	-3.62	-8.63		-3.2	-8.45
0.85	-8.5	-4.2	-10.2	-8.5	-3.5	-9.7		-3.03	-9.48
0.9	-9.0	-4.13	-10.74	-9.0	-3.4	-10.2		-2.95	-9.99
0.95	-9.5	-4.06	-11.26	-9.5	-3.325	-10.73		-2.86	-10.48
1.0	-10.0	-4.0	-11.78	-10.0	-3.2674	-11.25		-2.79	-10.99

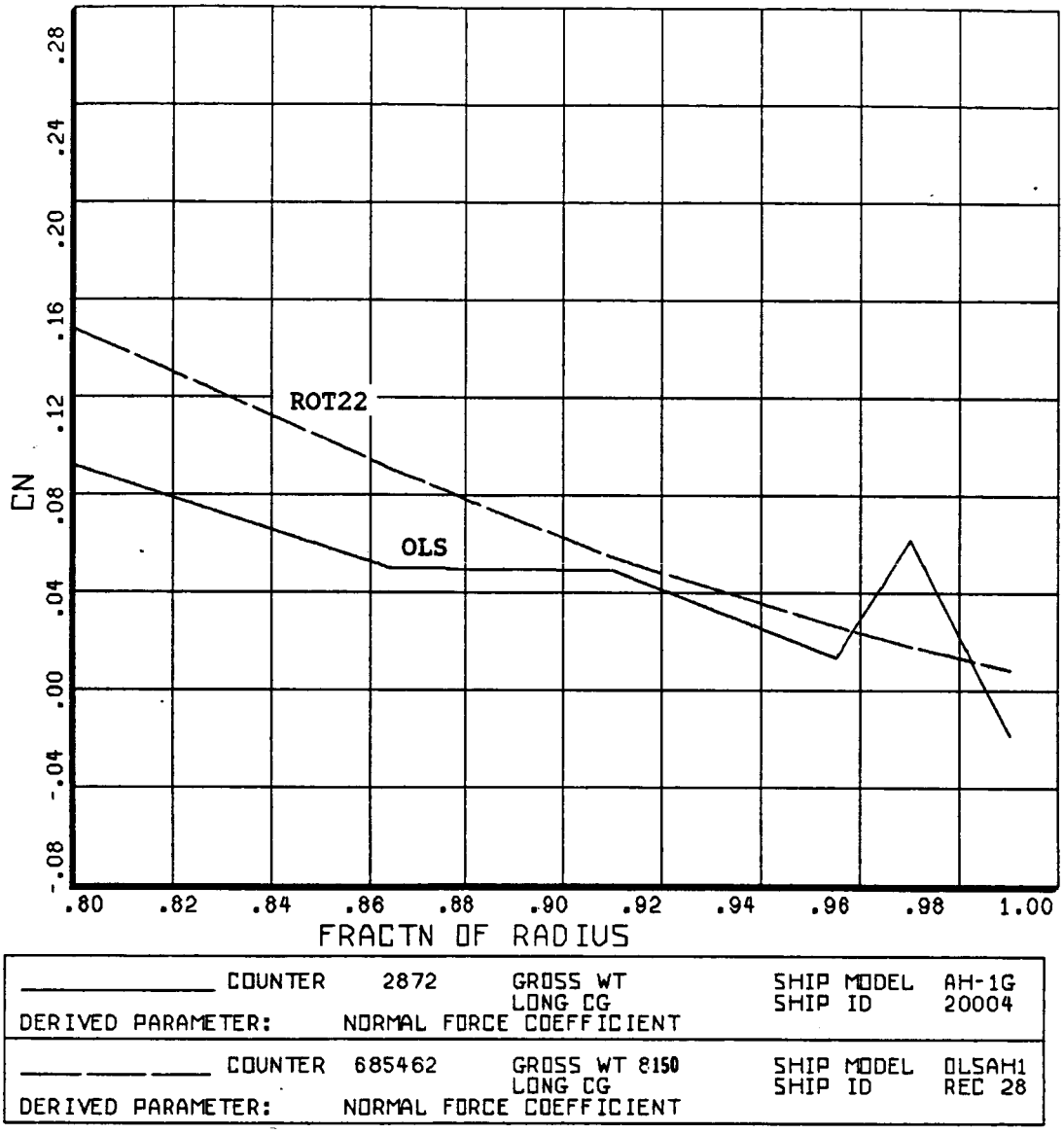

BHT,USARTL DATAMAP (VERS 3.10 - 24/02/82) 05/17/83 BELL HELICOPTER

Figure 2. Normal force coefficient for Record 2872.

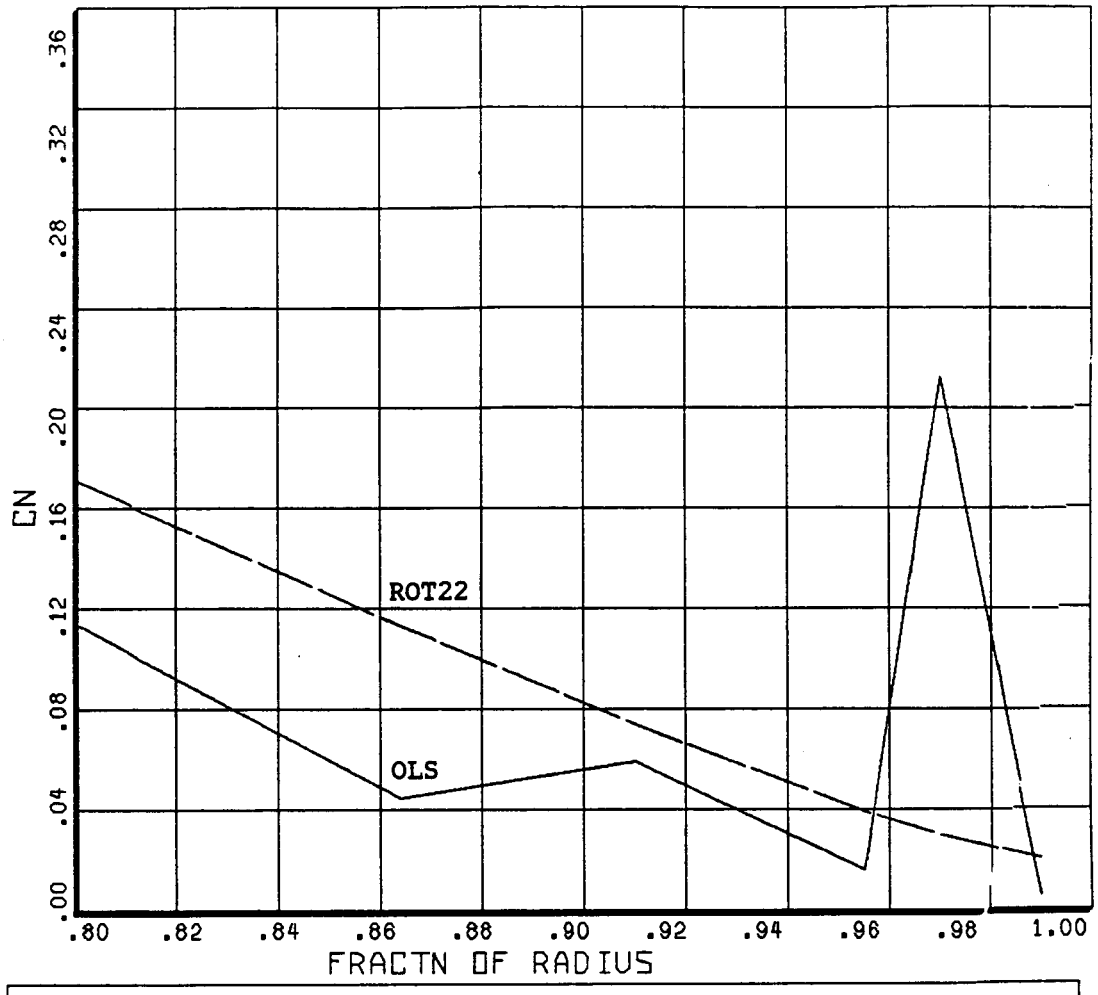

BHT,USARTL DATAMAP (VERS 3.10 - 24/02/82) 05/17/83 BELL HELICOPTER

Figure 3. Normal force coefficient for Record 2873.

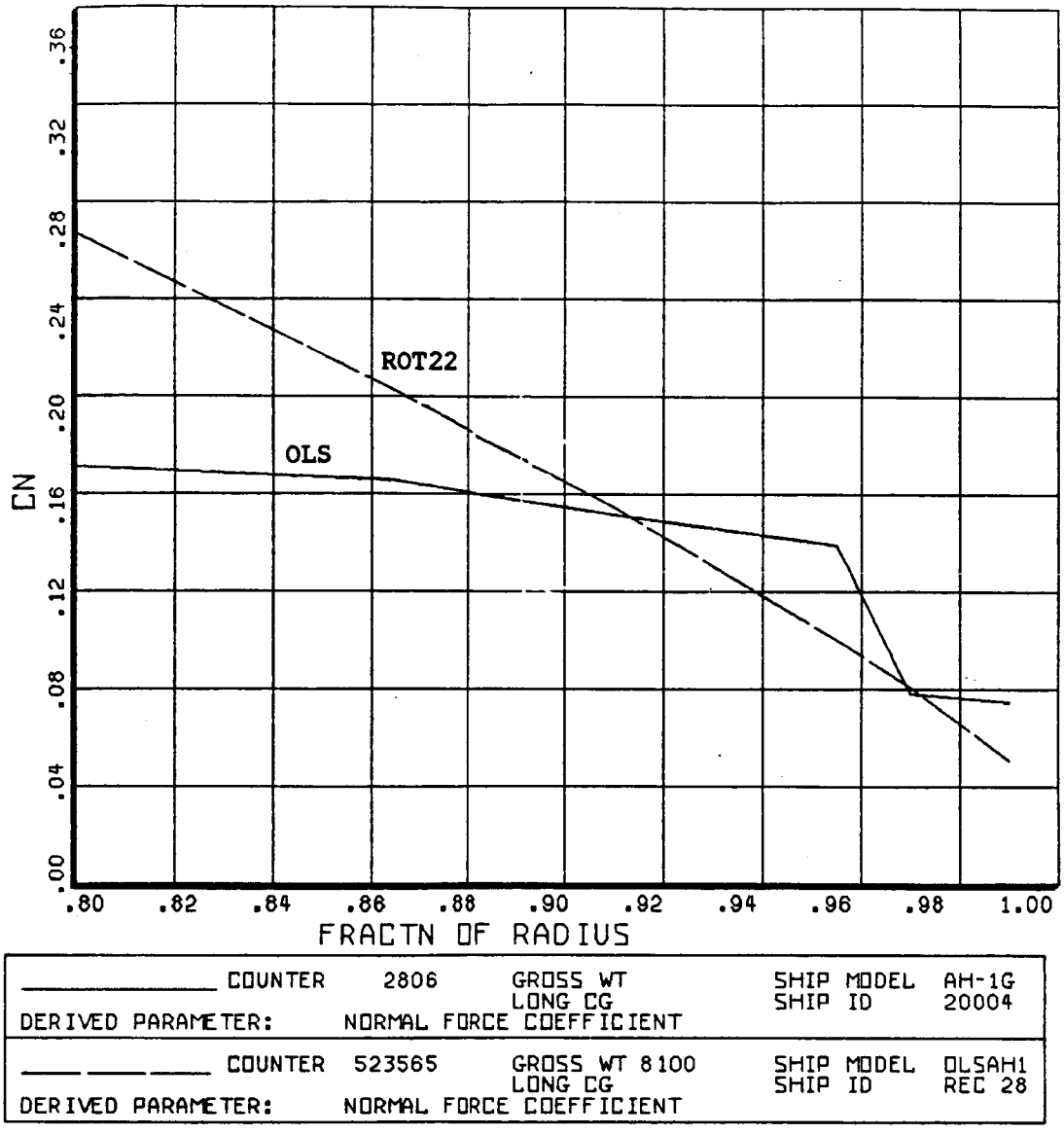

BHT.USARTL DATAMAP (VERS 3.10 - 24/02/82) 05/19/83 BELL HELICOPTER

Figure 4. Normal force coefficient for Record 2806.

RESULTS

In this section, the sectional pressure coefficients calculated by ROT22 are compared with those from flight tests. Then the sectional pressure coefficients and surface pressure contours obtained after modifying the tip region twist to approximately match the pressure coefficients are provided for each of the records. In addition, measured surface pressure contours are also provided. Finally some discussion of these results is provided.

Record 2872

Sectional pressure coefficients calculated by ROT22 program using the equivalent angles provided in Table 3 are compared with the flight test results in Figures 5 through 9. From these it was concluded that the upper surface suction was underestimated considerably. This mandated an increase in the twist in the tip region. After a few iterations, the new twist rate provided in Table 4 was determined. The results from ROT22 after modifying the tip region twist angles are shown in Figures 10 through 16. Here, the pressure contours from ROT22 results shown in Figures 15 and 16 may be compared with those from flight tests (Figures 17 and 18). The normal force coefficients calculated after modifying the twist are provided in Figure 19. As mentioned in the earlier section, the agreement between the theory and flight tests has worsened when compared with Figure 2.

Record 2873

Results for Record 2873 are provided in a manner identical to Record 2872. Here the sectional coefficients of pressure before adjusting the twist are provided in Figures 20 through 24. The same after adjusting the twist are shown in Figures 25 through 29.

The surface pressure contours from ROT22 results are provided in Figures 30 and 31. These may be compared with those in Figures 32 and 33 where the flight test results are used. Finally, the normal force coefficients obtained

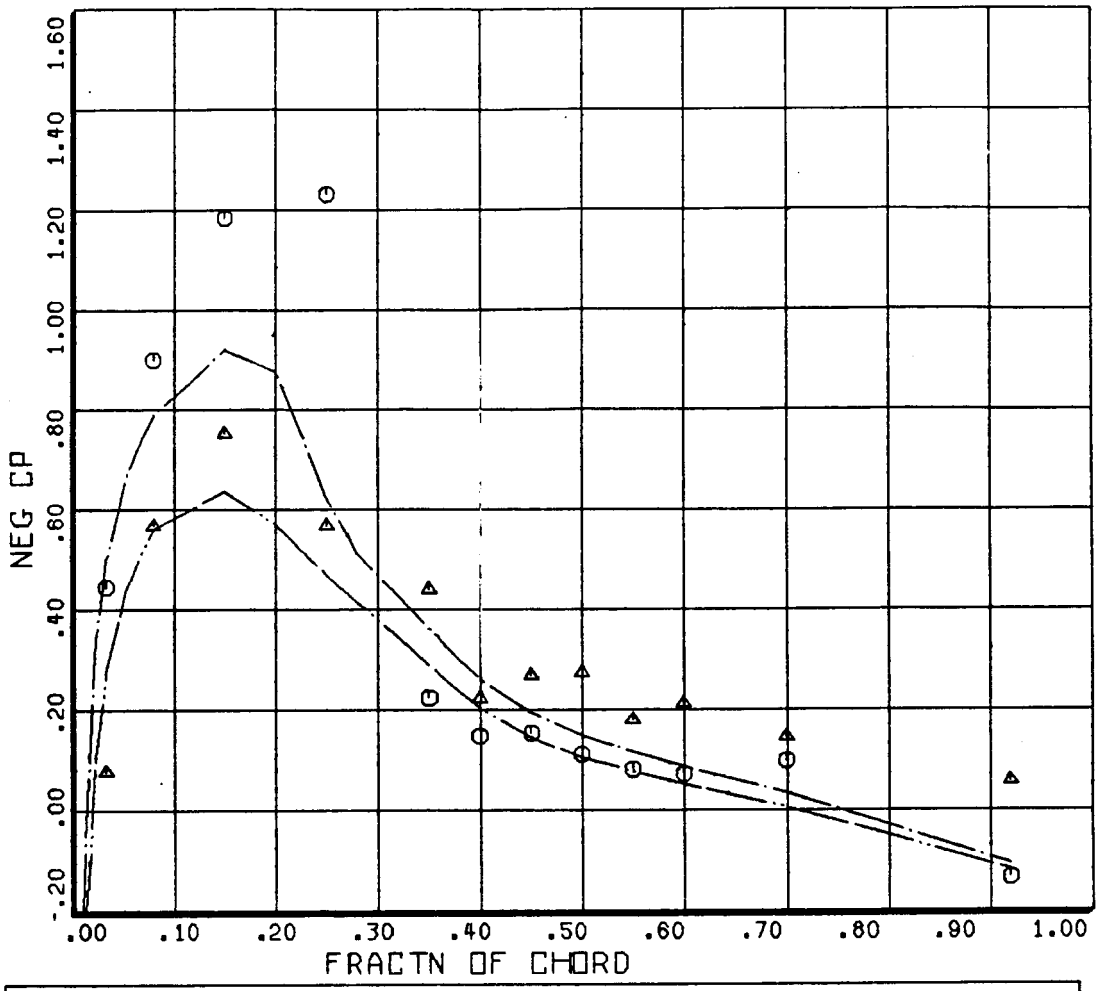

⊙ ⊙ ⊙	COUNTER .86	2872 R/RADIUS	GROSS WT LONG CG	SHIP MODEL AH-1G UPPER SURFACE
DERIVED PARAMETER:		BLADE STATIC PRESSURE COEFF		
△ △ △	COUNTER .86	2872 R/RADIUS	GROSS WT LONG CG	SHIP MODEL AH-1G LOWER SURFACE
DERIVED PARAMETER:		BLADE STATIC PRESSURE COEFF		
——·——·——	COUNTER .86	685462 R/RADIUS	GROSS WT 8150 LONG CG	SHIP MODEL OLSAH1 UPPER SURFACE
CYCLE AVERAGE:		LOCAL NEG CP: ROT22		
——·——·——	COUNTER .86	685462 R/RADIUS	GROSS WT 8150 LONG CG	SHIP MODEL OLSAH1 LOWER SURFACE
CYCLE AVERAGE:		LOCAL NEG CP: ROT22		

BHT.USARTL DATAMAP (VERS 3.10 - 24/02/82) 04/16/83 BELL HELICOPTER

Figure 5. Sectional pressure coefficient at 86% radius for Record 2872.

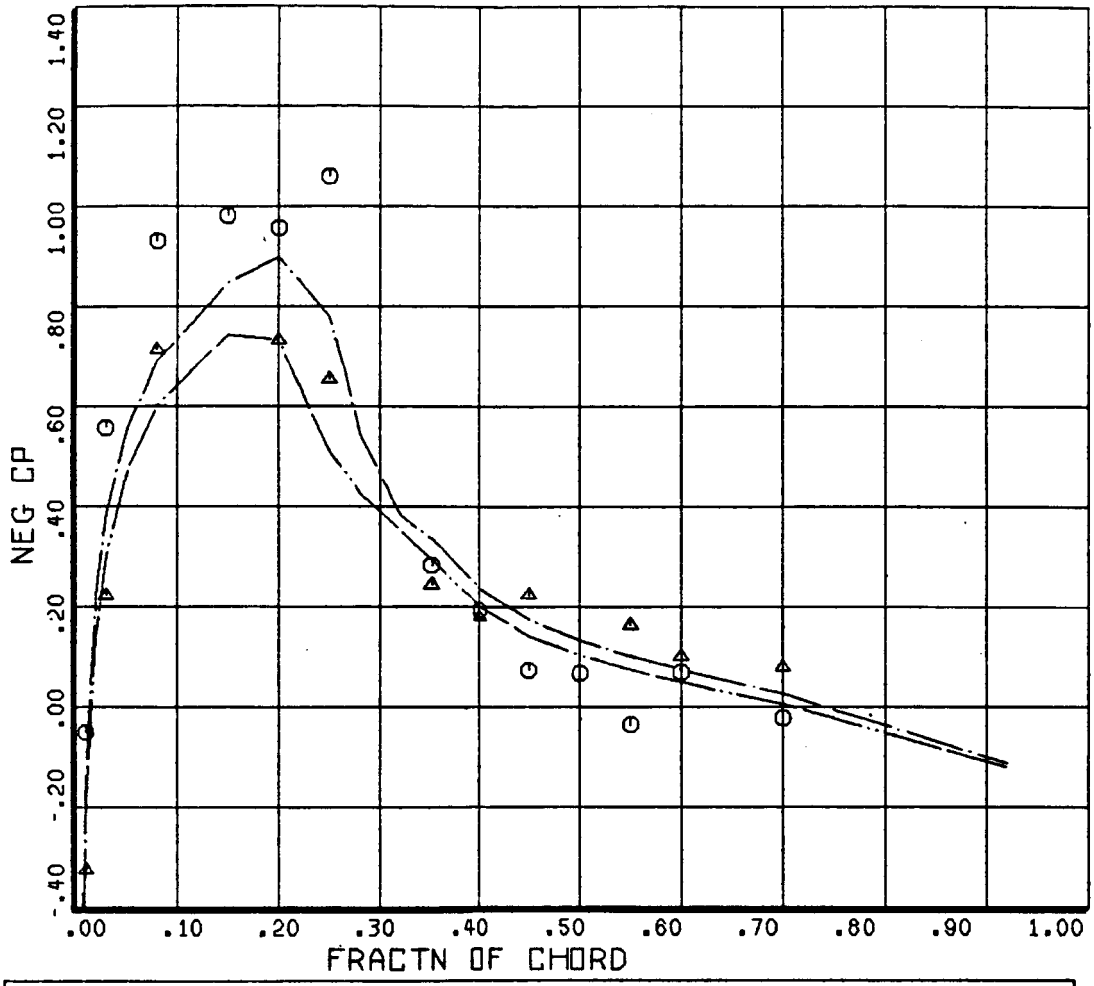

⊙ ⊙ ⊙	COUNTER .91	2872 R/RADIUS	GROSS WT LONG CG	SHIP MODEL AH-1G UPPER SURFACE
DERIVED PARAMETER:		BLADE STATIC PRESSURE COEFF		
△ △ △	COUNTER .91	2872 R/RADIUS	GROSS WT LONG CG	SHIP MODEL AH-1G LOWER SURFACE
DERIVED PARAMETER:		BLADE STATIC PRESSURE COEFF		
——·——·——	COUNTER .91	685462 R/RADIUS	GROSS WT 8150 LONG CG	SHIP MODEL OLSAH1 UPPER SURFACE
CYCLE AVERAGE:		LOCAL NEG CP: ROT22		
——·—— ——	COUNTER .91	685462 R/RADIUS	GROSS WT 8150 LONG CG	SHIP MODEL OLSAH1 LOWER SURFACE
CYCLE AVERAGE:		LOCAL NEG CP: ROT22		

BHT.USARTL DATAMAP (VERS 3.10 - 24/02/82) 04/16/83 BELL HELICOPTER

Figure 6. Sectional pressure coefficient at 91% radius for Record 2872.

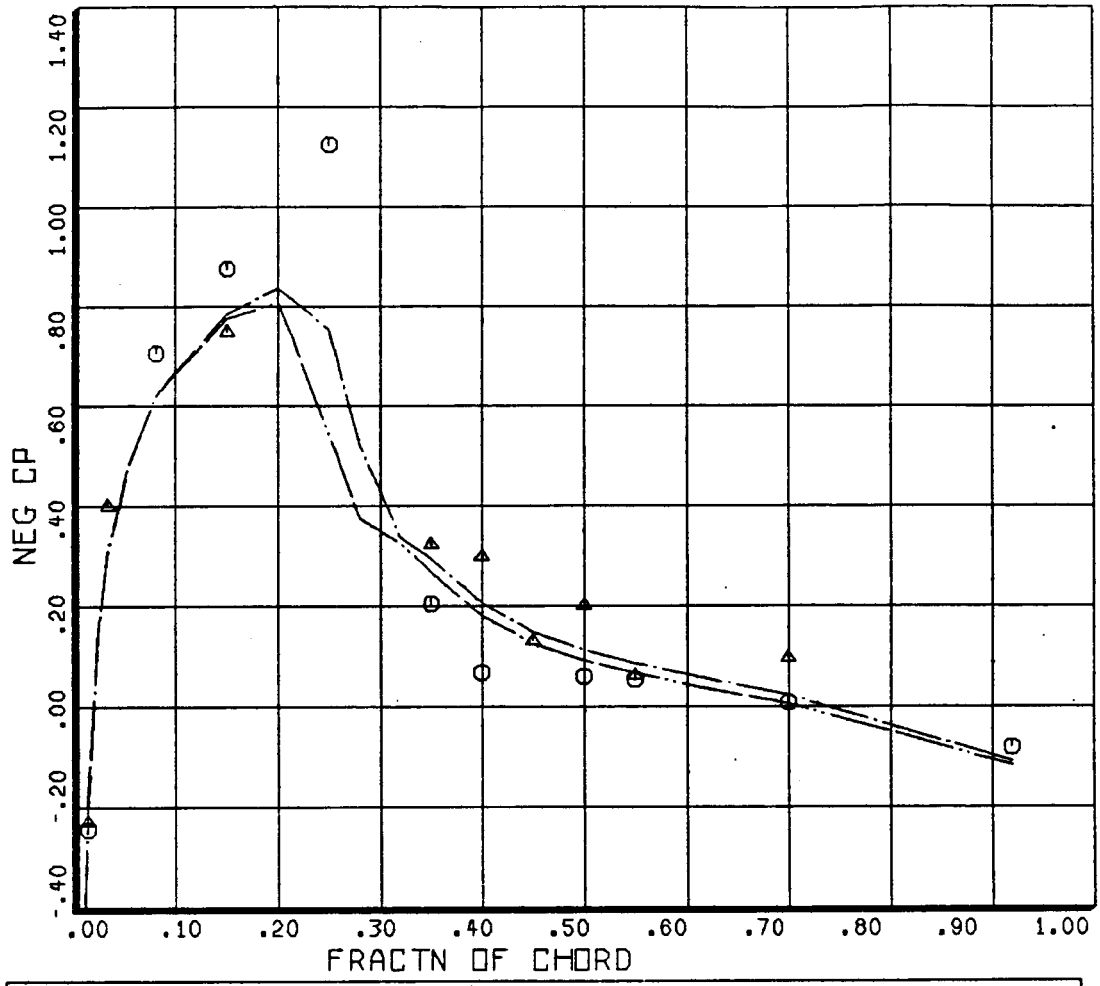

Figure 7. Sectional pressure coefficient at 95% radius for Record 2872.

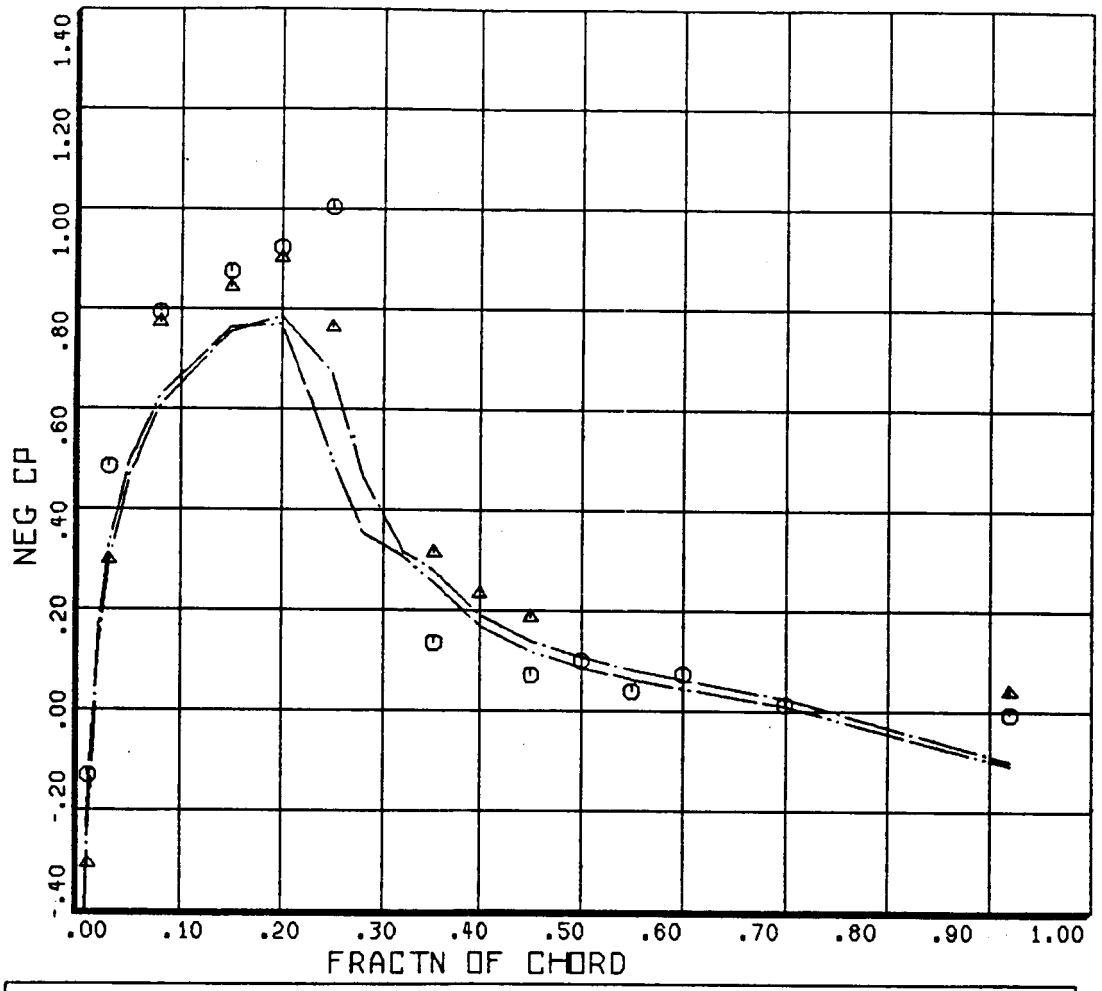

⊙ ⊙ ⊙	COUNTER .97	2872 R/RADIUS	GROSS WT LONG CG	SHIP MODEL AH-1G UPPER SURFACE
DERIVED PARAMETER:		BLADE STATIC PRESSURE COEFF		
△ △ △	COUNTER .97	2872 R/RADIUS	GROSS WT LONG CG	SHIP MODEL AH-1G LOWER SURFACE
DERIVED PARAMETER:		BLADE STATIC PRESSURE COEFF		
——·——·——	COUNTER .97	685462 R/RADIUS	GROSS WT 8150 LONG CG	SHIP MODEL OLSAH1 UPPER SURFACE
CYCLE AVERAGE:		LOCAL NEG CP: ROT22		
——·——·——	COUNTER .97	685462 R/RADIUS	GROSS WT 8150 LONG CG	SHIP MODEL OLSAH1 LOWER SURFACE
CYCLE AVERAGE:		LOCAL NEG CP: ROT22		

BHT.USARTL DATAMAP (VERS 3.10 - 24/02/82) 04/16/83 BELL HELICOPTER

Figure 8. Sectional pressure coefficient at 97% radius for Record 2872.

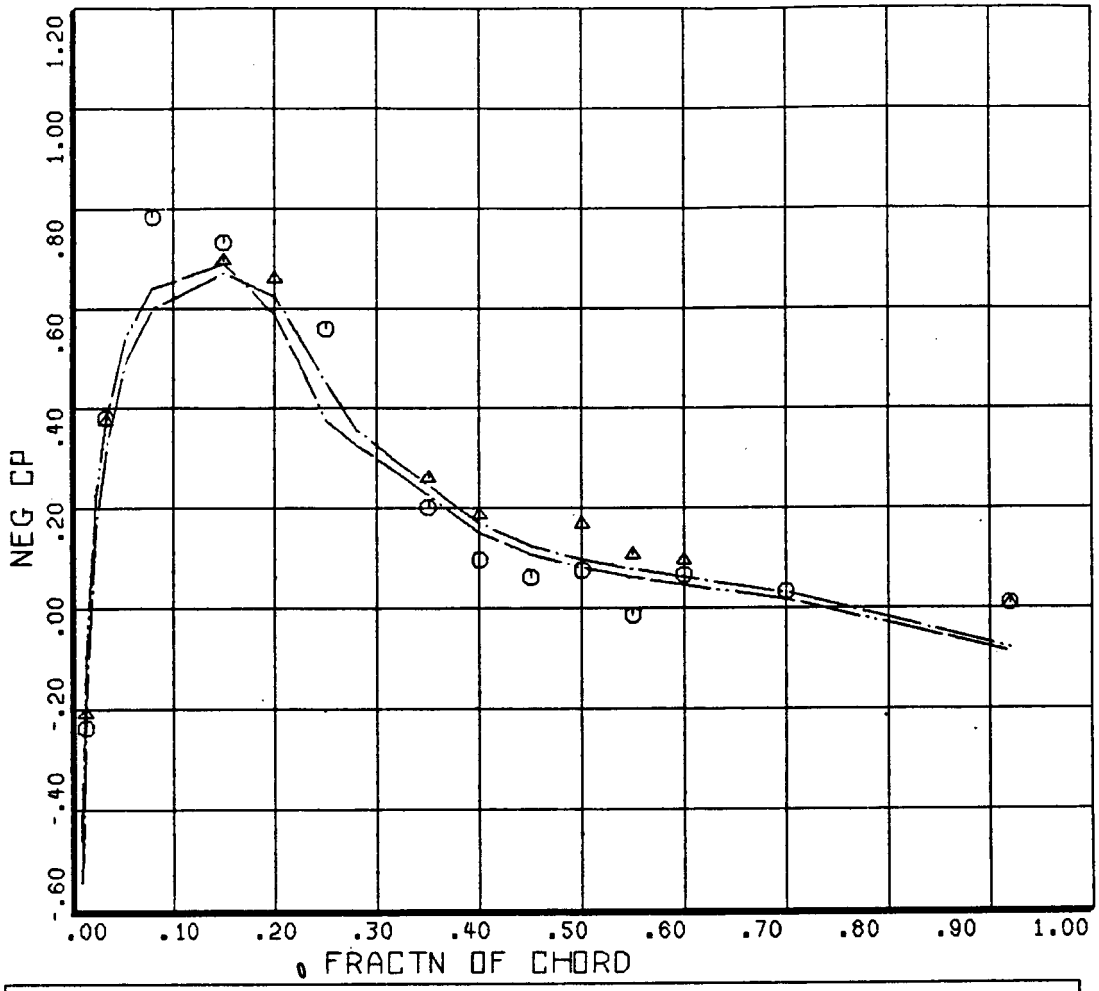

⊙ ⊙ ⊙	COUNTER .99	2872 R/RADIUS	GROSS WT LONG CG	SHIP MODEL AH-1G UPPER SURFACE
DERIVED PARAMETER:	BLADE STATIC PRESSURE COEFF			
△ △ △	COUNTER .99	2872 R/RADIUS	GROSS WT LONG CG	SHIP MODEL AH-1G LOWER SURFACE
DERIVED PARAMETER:	BLADE STATIC PRESSURE COEFF			
——·——·——	COUNTER .99	685462 R/RADIUS	GROSS WT 8150 LONG CG	SHIP MODEL OLSAH1 UPPER SURFACE
CYCLE AVERAGE:	LOCAL NEG CP: ROT22			
——·——·——	COUNTER .99	685462 R/RADIUS	GROSS WT 8150 LONG CG	SHIP MODEL OLSAH1 LOWER SURFACE
CYCLE AVERAGE:	LOCAL NEG CP: ROT22			

BHT,USARTL DATAMAP (VERS 3.10 - 24/02/82) 04/16/83 BELL HELICOPTER

Figure 9. Sectional pressure coefficient at 99% radius for Record 2872.

TABLE 4. TWIST RATES, $(\theta_{T_R})_{EQ}$, TO MATCH SURFACE PRESSURES

r/R	Record 2872	Record 2873	Record 2806
0.75	-9.37	-8.63	-8.45
0.85	-10.20	-10.0	-9.50
0.90	-10.74	-10.40	-9.70
0.95	-10.50	-10.10	-9.10
1.0	-11.40	-11.00	-10.0

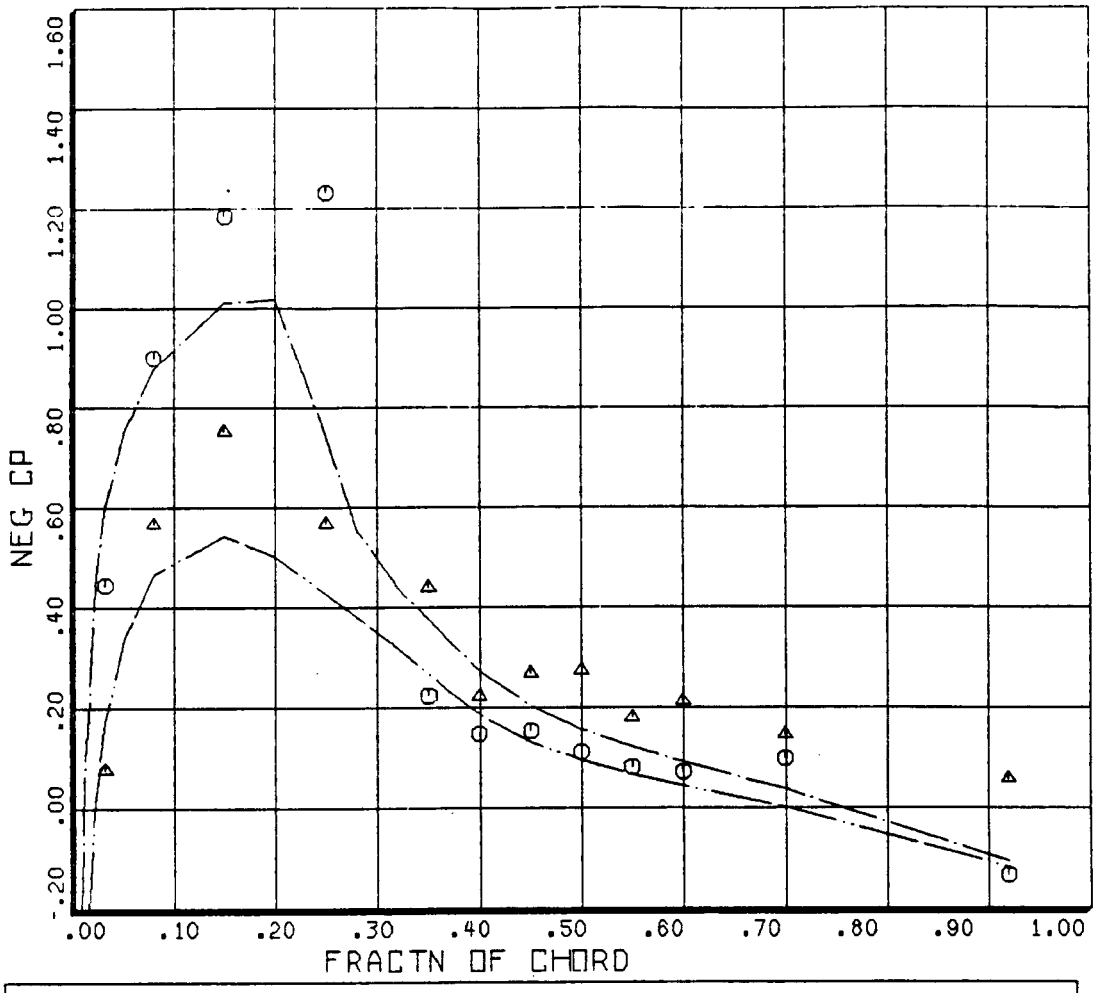

⊙ ⊙ ⊙ DERIVED PARAMETER:	COUNTER .86 2872 R/RADIUS BLADE STATIC PRESSURE COEFF	GROSS WT LONG CG	SHIP MODEL AH-1G UPPER SURFACE
△ △ △ DERIVED PARAMETER:	COUNTER .86 2872 R/RADIUS BLADE STATIC PRESSURE COEFF	GROSS WT LONG CG	SHIP MODEL AH-1G LOWER SURFACE
CYCLE AVERAGE:	COUNTER .86 947609 R/RADIUS LOCAL NEG CP: ROT22	GROSS WT 8150 LONG CG	SHIP MODEL OLSAH1 UPPER SURFACE
CYCLE AVERAGE:	COUNTER .86 947609 R/RADIUS LOCAL NEG CP: ROT22	GROSS WT 8150 LONG CG	SHIP MODEL OLSAH1 LOWER SURFACE

BHT,USARTL DATAMAP (VERS 3.10 - 24/02/82) 04/25/83 BELL HELICOPTER

Figure 10. Sectional pressure coefficient at 86% radius for Record 2872 (modified twist).

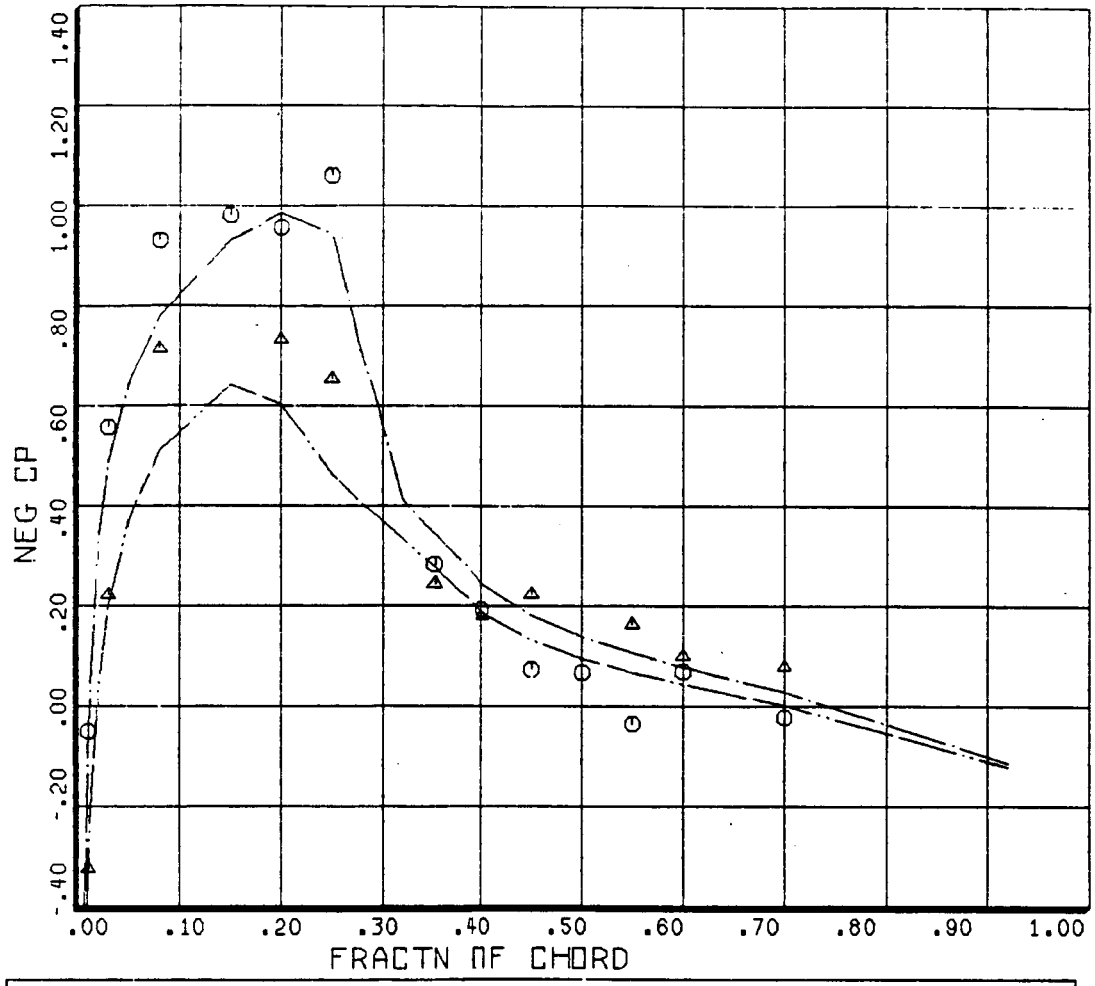

⊙ ⊙ ⊙	COUNTER 2872	GROSS WT	SHIP MODEL AH-1G
	.91 R/RADIUS	LONG CG	UPPER SURFACE
DERIVED PARAMETER:	BLADE STATIC PRESSURE COEFF		
△ △ △	COUNTER 2872	GROSS WT	SHIP MODEL AH-1G
	.91 R/RADIUS	LONG CG	LOWER SURFACE
DERIVED PARAMETER:	BLADE STATIC PRESSURE COEFF		
——·——·——	COUNTER 947609	GROSS WT 8150	SHIP MODEL OLSAH1
	.91 R/RADIUS	LONG CG	UPPER SURFACE
CYCLE AVERAGE:	LOCAL NEG CP: ROT22		
——·——·——	COUNTER 947609	GROSS WT 8150	SHIP MODEL OLSAH1
	.91 R/RADIUS	LONG CG	LOWER SURFACE
CYCLE AVERAGE:	LOCAL NEG CP: ROT22		

BHT.USARTL DATAMAP (VERS 3.10 - 24/02/82) 04/25/83 BELL HELICOPTER

Figure 11. Sectional pressure coefficient at 91% radius for Record 2872 (modified twist).

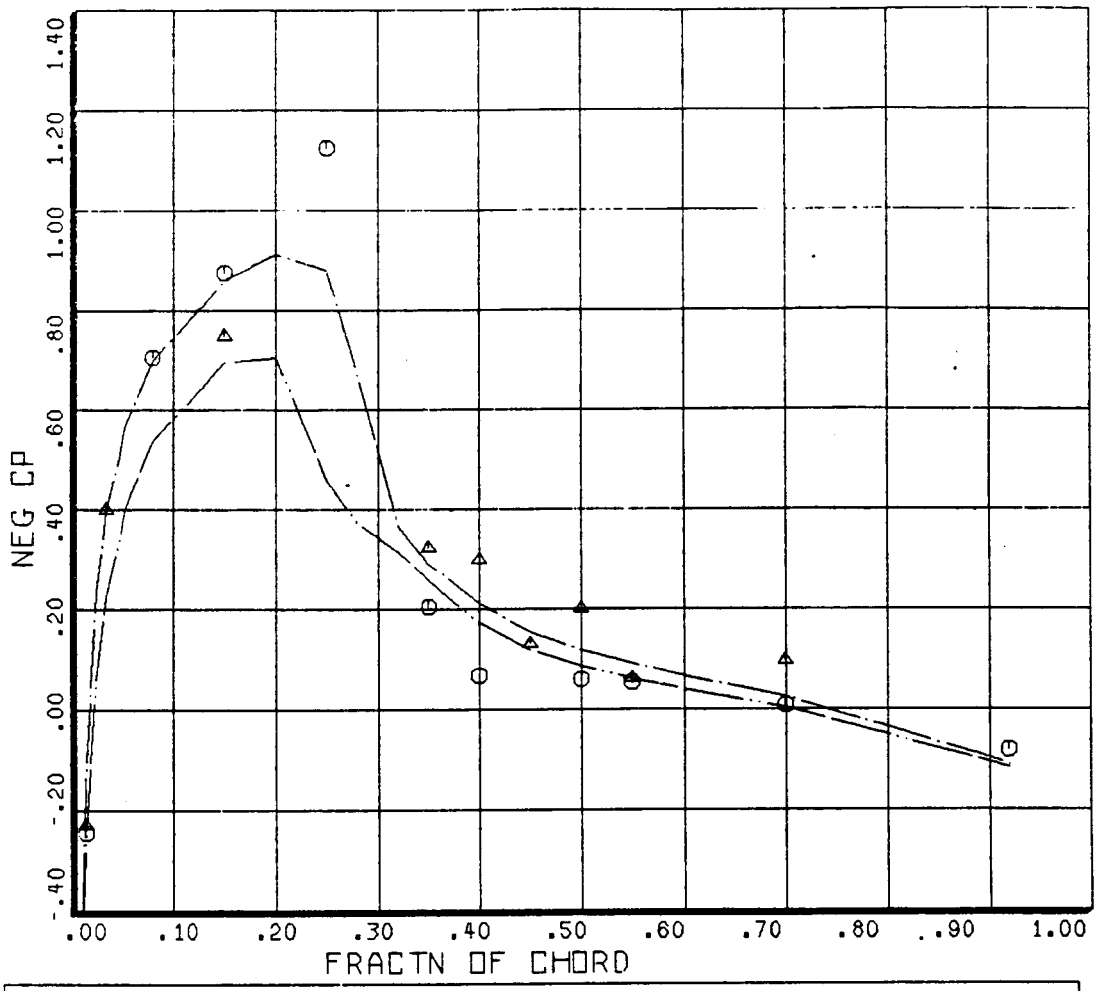

Figure 12. Sectional pressure coefficient at 95% radius for Record 2872 (modified twist).

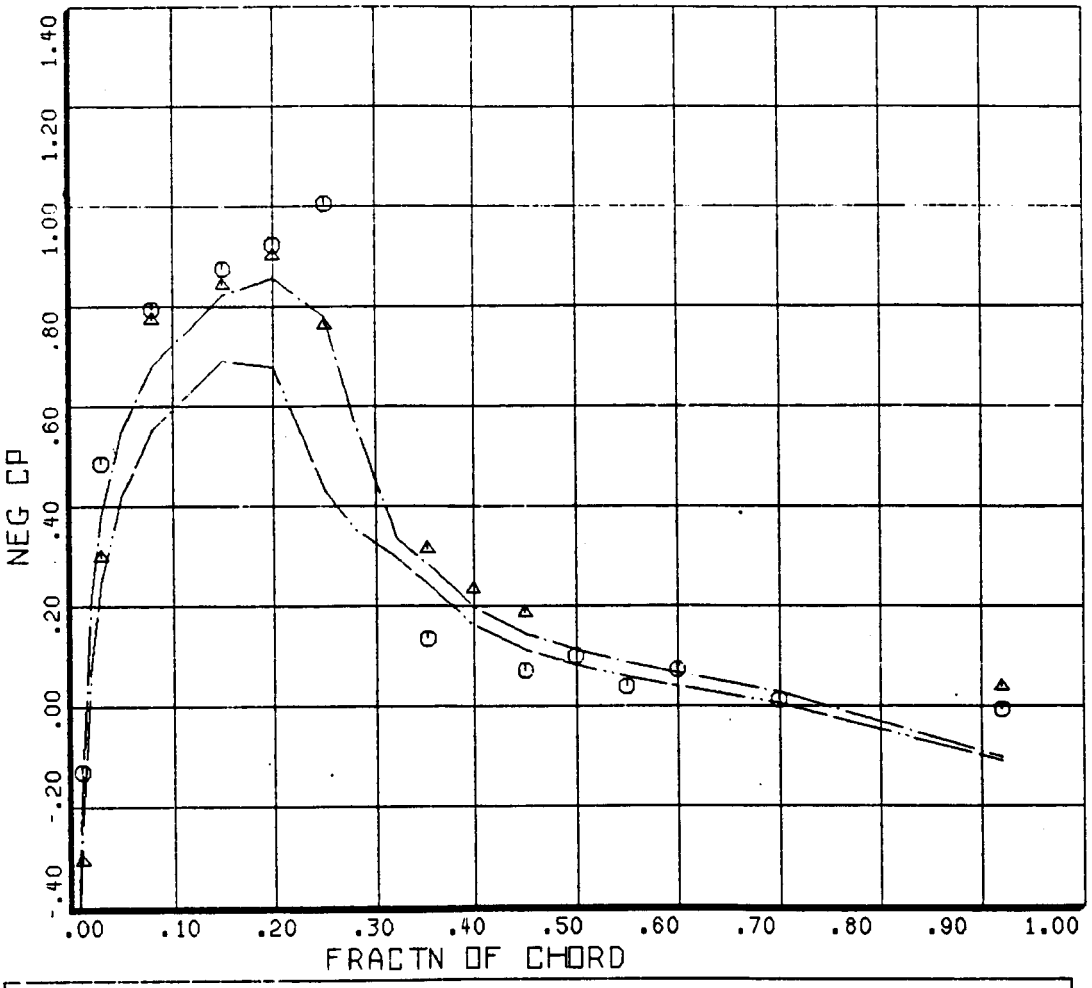

⊖ ⊖ ⊖ DERIVED PARAMETER:	COUNTER .97 2872 R/RADIUS GROSS WT LONG CG BLADE STATIC PRESSURE COEFF		SHIP MODEL AH-1G UPPER SURFACE
△ △ △ DERIVED PARAMETER:	COUNTER .97 2872 R/RADIUS GROSS WT LONG CG BLADE STATIC PRESSURE COEFF		SHIP MODEL AH-1G LOWER SURFACE
——·——·—— CYCLE AVERAGE:	COUNTER .97 947609 R/RADIUS GROSS WT 8150 LONG CG LOCAL NEG CP: ROT22		SHIP MODEL OLSAH1 UPPER SURFACE
——·——·—— CYCLE AVERAGE:	COUNTER .97 947609 R/RADIUS GROSS WT 8150 LONG CG LOCAL NEG CP: ROT22		SHIP MODEL OLSAH1 LOWER SURFACE

BHT.USARTL DATAMAP (VERS 3.10 - 24/02/82) 04/25/83 BELL HELICOPTER

Figure 13. Sectional pressure coefficient at 97% radius for Record 2872 (modified twist).

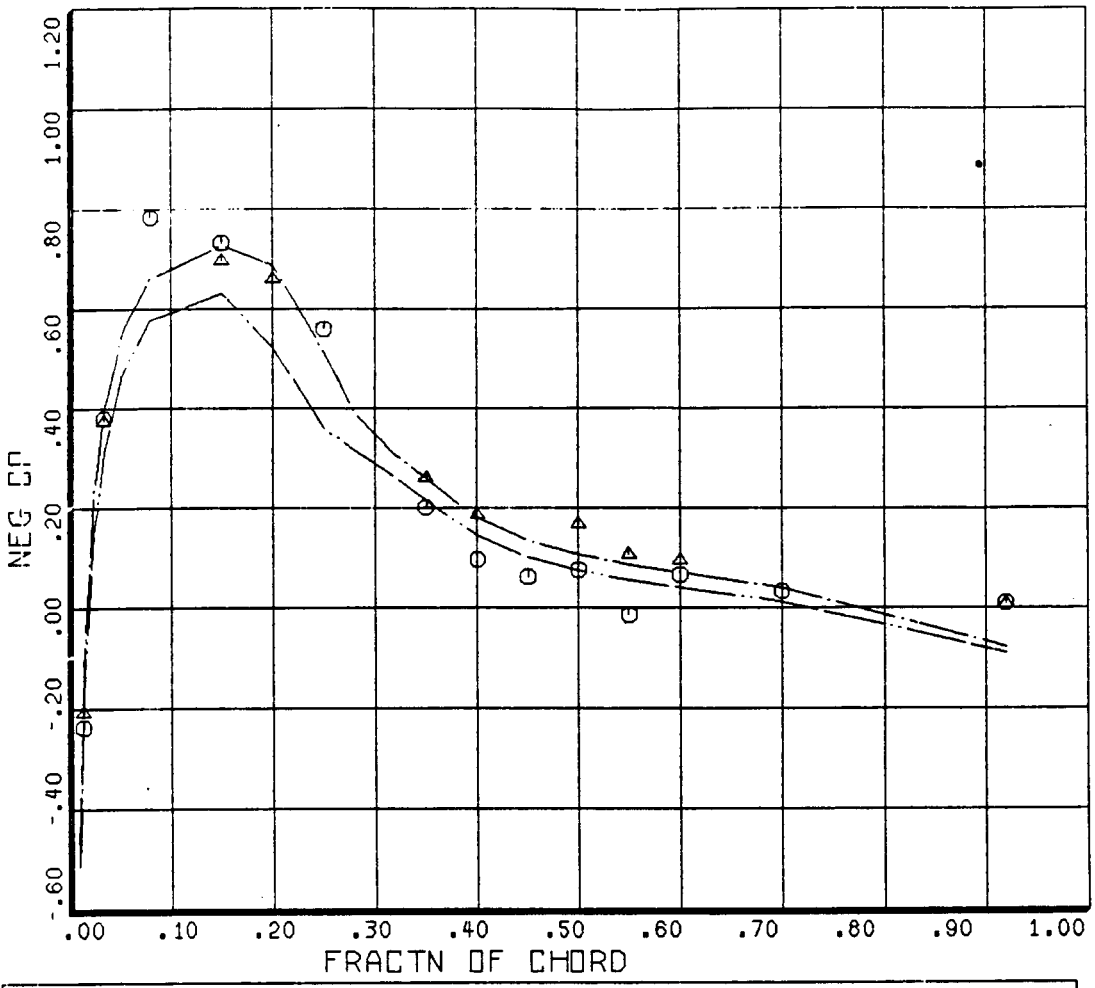

⊙ ⊙ ⊙ DERIVED PARAMETER:	COUNTER .99	2872 R/RADIUS BLADE STATIC PRESSURE COEFF	GROSS WT LONG CG	SHIP MODEL AH-1G UPPER SURFACE
△ △ △ DERIVED PARAMETER:	COUNTER .99	2872 R/RADIUS BLADE STATIC PRESSURE COEFF	GROSS WT LONG CG	SHIP MODEL AH-1G LOWER SURFACE
——·——·—— CYCLE AVERAGE:	COUNTER .99	947609 R/RADIUS LOCAL NEG CP: ROT22	GROSS WT 8150 LONG CG	SHIP MODEL OLSAH1 UPPER SURFACE
——··——·—— CYCLE AVERAGE:	COUNTER .99	947609 R/RADIUS LOCAL NEG CP: ROT22	GROSS WT 8150 LONG CG	SHIP MODEL OLSAH1 LOWER SURFACE

BHT,USARTL DATAMAP (VERS 3.10 · 24/02/82) 04/25/83 BELL HELICOPTER

Figure 14. Sectional pressure coefficient at 99% radius for Record 2872 (modified twist).

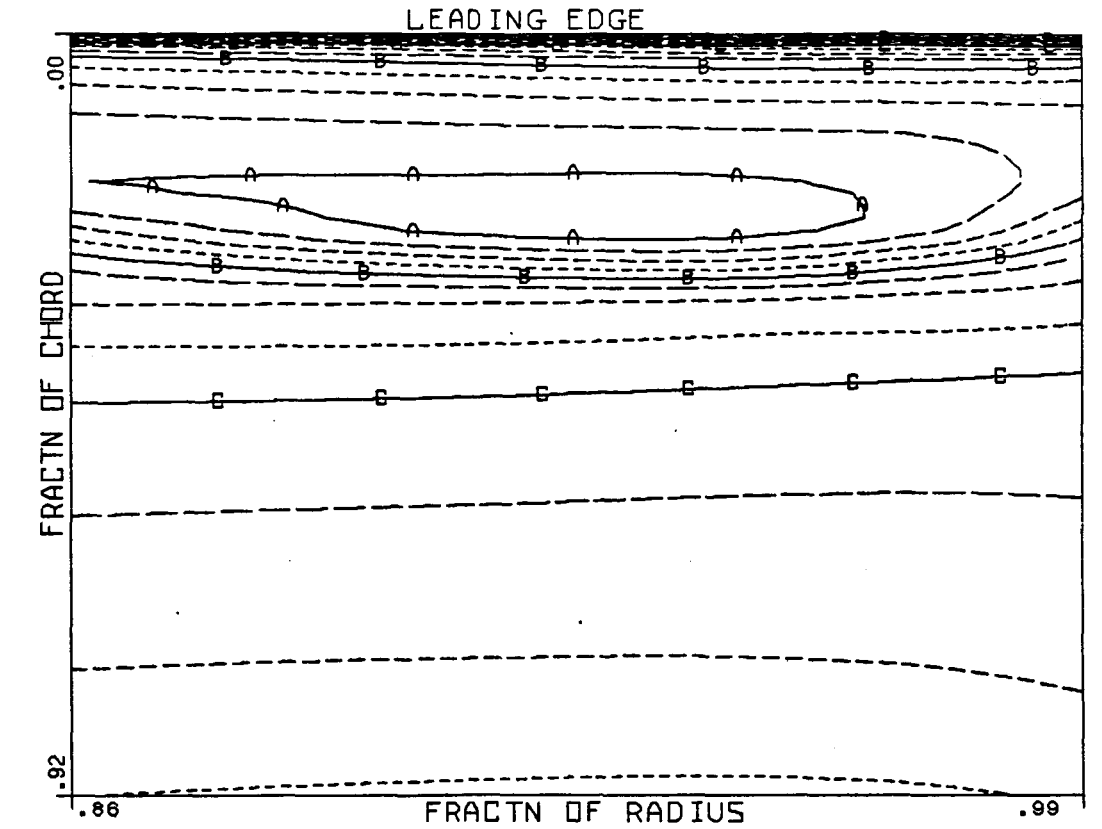

Figure 15. ROT22 blade tip pressure contours for Record 2872 (upper surface).

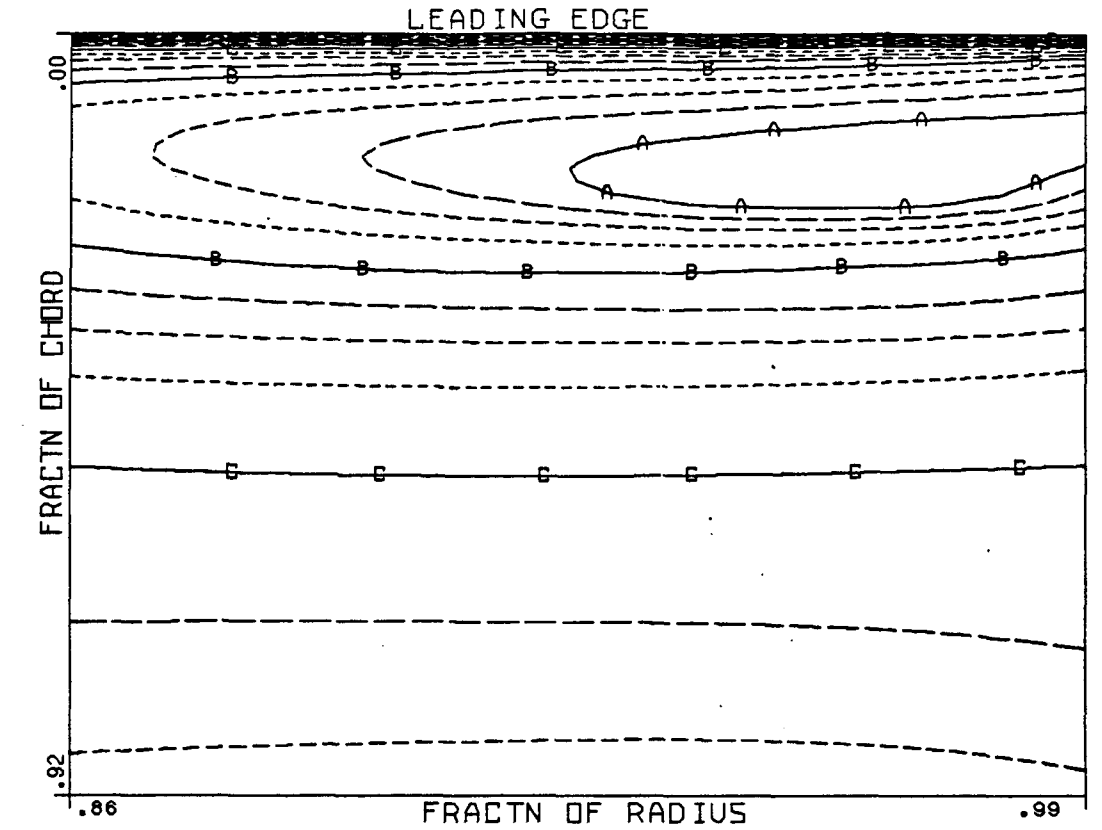

Figure 16. ROT22 blade tip pressure contours for Record 2872 (lower surface).

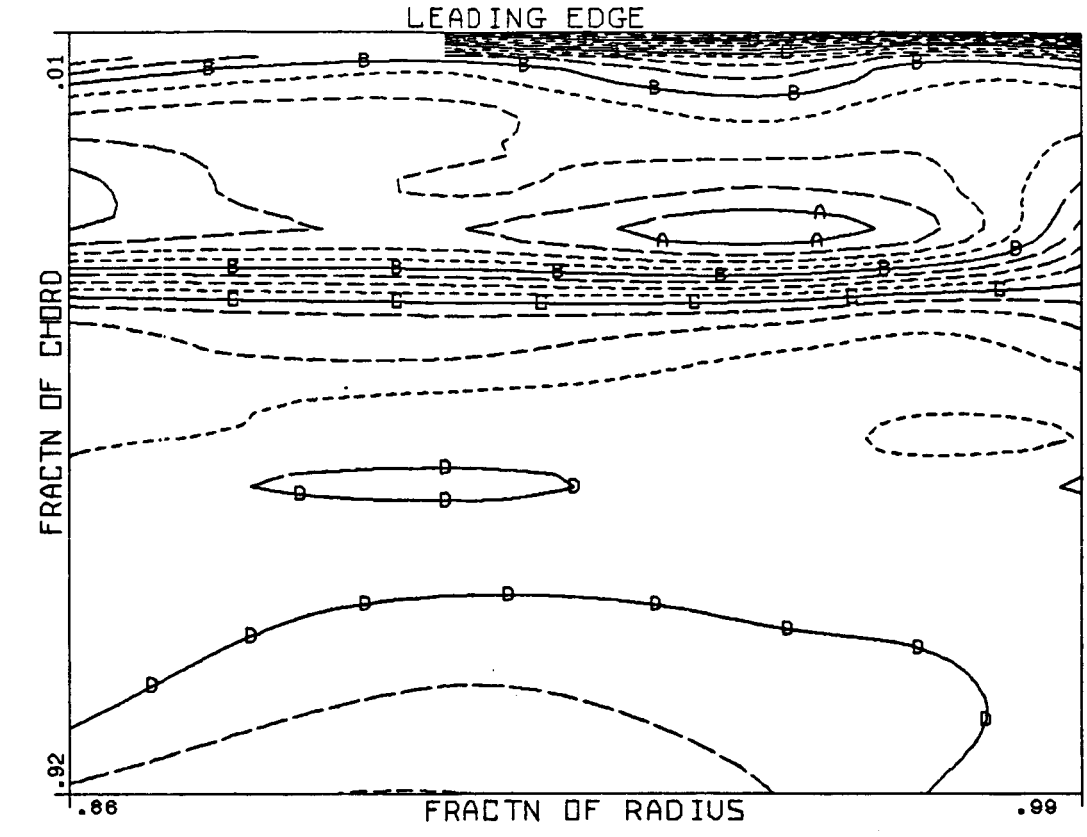

Figure 17. Flight test blade tip pressure contours for Record 2872 (upper surface).

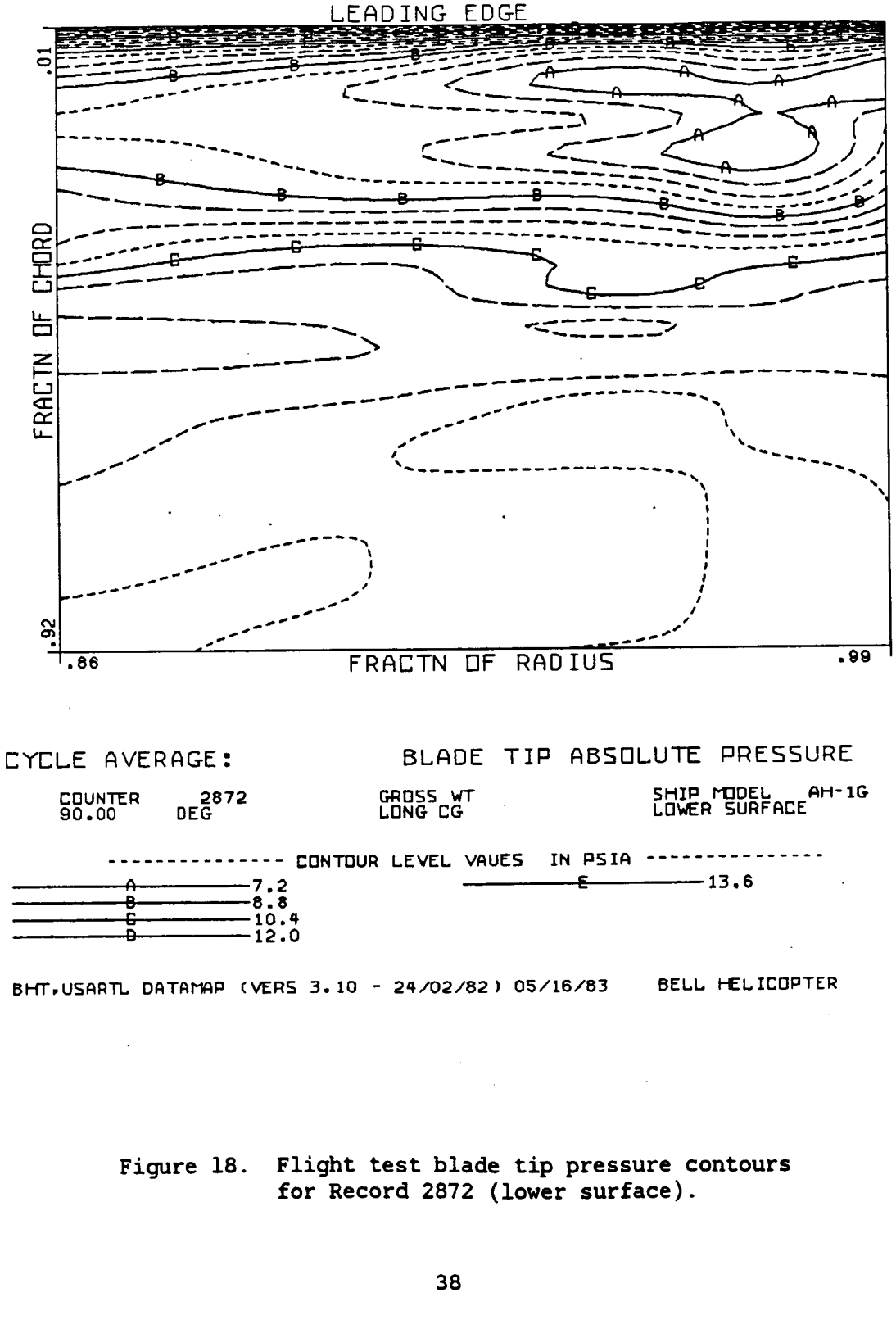

Figure 18. Flight test blade tip pressure contours for Record 2872 (lower surface).

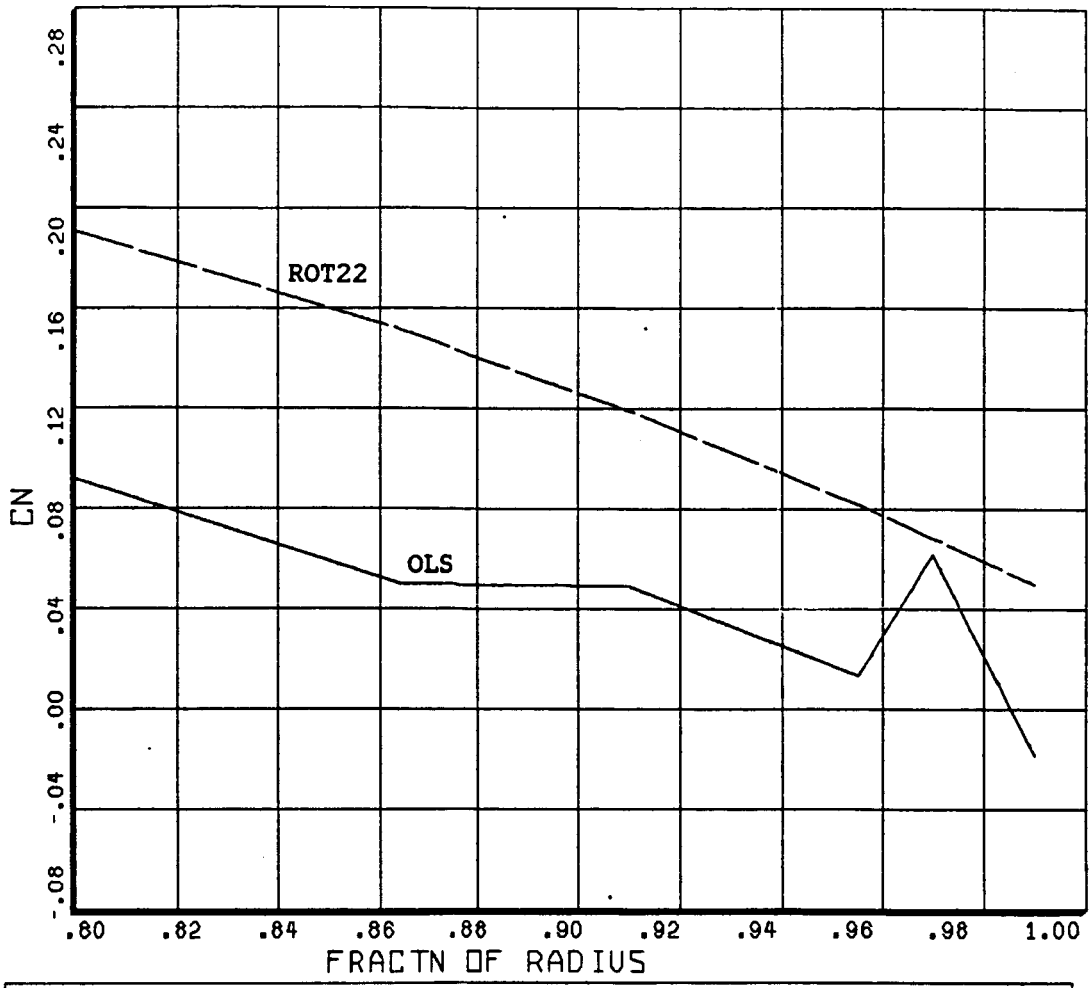

BHT.USARTL DATAMAP (VERS 3.10 - 24/02/82) 05/17/83 BELL HELICOPTER

Figure 19. Normal force coefficient for Record 2872 (modified twist).

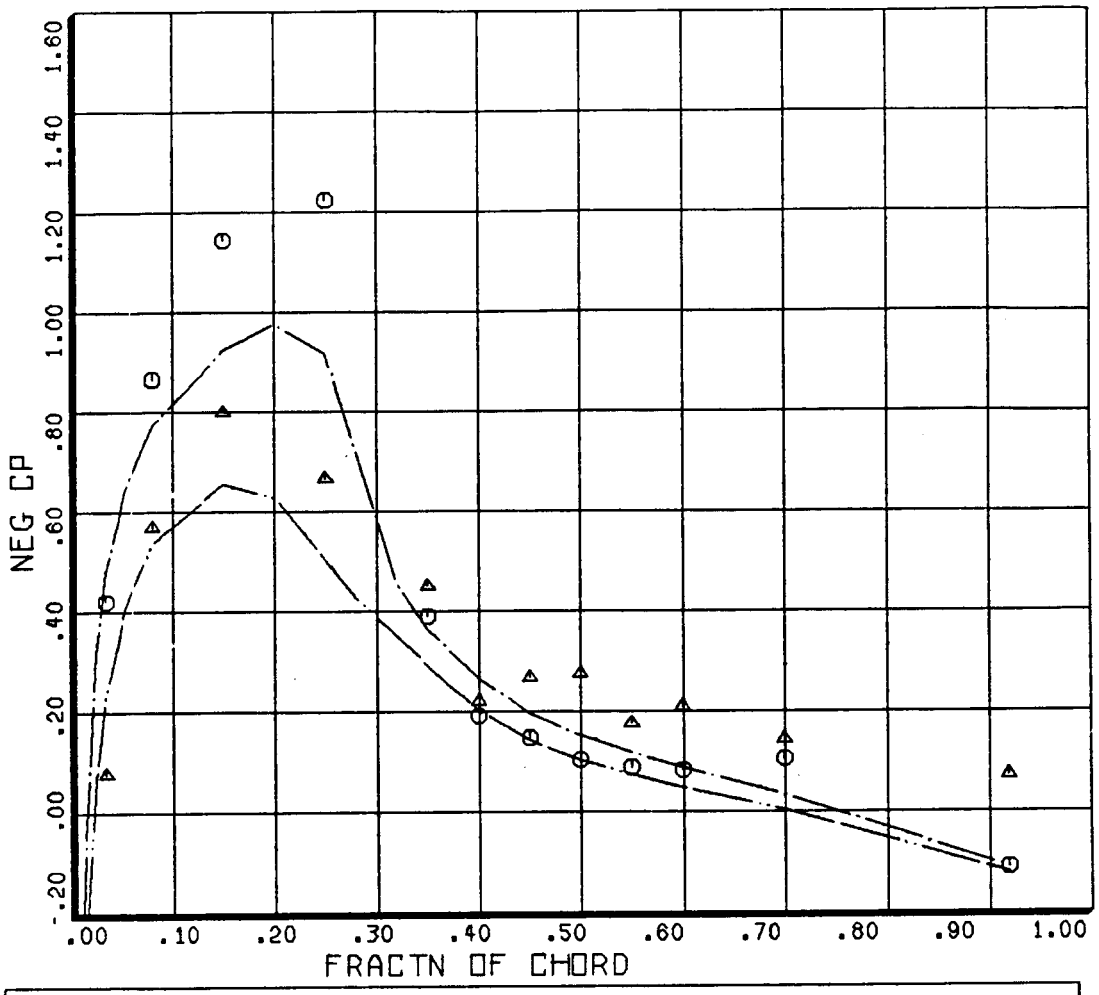

⊙ ⊙ ⊙	COUNTER 2873	GROSS WT	SHIP MODEL AH-1G
	.86 R/RADIUS	LONG CG	UPPER SURFACE
DERIVED PARAMETER:	BLADE STATIC PRESSURE COEFF		
△ △ △	COUNTER 2873	GROSS WT	SHIP MODEL AH-1G
	.86 R/RADIUS	LONG CG	LOWER SURFACE
DERIVED PARAMETER:	BLADE STATIC PRESSURE COEFF		
——·——·——	COUNTER 441053	GROSS WT 8050	SHIP MODEL OLSAH1
	.86 R/RADIUS	LONG CG	UPPER SURFACE
CYCLE AVERAGE:	LOCAL NEG CP: ROT22		
——··——··——	COUNTER 441053	GROSS WT 8050	SHIP MODEL OLSAH1
	.86 R/RADIUS	LONG CG	LOWER SURFACE
CYCLE AVERAGE:	LOCAL NEG CP: ROT22		

BHT,USARTL DATAMAP (VERS 3.10 - 24/02/82) 04/16/83 BELL HELICOPTER

Figure 20. Sectional pressure coefficient at 86% radius for Record 2873.

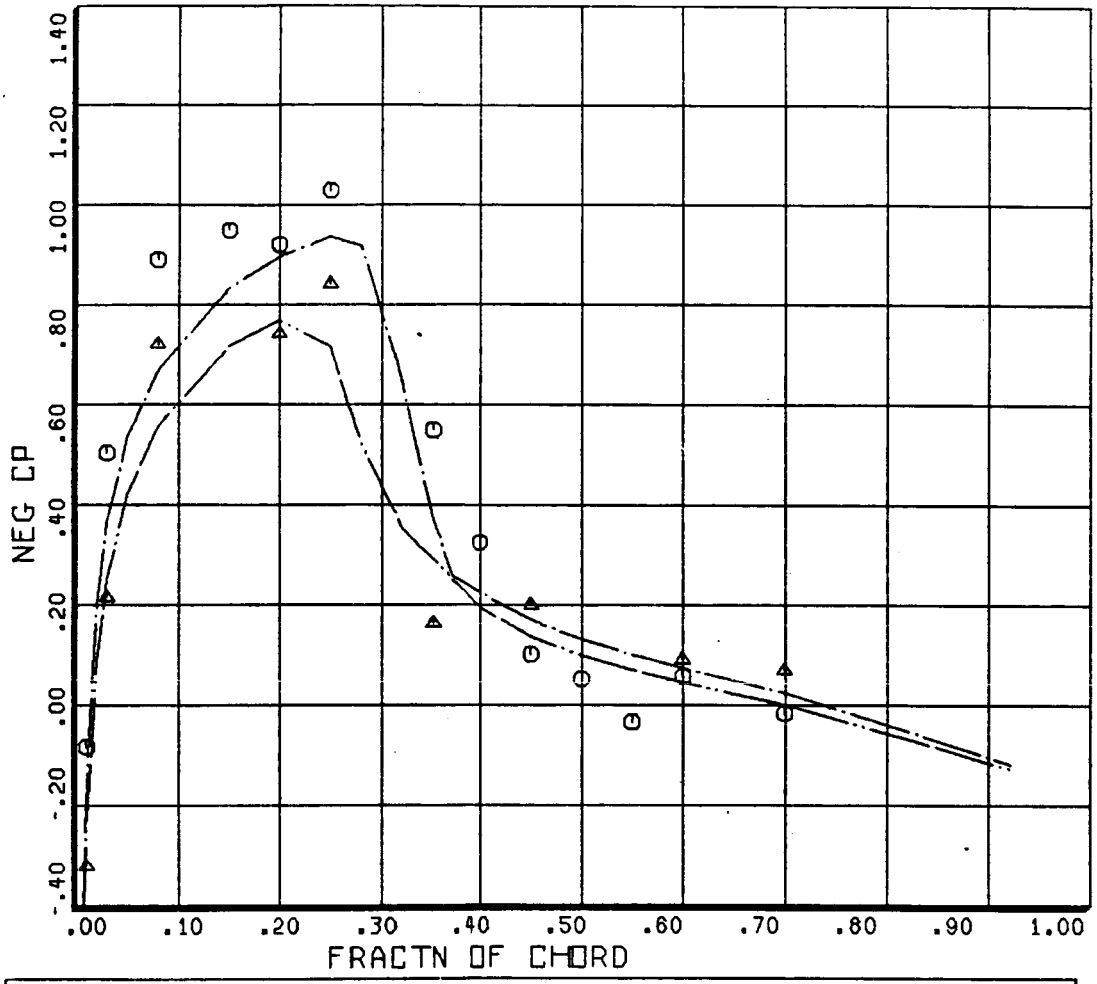

⏲ ⏲ ⏲ DERIVED PARAMETER:	COUNTER .91 BLADE STATIC PRESSURE COEFF	2873 R/RADIUS	GROSS WT LONG CG	SHIP MODEL AH-1G UPPER SURFACE
△ △ △ DERIVED PARAMETER:	COUNTER .91 BLADE STATIC PRESSURE COEFF	2873 R/RADIUS	GROSS WT LONG CG	SHIP MODEL AH-1G LOWER SURFACE
——·——·—— CYCLE AVERAGE:	COUNTER .91 LOCAL NEG CP: ROT22	441053 R/RADIUS	GROSS WT 8050 LONG CG	SHIP MODEL OLSAH1 UPPER SURFACE
——·———·—— CYCLE AVERAGE:	COUNTER .91 LOCAL NEG CP: ROT22	441053 R/RADIUS	GROSS WT 8050 LONG CG	SHIP MODEL OLSAH1 LOWER SURFACE

BHT,USARTL DATAMAP (VERS 3.10 - 24/02/82) 04/16/83 BELL HELICOPTER

Figure 21. Sectional pressure coefficient at 91% radius for Record 2873.

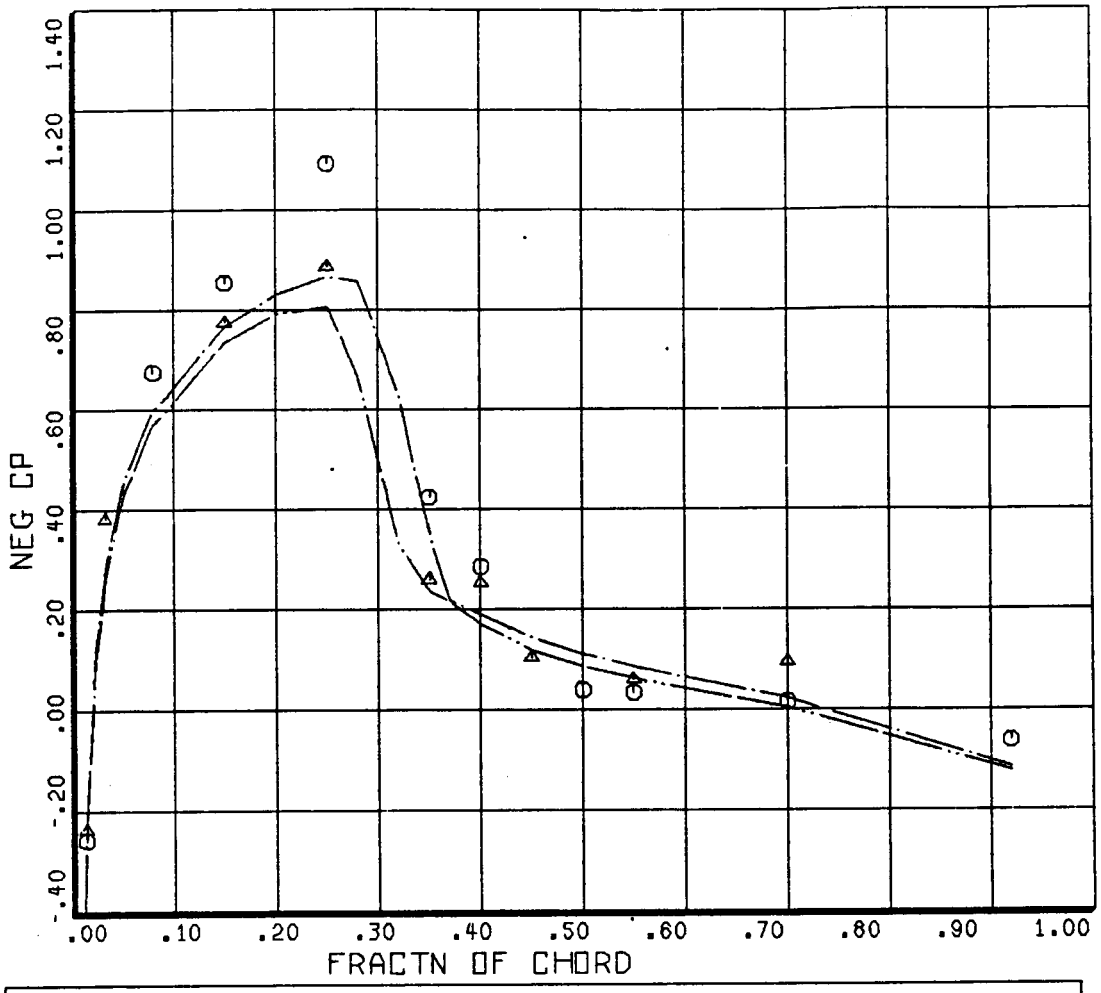

⊙ ⊙ ⊙ DERIVED PARAMETER:	COUNTER .95 R/RADIUS BLADE STATIC PRESSURE COEFF	2873	GROSS WT LONG CG	SHIP MODEL AH-1G UPPER SURFACE
△ △ △ DERIVED PARAMETER:	COUNTER .95 R/RADIUS BLADE STATIC PRESSURE COEFF	2873	GROSS WT LONG CG	SHIP MODEL AH-1G LOWER SURFACE
CYCLE AVERAGE:	COUNTER .95 R/RADIUS LOCAL NEG CP: ROT22	441053	GROSS WT 8050 LONG CG	SHIP MODEL OLSAH1 UPPER SURFACE
CYCLE AVERAGE:	COUNTER .95 R/RADIUS LOCAL NEG CP: ROT22	441053	GROSS WT 8050 LONG CG	SHIP MODEL OLSAH1 LOWER SURFACE

BHT,USARTL DATAMAP (VERS 3.10 - 24/02/82) 04/16/83 BELL HELICOPTER

Figure 22. Sectional pressure coefficient at 95% radius for Record 2873.

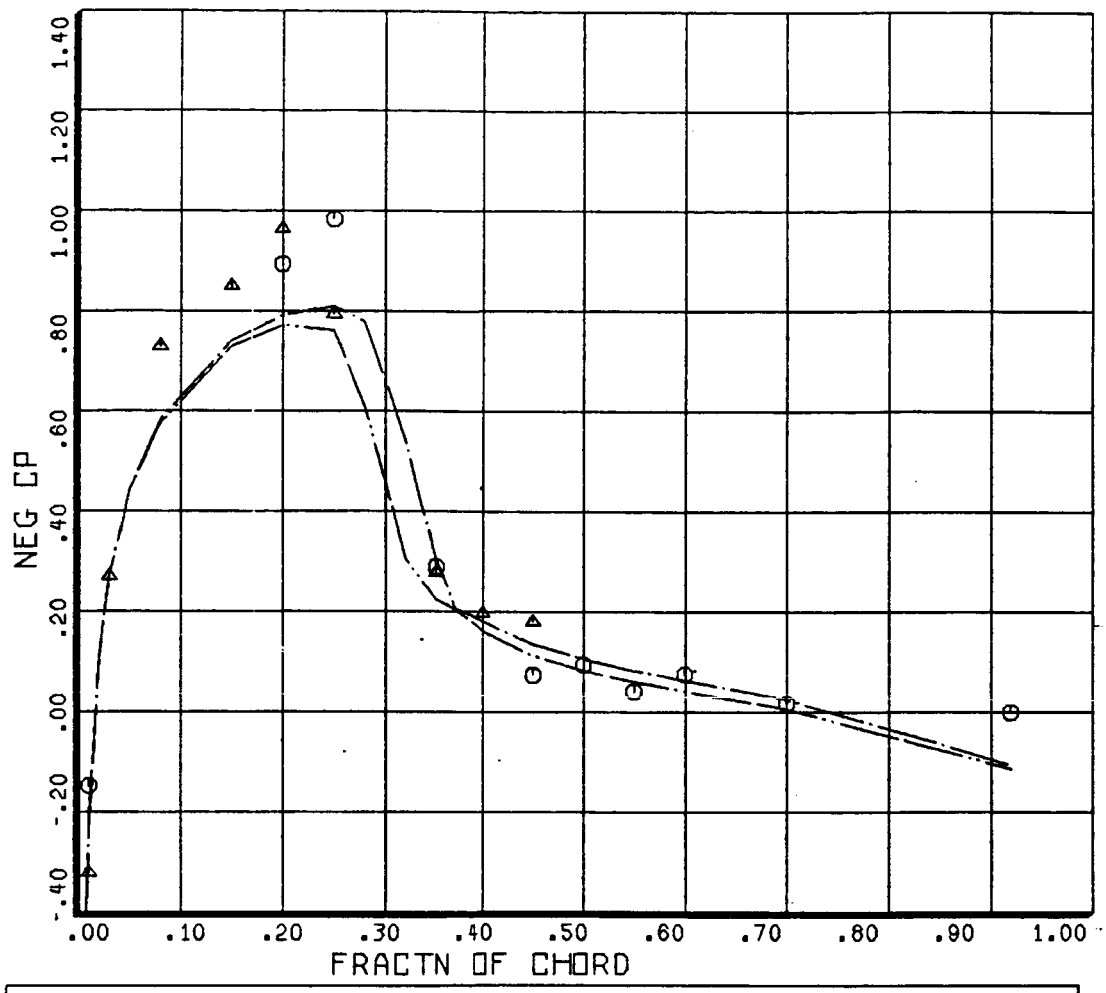

Figure 23. Sectional pressure coefficient at 97% radius for Record 2873.

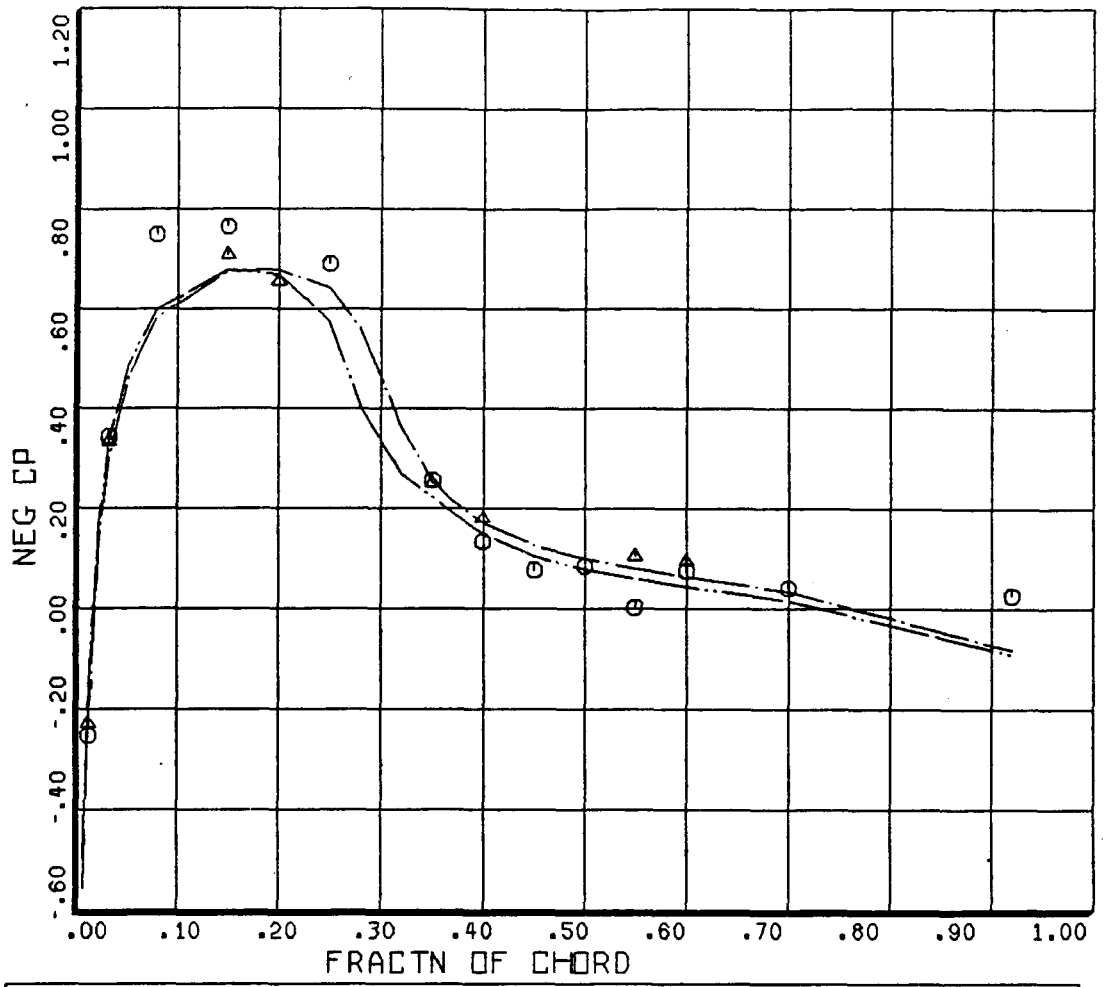

⊙ ⊙ ⊙	COUNTER 2873	GROSS WT	SHIP MODEL AH-1G
	.99 R/RADIUS	LONG CG	UPPER SURFACE
DERIVED PARAMETER:	BLADE STATIC PRESSURE COEFF		
△ △ △	COUNTER 2873	GROSS WT	SHIP MODEL AH-1G
	.99 R/RADIUS	LONG CG	LOWER SURFACE
DERIVED PARAMETER:	BLADE STATIC PRESSURE COEFF		
——·——·——	COUNTER 441053	GROSS WT 8050	SHIP MODEL DLSAH1
	.99 R/RADIUS	LONG CG	UPPER SURFACE
CYCLE AVERAGE:	LOCAL NEG CP: ROT22		
——·——·——	COUNTER 441053	GROSS WT 8050	SHIP MODEL DLSAH1
	.99 R/RADIUS	LONG CG	LOWER SURFACE
CYCLE AVERAGE:	LOCAL NEG CP: ROT22		

BHT,USARTL DATAMAP (VERS 3.10 - 24/02/82) 04/16/83 BELL HELICOPTER

Figure 24. Sectional pressure coefficient at 99% radius for Record 2873.

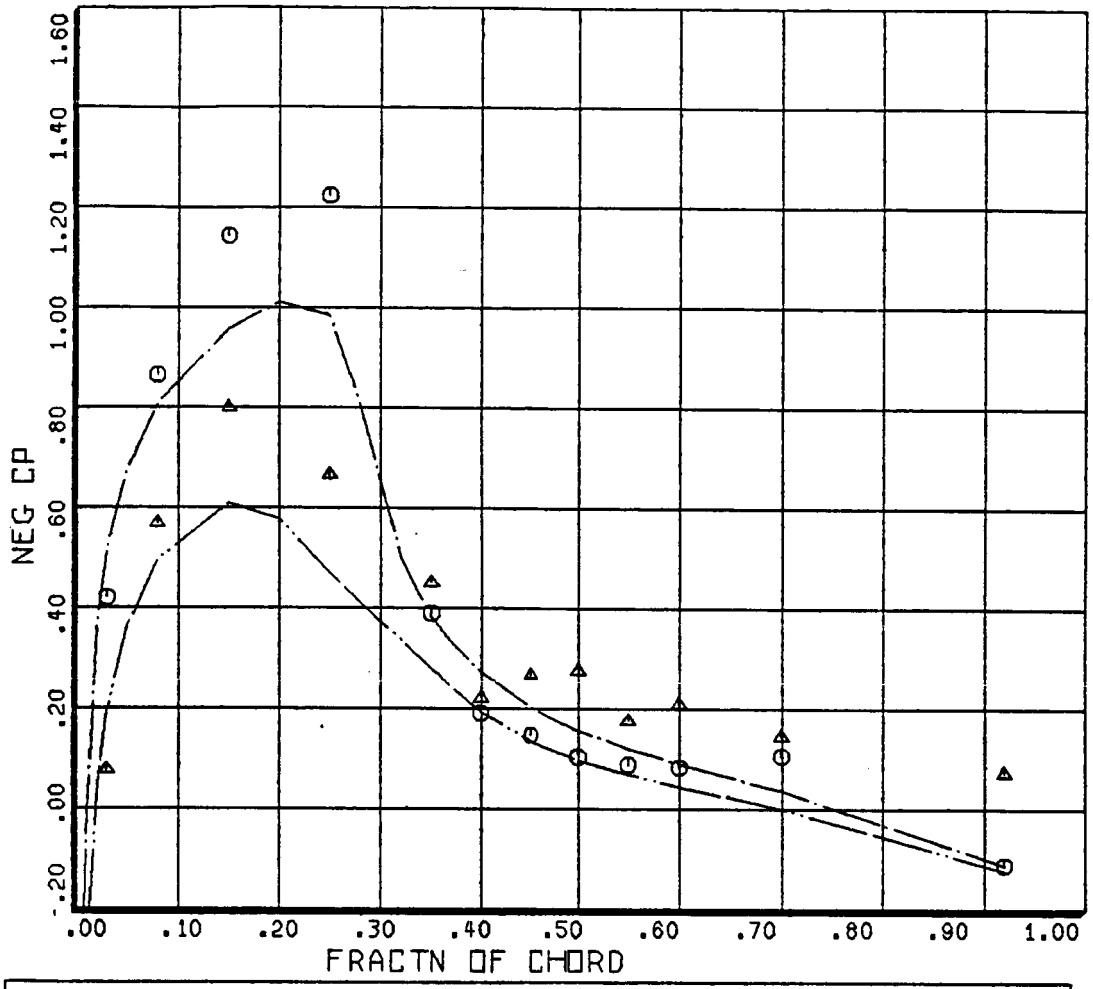

⊙ ⊙ ⊙ DERIVED PARAMETER:	COUNTER .86 R/RADIUS BLADE STATIC PRESSURE COEFF	2873 LONG CG	GROSS WT SHIP MODEL AH-1G UPPER SURFACE
△ △ △ DERIVED PARAMETER:	COUNTER .86 R/RADIUS BLADE STATIC PRESSURE COEFF	2873 LONG CG	GROSS WT SHIP MODEL AH-1G LOWER SURFACE
CYCLE AVERAGE:	COUNTER .86 R/RADIUS LOCAL NEG CP: ROT22	344575 LONG CG	GROSS WT 8050 SHIP MODEL OLSAH1 UPPER SURFACE
CYCLE AVERAGE:	COUNTER .86 R/RADIUS LOCAL NEG CP: ROT22	344575 LONG CG	GROSS WT 8050 SHIP MODEL OLSAH1 LOWER SURFACE

BHT.USARTL DATAMAP (VERS 3.10 - 24/02/82) 04/26/83 BELL HELICOPTER

Figure 25. Sectional pressure coefficient at 86% radius for Record 2873 (modified twist).

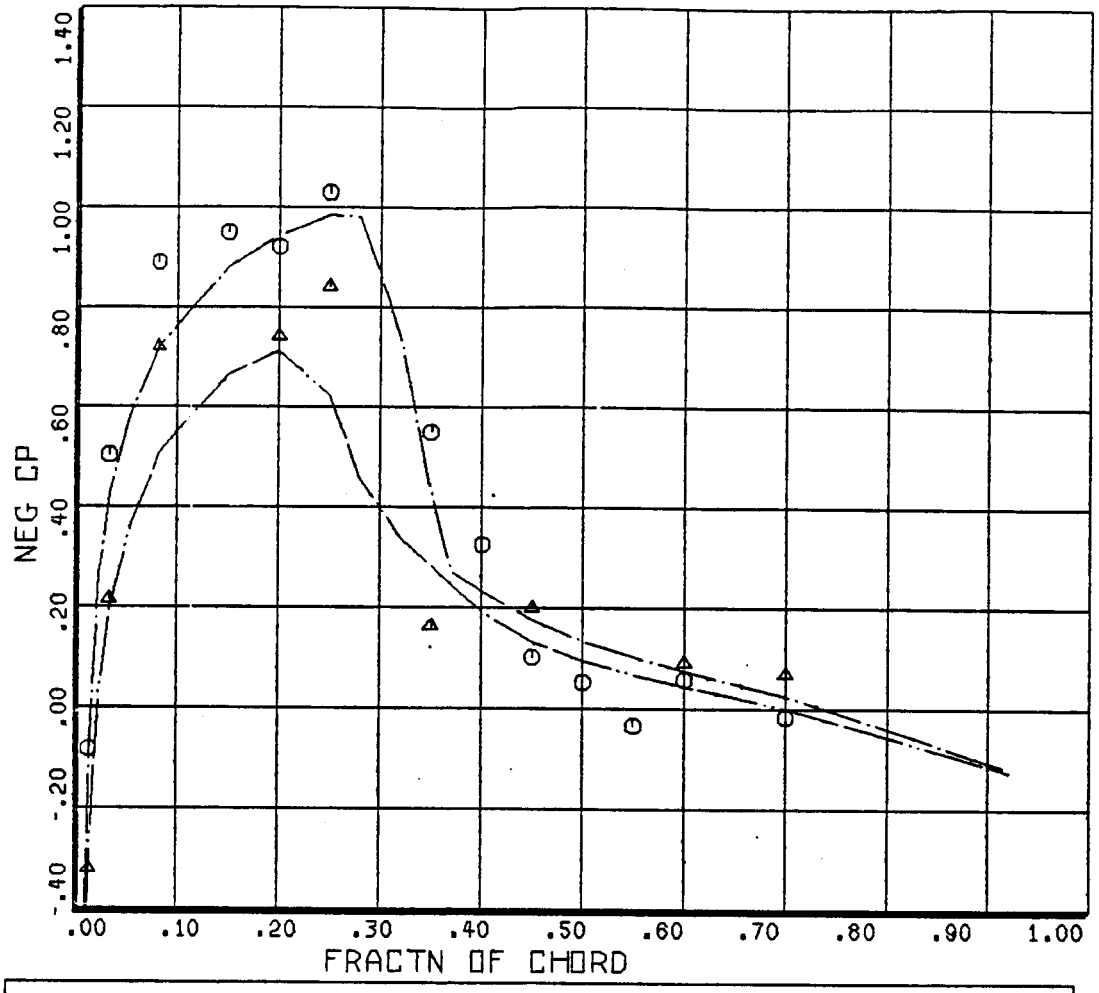

⏲ ⏲ ⏲ DERIVED PARAMETER:	COUNTER .91 BLADE STATIC PRESSURE COEFF	2873 R/RADIUS	GROSS WT LONG CG	SHIP MODEL AH-1G UPPER SURFACE
△ △ △ DERIVED PARAMETER:	COUNTER .91 BLADE STATIC PRESSURE COEFF	2873 R/RADIUS	GROSS WT LONG CG	SHIP MODEL AH-1G LOWER SURFACE
CYCLE AVERAGE:	COUNTER .91 LOCAL NEG CP: ROT22	344575 R/RADIUS	GROSS WT 8050 LONG CG	SHIP MODEL OLSAH1 UPPER SURFACE
CYCLE AVERAGE:	COUNTER .91 LOCAL NEG CP: ROT22	344575 R/RADIUS	GROSS WT 8050 LONG CG	SHIP MODEL OLSAH1 LOWER SURFACE

BHT,USARTL DATAMAP (VERS 3.10 - 24/02/82) 04/26/83 BELL HELICOPTER

Figure 26. Sectional pressure coefficient at 91% radius for Record 2873 (modified twist).

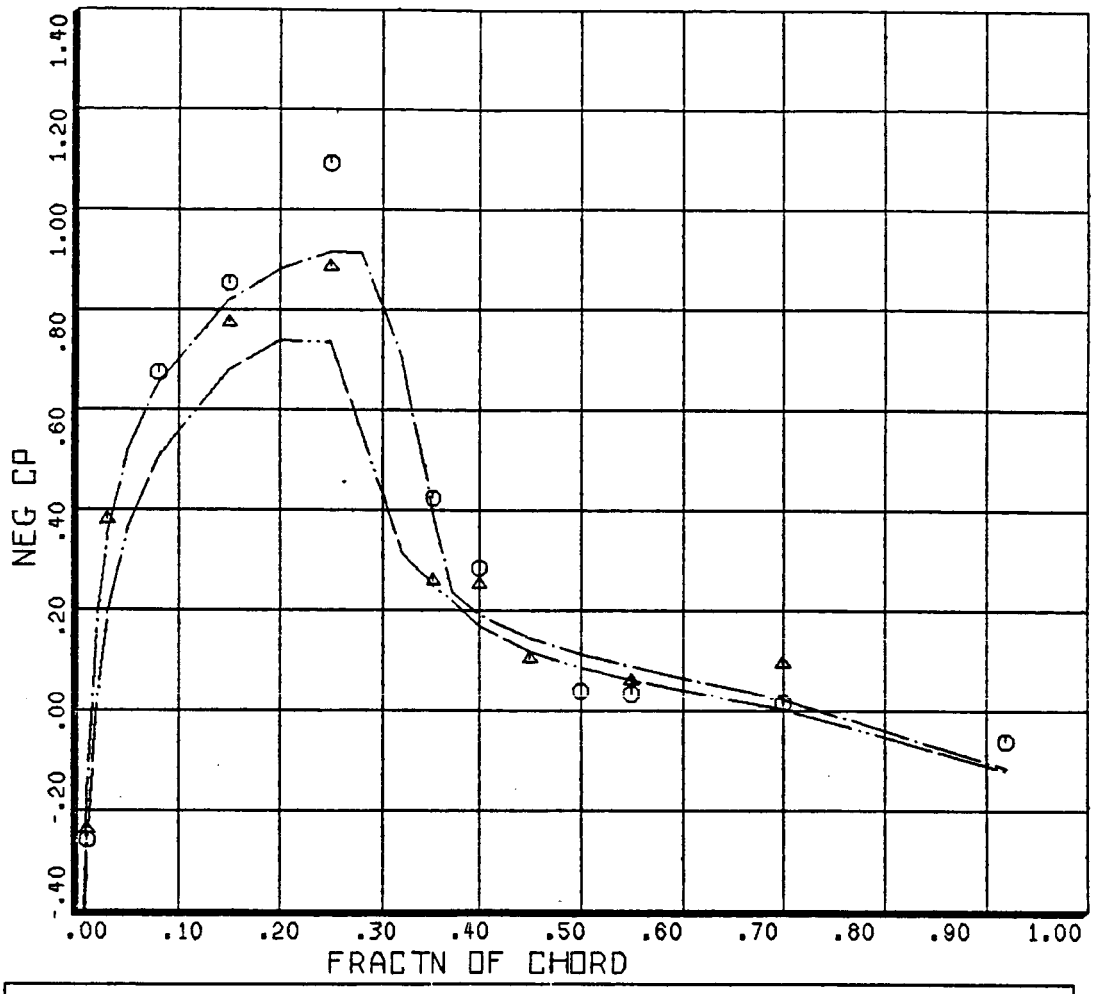

⊙ ⊙ ⊙	COUNTER .95	2873 R/RADIUS	GROSS WT LONG CG	SHIP MODEL AH-1G UPPER SURFACE
DERIVED PARAMETER:		BLADE STATIC PRESSURE COEFF		
△ △ △	COUNTER .95	2873 R/RADIUS	GROSS WT LONG CG	SHIP MODEL AH-1G LOWER SURFACE
DERIVED PARAMETER:		BLADE STATIC PRESSURE COEFF		
——·——·——	COUNTER .95	344575 R/RADIUS	GROSS WT 8050 LONG CG	SHIP MODEL OLSAH1 UPPER SURFACE
CYCLE AVERAGE:		LOCAL NEG CP: ROT22		
——··——··——	COUNTER .95	344575 R/RADIUS	GROSS WT 8050 LONG CG	SHIP MODEL OLSAH1 LOWER SURFACE
CYCLE AVERAGE:		LOCAL NEG CP: ROT22		

BHT.USARTL DATAMAP (VERS 3.10 - 24/02/82) 04/26/83 BELL HELICOPTER

Figure 27. Sectional pressure coefficient at 95% radius for Record 2873 (modified twist).

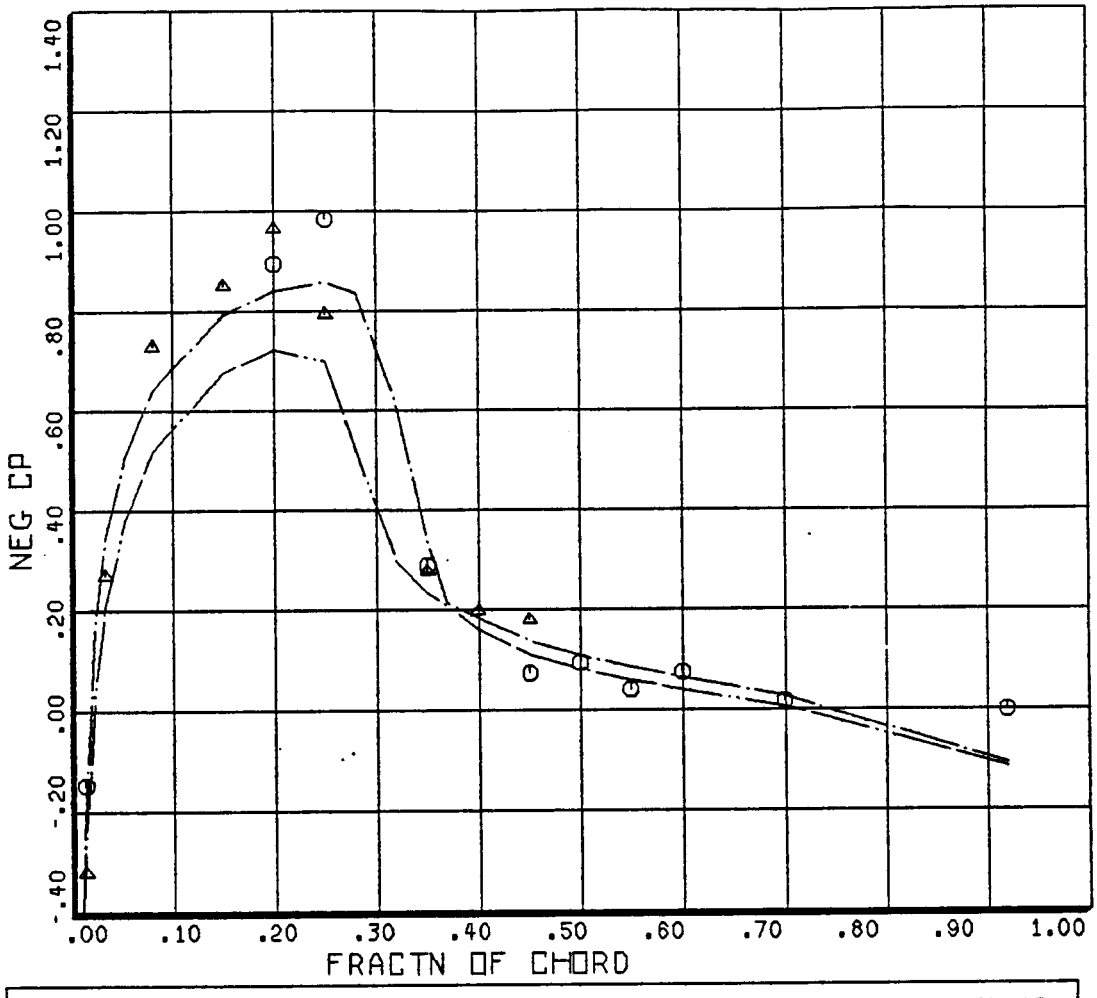

⊙ ⊙ ⊙ DERIVED PARAMETER:	COUNTER .97	2873 R/RADIUS BLADE STATIC PRESSURE COEFF	GROSS WT LONG CG	SHIP MODEL AH-1G UPPER SURFACE
△ △ △ DERIVED PARAMETER:	COUNTER .97	2873 R/RADIUS BLADE STATIC PRESSURE COEFF	GROSS WT LONG CG	SHIP MODEL AH-1G LOWER SURFACE
CYCLE AVERAGE:	COUNTER .97	344575 R/RADIUS LOCAL NEG CP: ROT22	GROSS WT 8050 LONG CG	SHIP MODEL OLSAH1 UPPER SURFACE
CYCLE AVERAGE:	COUNTER .97	344575 R/RADIUS LOCAL NEG CP: ROT22	GROSS WT 8050 LONG CG	SHIP MODEL OLSAH1 LOWER SURFACE

BHT,USARTL DATAMAP (VERS 3.10 - 24/02/82) 04/26/83 BELL HELICOPTER

Figure 28. Sectional pressure coefficient at 97% radius for Record 2873 (modified twist).

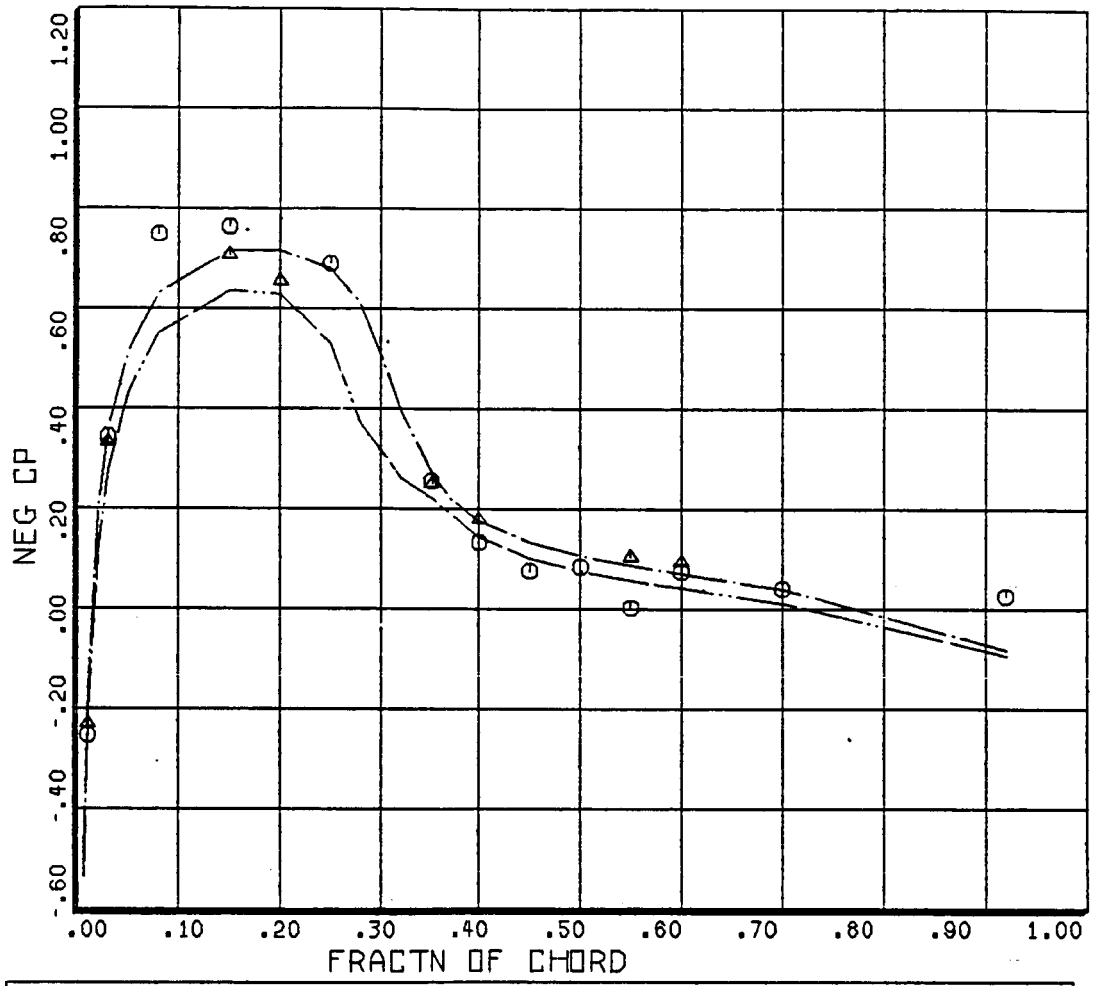

⊙ ⊙ ⊙	COUNTER .99	2873 R/RADIUS	GROSS WT LONG CG	SHIP MODEL AH-1G UPPER SURFACE
DERIVED PARAMETER:		BLADE STATIC PRESSURE COEFF		
△ △ △	COUNTER .99	2873 R/RADIUS	GROSS WT LONG CG	SHIP MODEL AH-1G LOWER SURFACE
DERIVED PARAMETER:		BLADE STATIC PRESSURE COEFF		
——·——·——	COUNTER .99	344575 R/RADIUS	GROSS WT 8050 LONG CG	SHIP MODEL OLSAH1 UPPER SURFACE
CYCLE AVERAGE:		LOCAL NEG CP: ROT22		
——·——·——	COUNTER .99	344575 R/RADIUS	GROSS WT 8050 LONG CG	SHIP MODEL OLSAH1 LOWER SURFACE
CYCLE AVERAGE:		LOCAL NEG CP: ROT22		

BHT.USARTL DATAMAP (VERS 3.10 - 24/02/82) 04/26/83 BELL HELICOPTER

Figure 29. Sectional pressure coefficient at 99% radius for Record 2873 (modified twist).

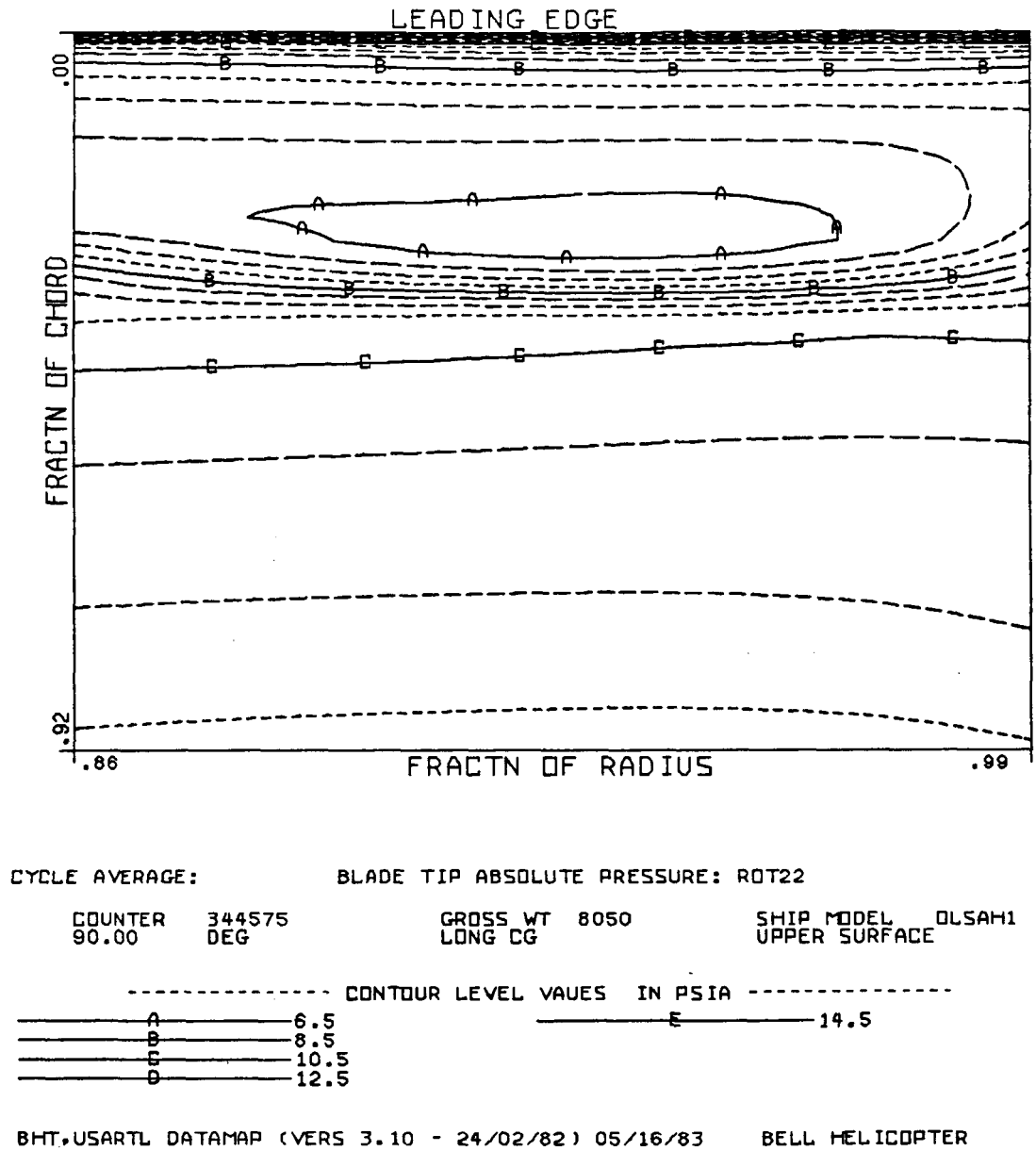

Figure 30. ROT22 blade tip pressure contours for Record 2873 (upper surface).

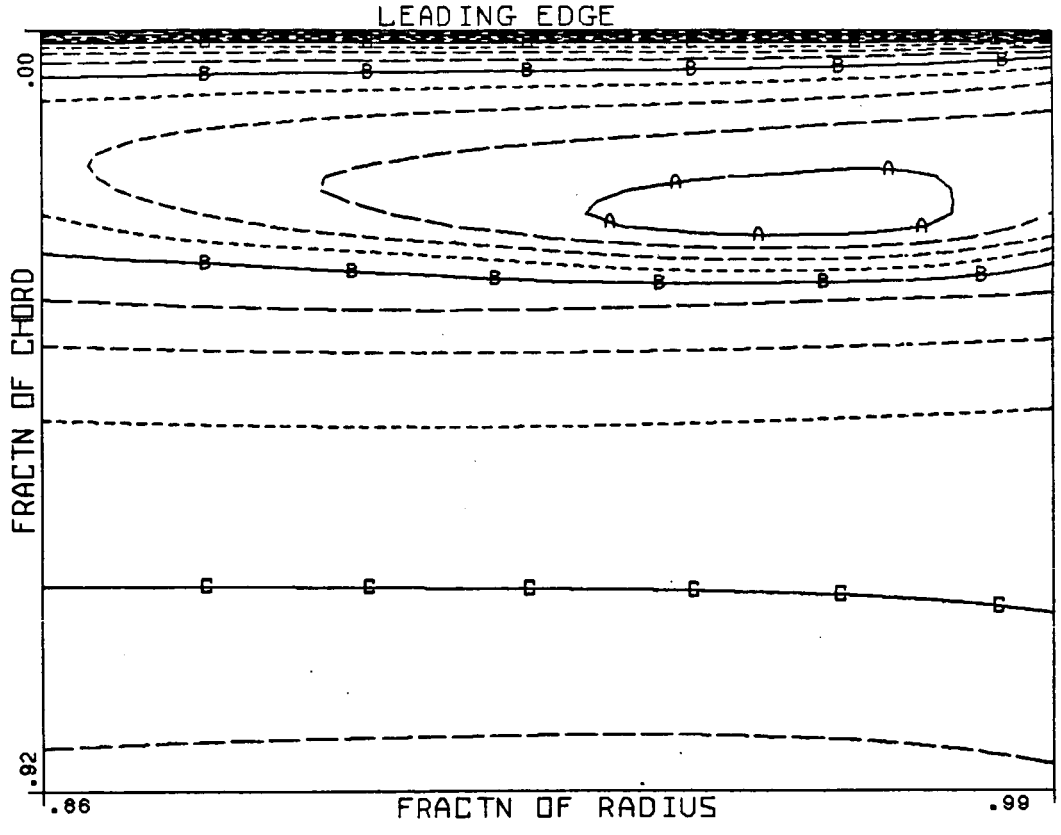

Figure 31. ROT22 blade tip pressure contours for Record 2873 (lower surface).

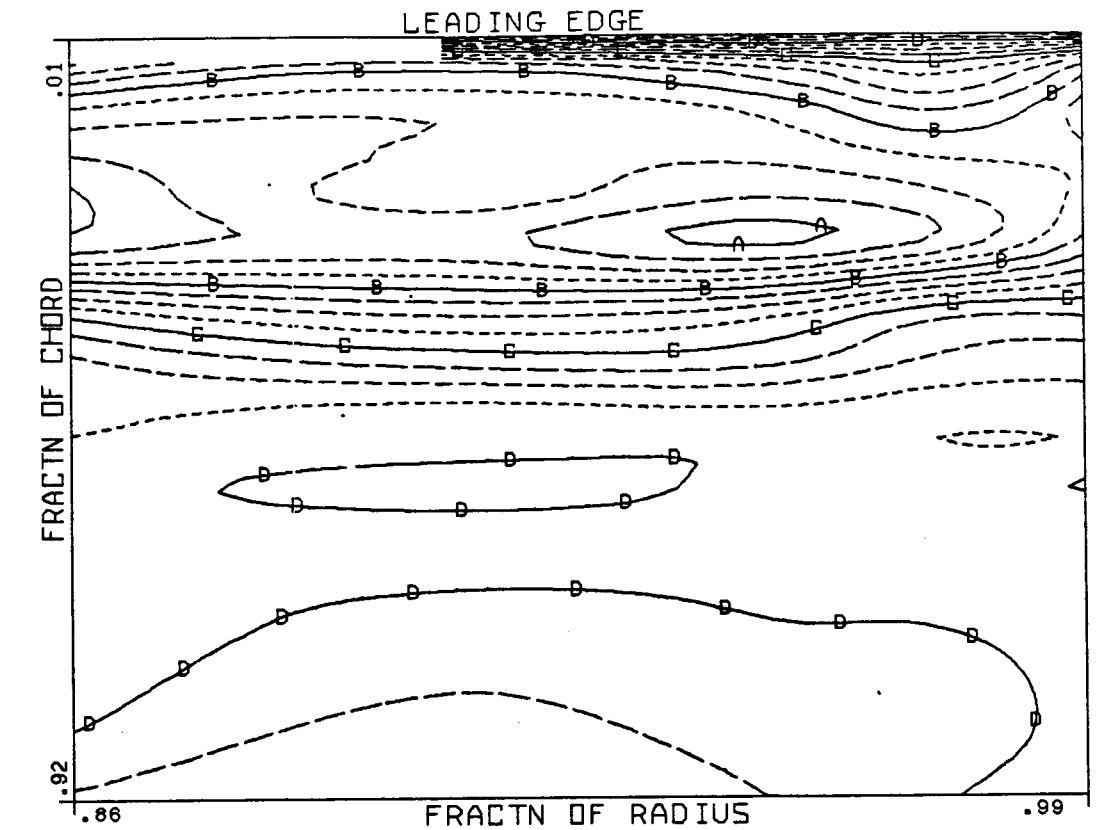

Figure 32. Flight test blade tip pressure contours for Record 2873 (upper surface).

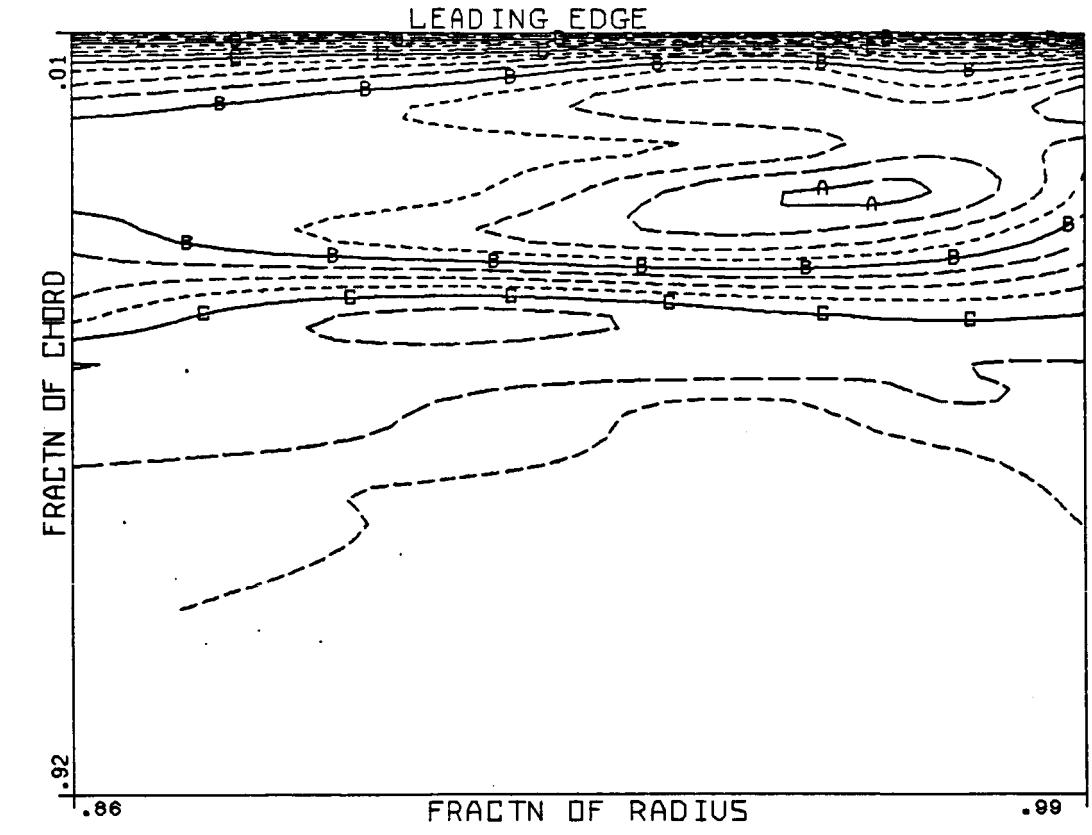

Figure 33. Flight test blade tip pressure contours for Record 2873 (lower surface).

after modifying the tip region twist input to ROT22 are compared with those from test data in Figure 34. As in the case of Record 2872, the agreement becomes worse when compared to the results shown in Figure 3.

Record 2806

The results here are presented for an azimuth angle of 60° in a manner identical to the preceding records. In other words, sectional pressure coefficients from ROT22 program are first provided in Figures 35 through 39. The twist input to ROT22 is then modified to improve pressure coefficient correlation in the tip region. The ensuing results are then provided in Figures 40 through 46. While Figures 40 through 44 provide the sectional pressure coefficients, Figures 45 and 46 provide computed surface pressure contours. These may be compared with the measured surface pressure contours provided in Figures 47 and 48. Finally, the normal force coefficients calculated from ROT22 results are compared with measurements in Figure 49.

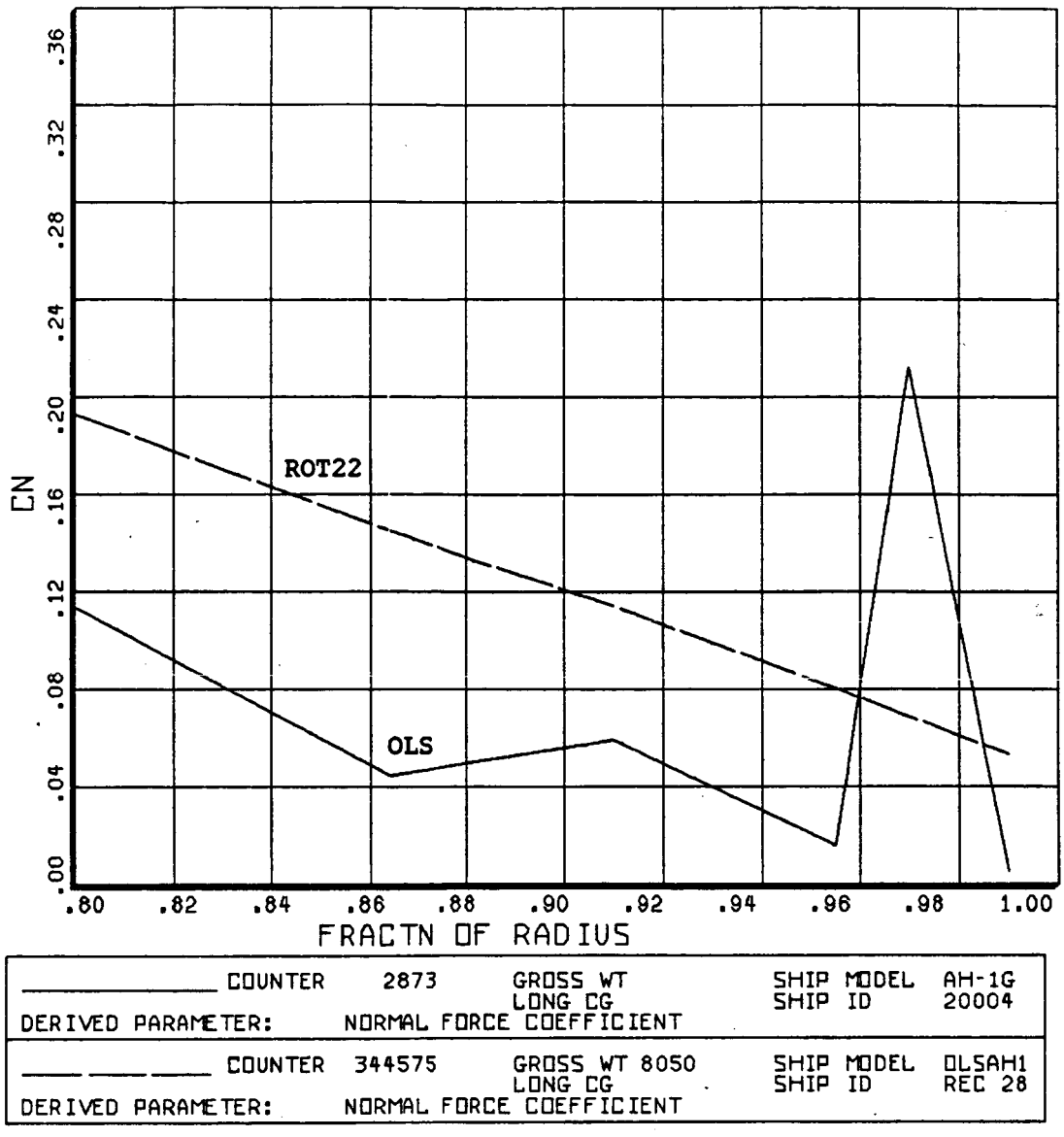

BHT,USARTL DATAMAP (VERS 3.10 - 24/02/82) 05/17/83 BELL HELICOPTER

Figure 34. Normal force coefficient for Record 2873 (modified twist).

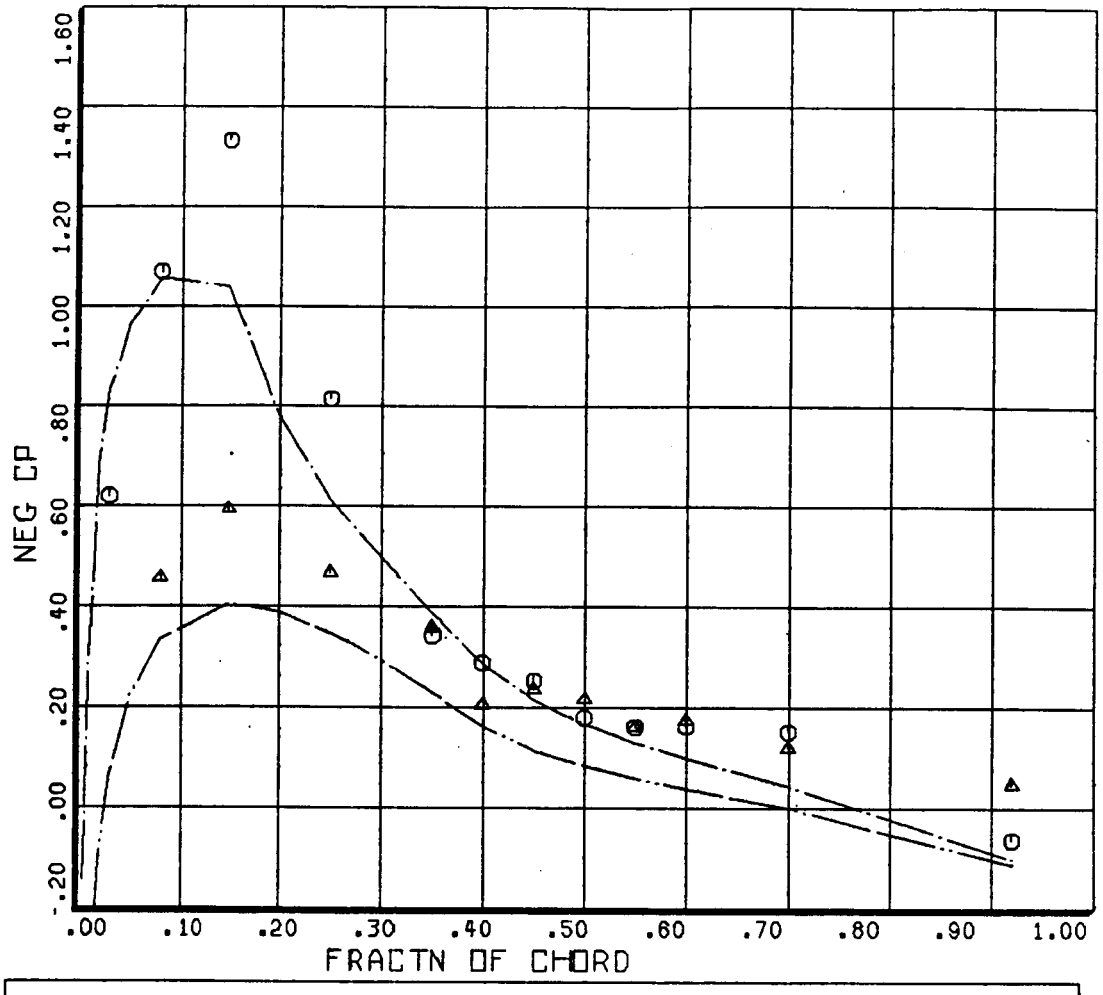

⊖ ⊖ ⊖ DERIVED PARAMETER:	COUNTER .86 R/RADIUS BLADE STATIC PRESSURE COEFF	2806 LONG CG	GROSS WT SHIP MODEL AH-1G UPPER SURFACE
▲ ▲ ▲ DERIVED PARAMETER:	COUNTER .86 R/RADIUS BLADE STATIC PRESSURE COEFF	2806 LONG CG	GROSS WT SHIP MODEL AH-1G LOWER SURFACE
CYCLE AVERAGE:	COUNTER .86 R/RADIUS LOCAL NEG CP: ROT22	523565 LONG CG	GROSS WT 8100 SHIP MODEL OLSAH1 UPPER SURFACE
CYCLE AVERAGE:	COUNTER .86 R/RADIUS LOCAL NEG CP: ROT22	523565 LONG CG	GROSS WT 8100 SHIP MODEL OLSAH1 LOWER SURFACE

BHT.USARTL DATAMAP (VERS 3.10 - 24/02/82) 04/16/83 BELL HELICOPTER

Figure 35. Sectional pressure coefficient at 86% radius for Record 2806.

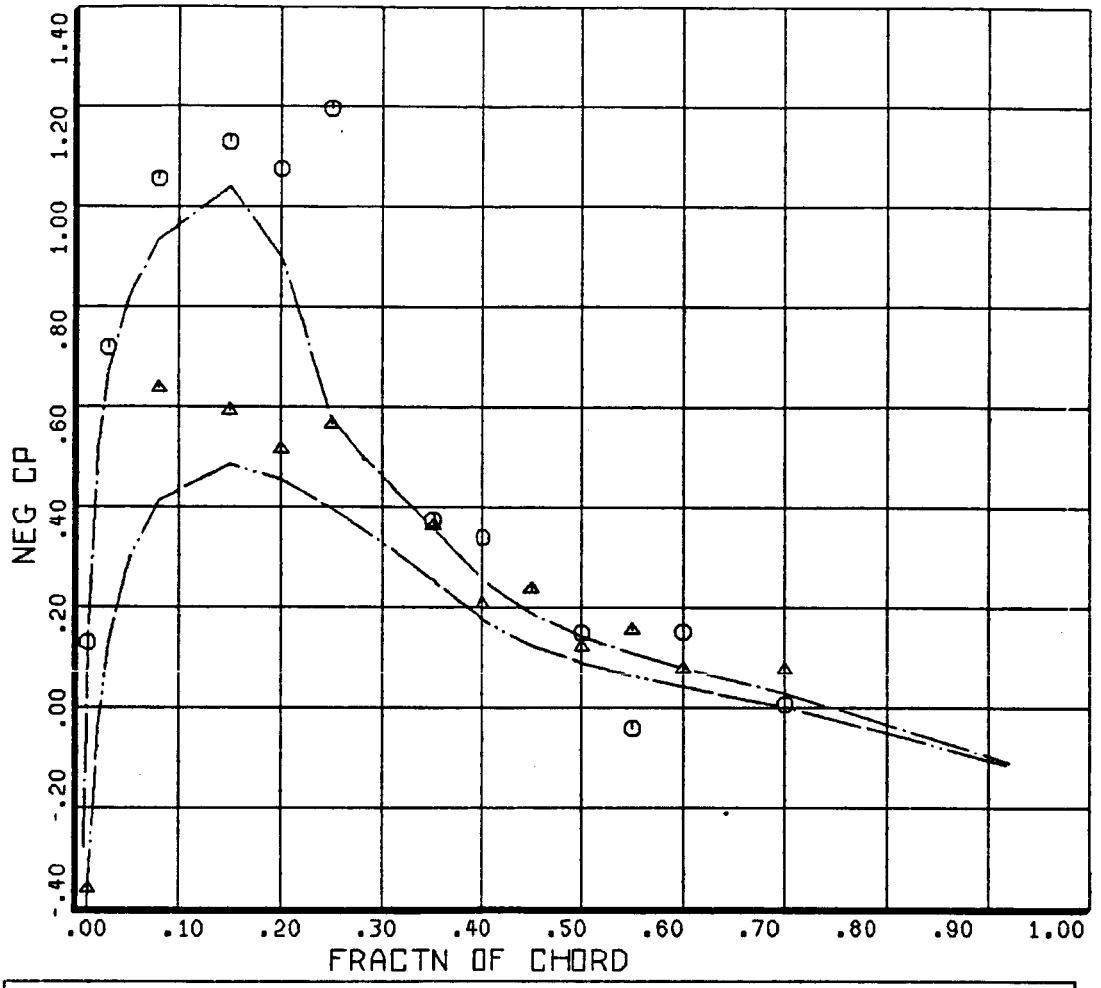

⊙ ⊙ ⊙	COUNTER 2806	GROSS WT	SHIP MODEL AH-1G
	.91 R/RADIUS	LONG CG	UPPER SURFACE
DERIVED PARAMETER:	BLADE STATIC PRESSURE COEFF		
△ △ △	COUNTER 2806	GROSS WT	SHIP MODEL AH-1G
	.91 R/RADIUS	LONG CG	LOWER SURFACE
DERIVED PARAMETER:	BLADE STATIC PRESSURE COEFF		
——·——·——	COUNTER 523565	GROSS WT 8100	SHIP MODEL OLSAH1
	.91 R/RADIUS	LONG CG	UPPER SURFACE
CYCLE AVERAGE:	LOCAL NEG CP: ROT22		
——·——·——	COUNTER 523565	GROSS WT 8100	SHIP MODEL OLSAH1
	.91 R/RADIUS	LONG CG	LOWER SURFACE
CYCLE AVERAGE:	LOCAL NEG CP: ROT22		

BHT.USARTL DATAMAP (VERS 3.10 - 24/02/82) 04/16/83 BELL HELICOPTER

Figure 36. Sectional pressure coefficient at 91% radius for Record 2806.

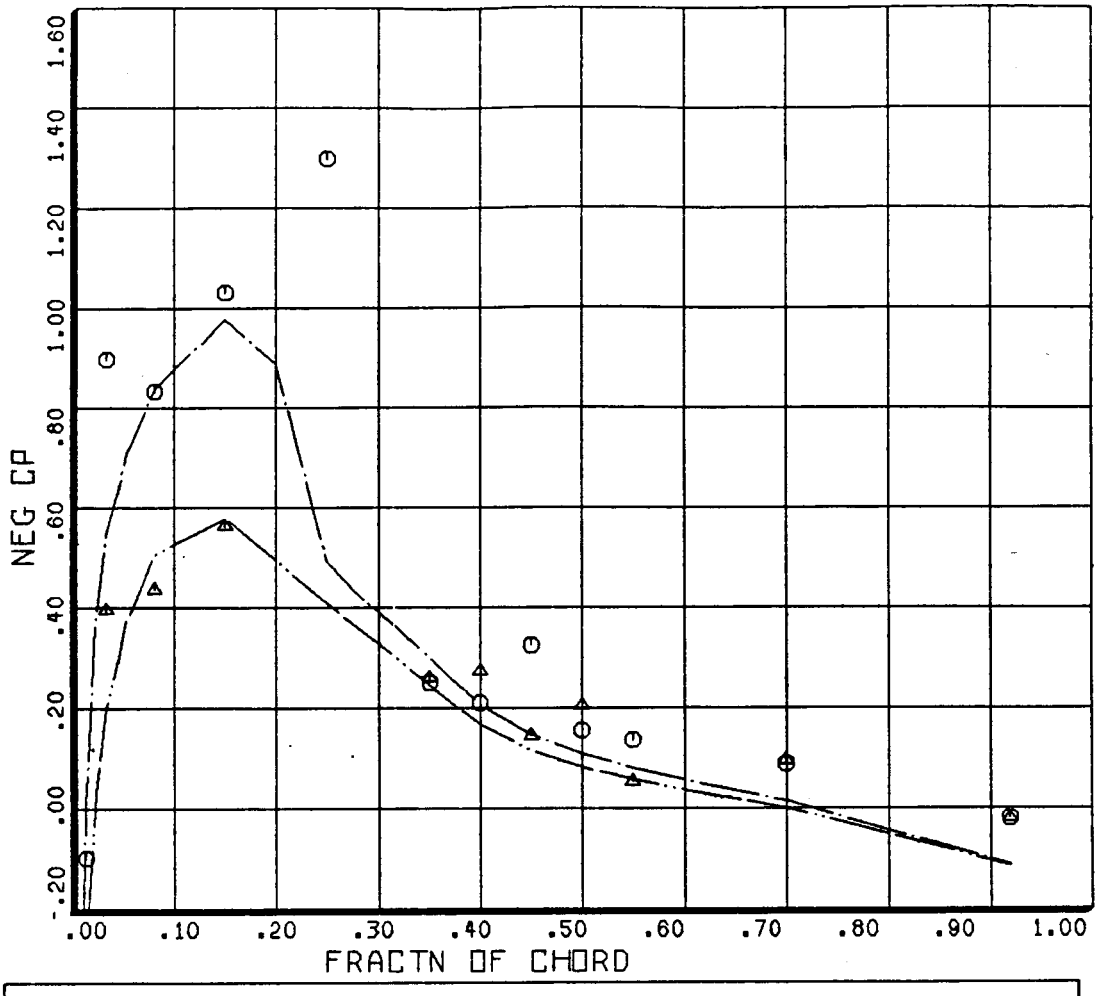

⏲ ⏲ ⏲	COUNTER .95	2806 R/RADIUS	GROSS WT LONG CG	SHIP MODEL AH-1G UPPER SURFACE
DERIVED PARAMETER:		BLADE STATIC PRESSURE COEFF		
△ △ △	COUNTER .95	2806 R/RADIUS	GROSS WT LONG CG	SHIP MODEL AH-1G LOWER SURFACE
DERIVED PARAMETER:		BLADE STATIC PRESSURE COEFF		
——·——·——	COUNTER .95	523565 R/RADIUS	GROSS WT 8100 LONG CG	SHIP MODEL OLSAH1 UPPER SURFACE
CYCLE AVERAGE:		LOCAL NEG CP: ROT22		
——·——·——	COUNTER .95	523565 R/RADIUS	GROSS WT 8100 LONG CG	SHIP MODEL OLSAH1 LOWER SURFACE
CYCLE AVERAGE:		LOCAL NEG CP: ROT22		

BHT,USARTL DATAMAP (VERS 3.10 - 24/02/82) 04/16/83 BELL HELICOPTER

Figure 37. Sectional pressure coefficient at 95% radius for Record 2806.

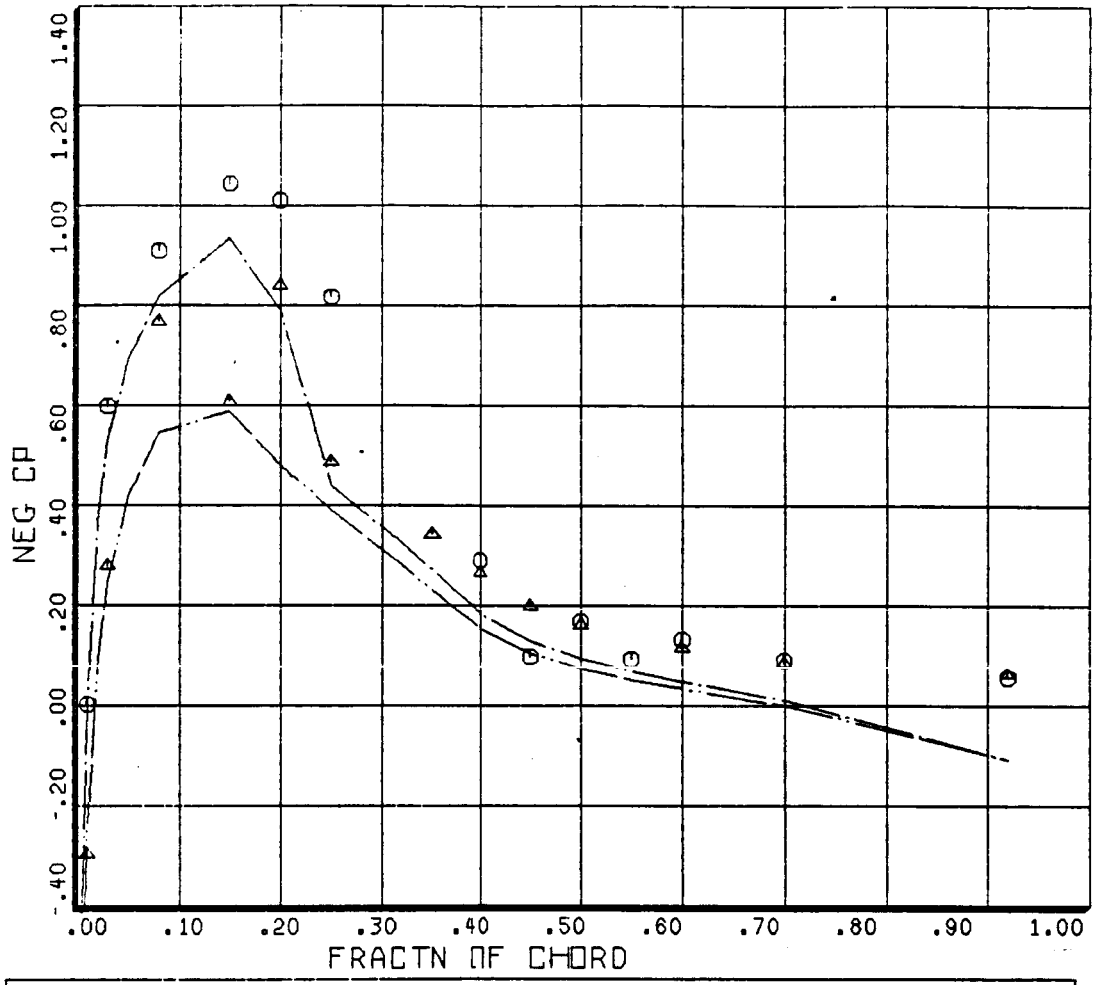

⏲ ⏲ ⏲ DERIVED PARAMETER:	COUNTER .97 R/RADIUS BLADE STATIC PRESSURE COEFF	2806 GROSS WT LONG CG	SHIP MODEL AH-1G UPPER SURFACE
△ △ △ DERIVED PARAMETER:	COUNTER .97 R/RADIUS BLADE STATIC PRESSURE COEFF	2806 GROSS WT LONG CG	SHIP MODEL AH-1G LOWER SURFACE
CYCLE AVERAGE:	COUNTER .97 R/RADIUS LOCAL NEG CP: ROT22	523565 GROSS WT 8100 LONG CG	SHIP MODEL OLSAH1 UPPER SURFACE
CYCLE AVERAGE:	COUNTER .97 R/RADIUS LOCAL NEG CP: ROT22	523565 GROSS WT 8100 LONG CG	SHIP MODEL OLSAH1 LOWER SURFACE

BHT.USARTL DATAMAP (VERS 3.10 - 24/02/82) 04/25/83 BELL HELICOPTER

Figure 38. Sectional pressure coefficient at 97% radius for Record 2806.

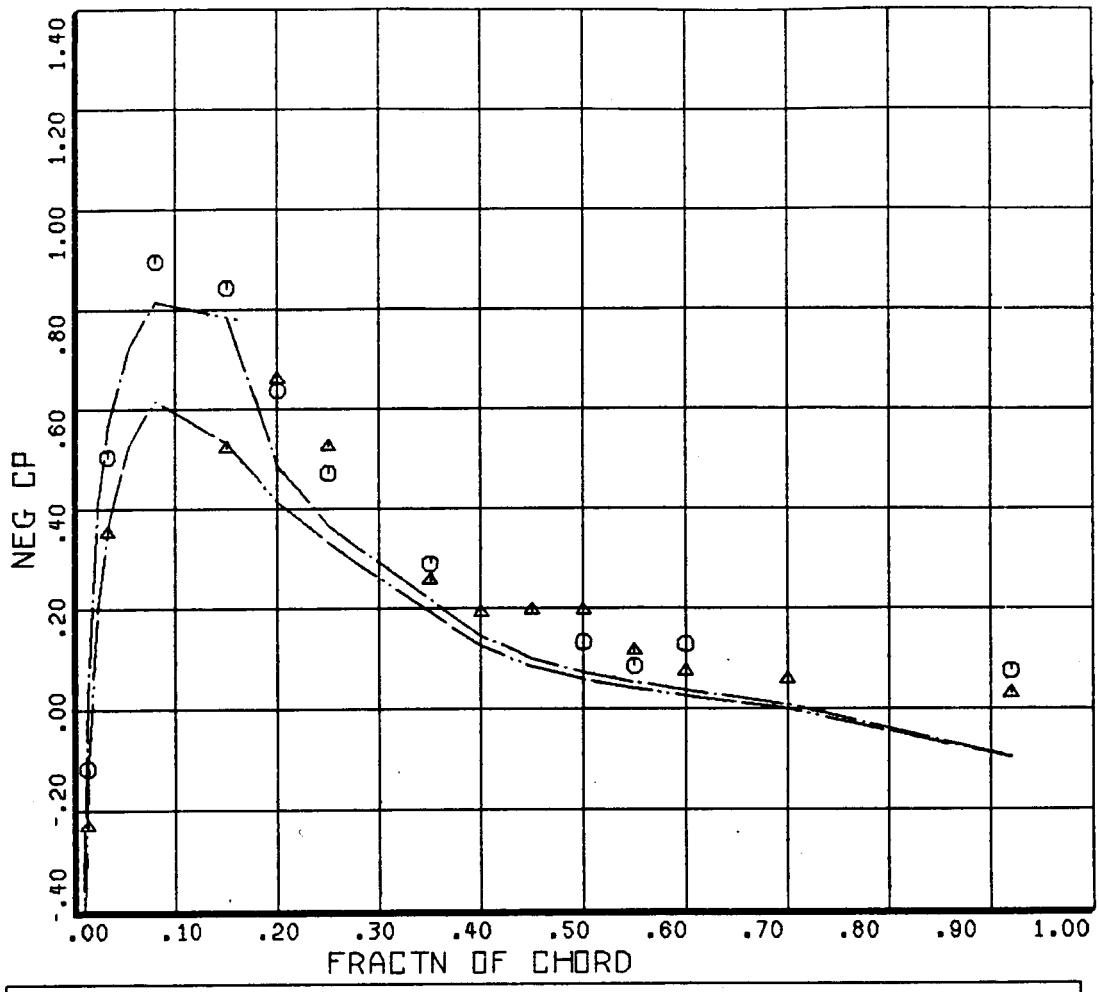

⊙ ⊙ ⊙ DERIVED PARAMETER:	COUNTER .99 BLADE STATIC PRESSURE COEFF	2806 R/RADIUS	GROSS WT LONG CG	SHIP MODEL AH-1G UPPER SURFACE
△ △ △ DERIVED PARAMETER:	COUNTER .99 BLADE STATIC PRESSURE COEFF	2806 R/RADIUS	GROSS WT LONG CG	SHIP MODEL AH-1G LOWER SURFACE
CYCLE AVERAGE:	COUNTER .99 LOCAL NEG CP: ROT22	523565 R/RADIUS	GROSS WT 8100 LONG CG	SHIP MODEL OLSAH1 UPPER SURFACE
CYCLE AVERAGE:	COUNTER .99 LOCAL NEG CP: ROT22	523565 R/RADIUS	GROSS WT 8100 LONG CG	SHIP MODEL OLSAH1 LOWER SURFACE

BHT.USARTL DATAMAP (VERS 3.10 - 24/02/82) 04/16/83 BELL HELICOPTER

Figure 39. Sectional pressure coefficient at 99% radius for Record 2806.

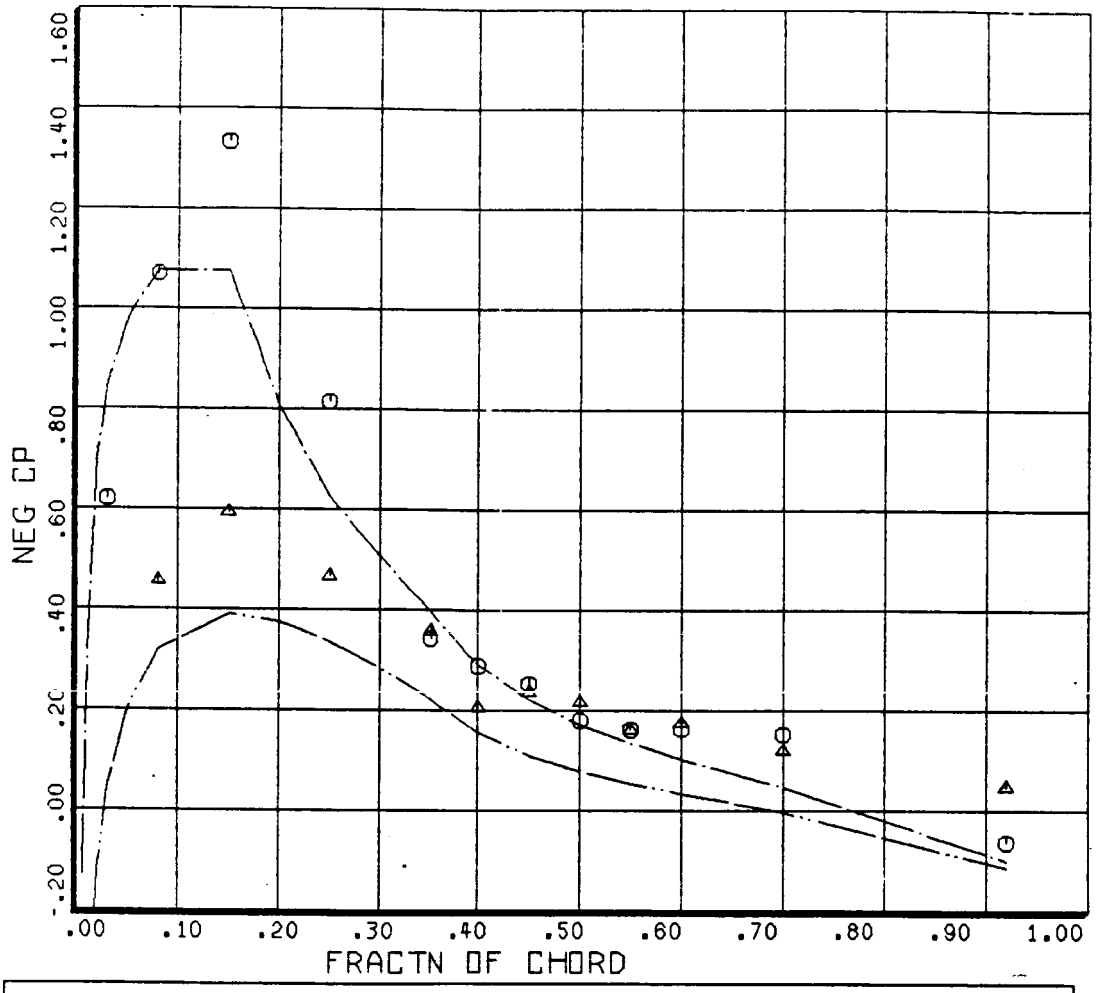

⊙ ⊙ ⊙ DERIVED PARAMETER:	COUNTER .86 BLADE STATIC	2806 R/RADIUS PRESSURE COEFF	GROSS WT LONG CG	SHIP MODEL AH-1G UPPER SURFACE
△ △ △ DERIVED PARAMETER:	COUNTER .86 BLADE STATIC	2806 R/RADIUS PRESSURE COEFF	GROSS WT LONG CG	SHIP MODEL AH-1G LOWER SURFACE
CYCLE AVERAGE:	COUNTER .86 LOCAL NEG CP:	273480 R/RADIUS ROT22	GROSS WT 8100 LONG CG	SHIP MODEL OLSAH1 UPPER SURFACE
CYCLE AVERAGE:	COUNTER .86 LOCAL NEG CP:	273480 R/RADIUS ROT22	GROSS WT 8100 LONG CG	SHIP MODEL OLSAH1 LOWER SURFACE

BHT.USARTL DATAMAP (VERS 3.10 - 24/02/82) 04/25/83 BELL HELICOPTER

Figure 40. Sectional pressure coefficient at 86% radius for Record 2806 (modified twist).

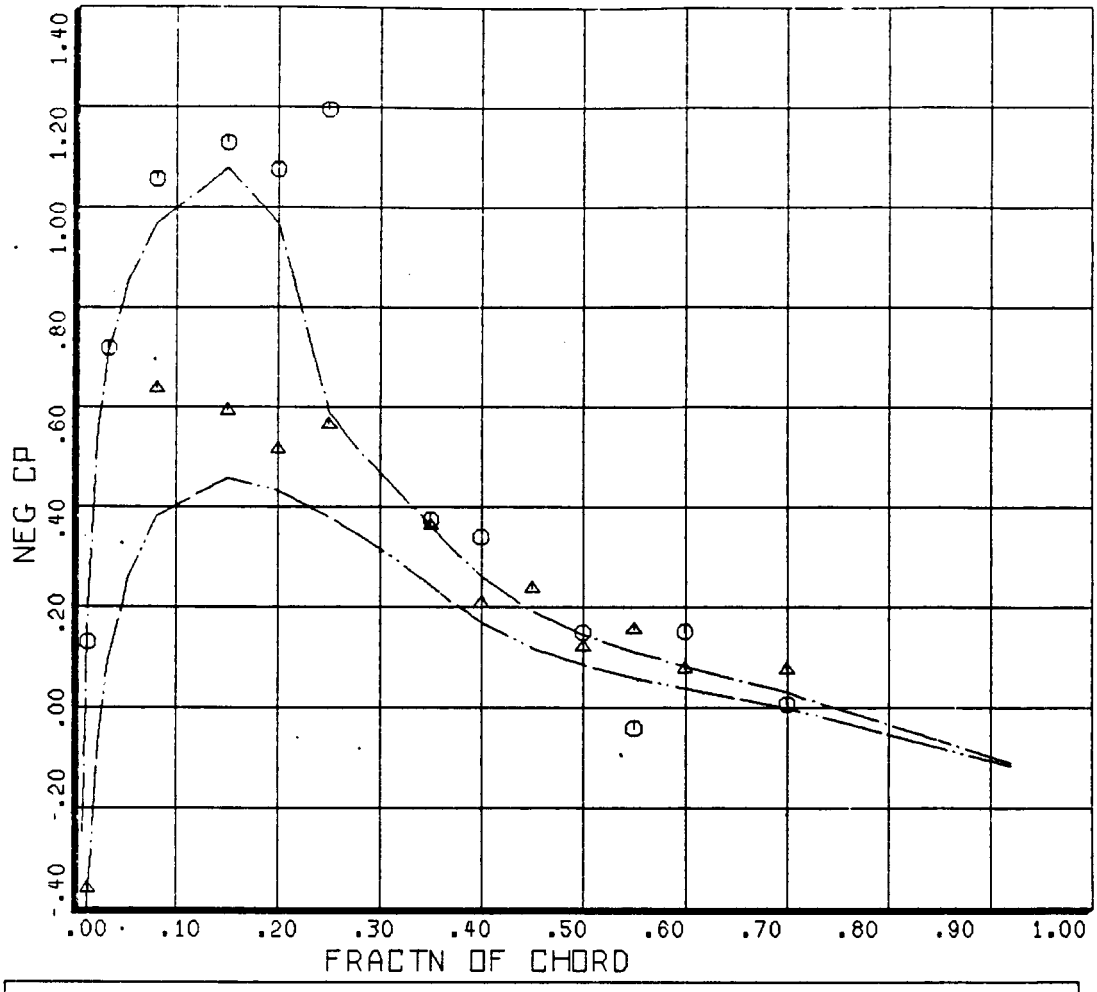

Figure 41. Sectional pressure coefficient at 91% radius for Record 2806 (modified twist).

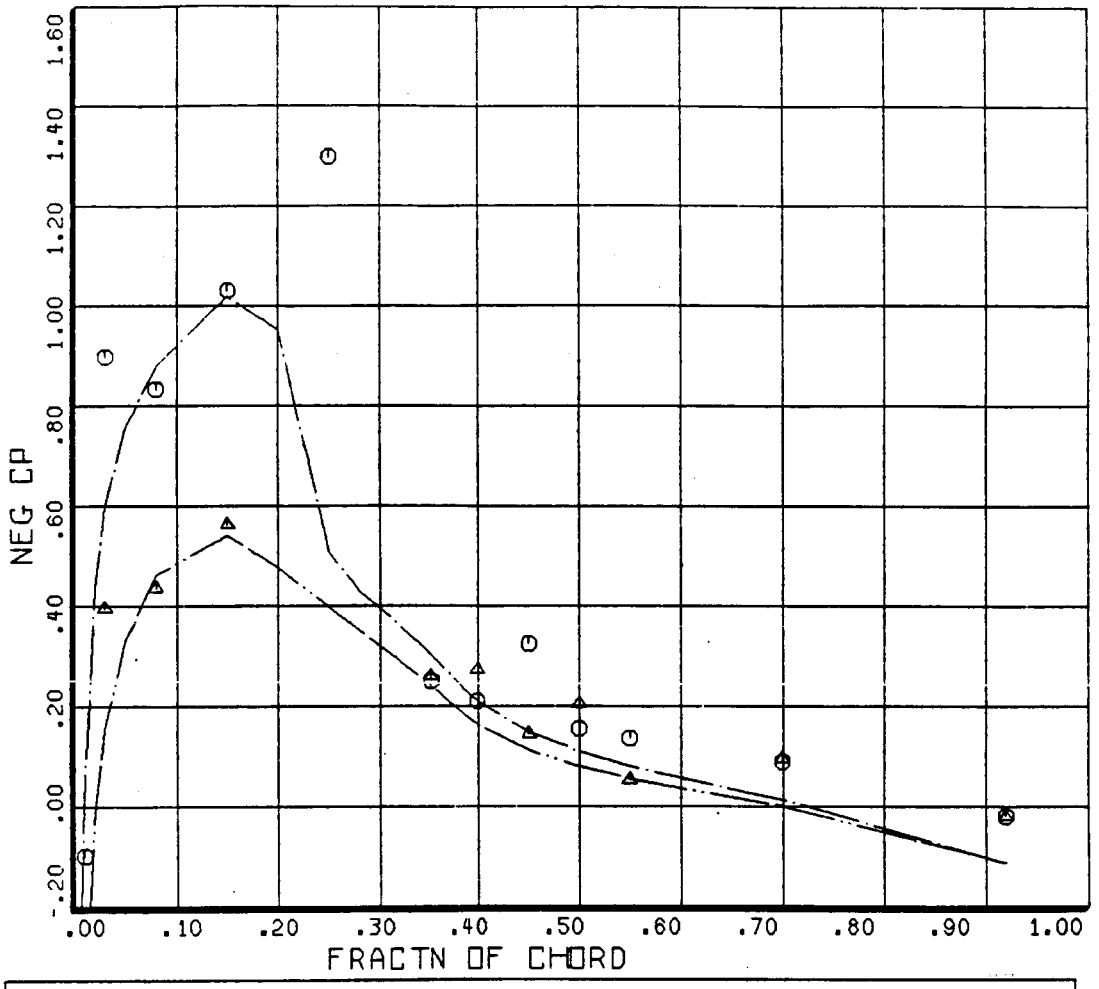

⏲ ⏲ ⏲ DERIVED PARAMETER:	COUNTER .95 BLADE STATIC PRESSURE COEFF	2806 R/RADIUS	GROSS WT LONG CG	SHIP MODEL AH-1G UPPER SURFACE
△ △ △ DERIVED PARAMETER:	COUNTER .95 BLADE STATIC PRESSURE COEFF	2806 R/RADIUS	GROSS WT LONG CG	SHIP MODEL AH-1G LOWER SURFACE
——— ——— CYCLE AVERAGE:	COUNTER .95 LOCAL NEG CP: ROT22	273480 R/RADIUS	GROSS WT 8100 LONG CG	SHIP MODEL OLSAH1 UPPER SURFACE
——— --- CYCLE AVERAGE:	COUNTER .95 LOCAL NEG CP: ROT22	273480 R/RADIUS	GROSS WT 8100 LONG CG	SHIP MODEL OLSAH1 LOWER SURFACE

BHT.USARTL DATAMAP (VERS 3.10 - 24/02/82) 04/25/83 BELL HELICOPTER

Figure 42. Sectional pressure coefficient at 95% radius for Record 2806 (modified twist).

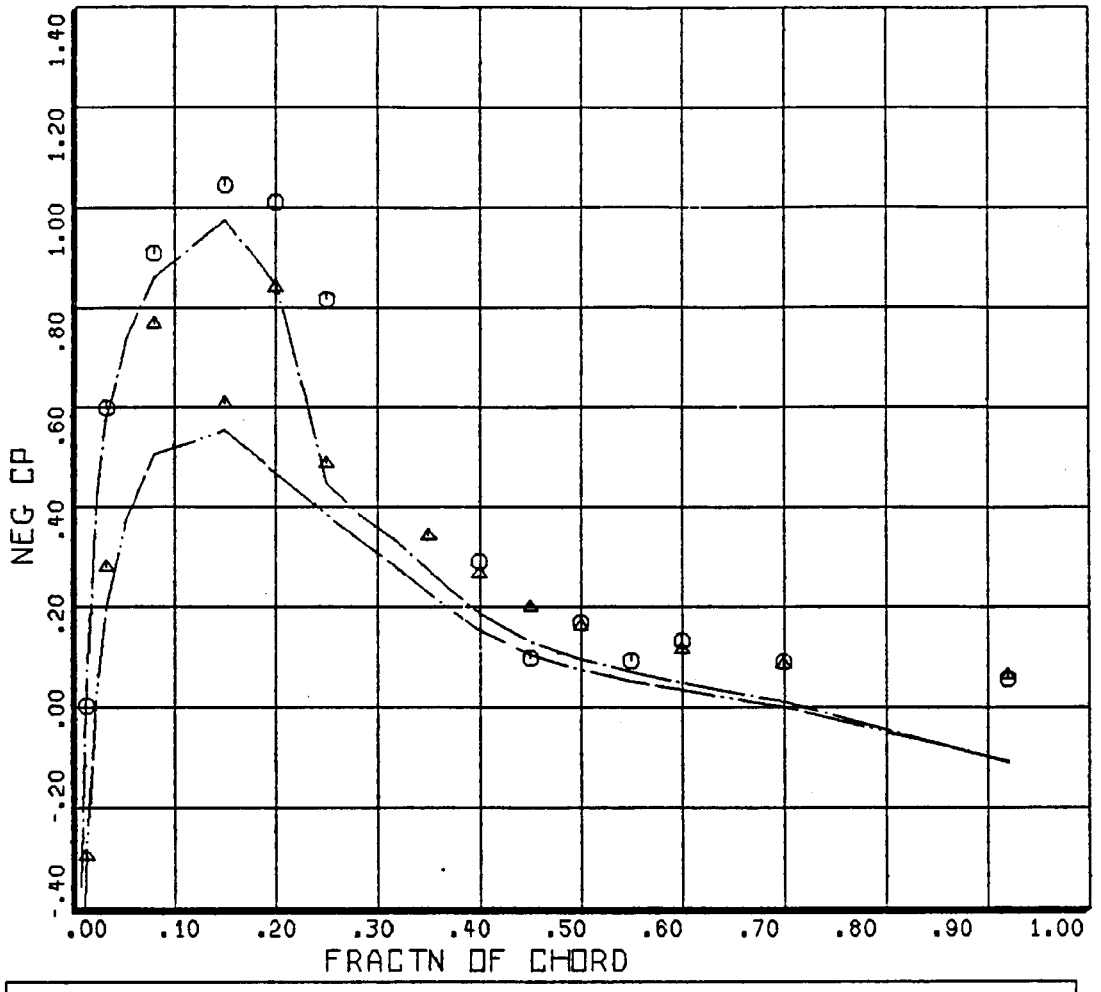

⏲ ⏲ ⏲	COUNTER 2806	GROSS WT	SHIP MODEL AH-1G
	.97 R/RADIUS	LONG CG	UPPER SURFACE
DERIVED PARAMETER:	BLADE STATIC PRESSURE COEFF		
△ △ △	COUNTER 2806	GROSS WT	SHIP MODEL AH-1G
	.97 R/RADIUS	LONG CG	LOWER SURFACE
DERIVED PARAMETER:	BLADE STATIC PRESSURE COEFF		
——·——·——	COUNTER 273480	GROSS WT 8100	SHIP MODEL OLSAH1
	.97 R/RADIUS	LONG CG	UPPER SURFACE
CYCLE AVERAGE:	LOCAL NEG CP: ROT22		
——·——·——	COUNTER 273480	GROSS WT 8100	SHIP MODEL OLSAH1
	.97 R/RADIUS	LONG CG	LOWER SURFACE
CYCLE AVERAGE:	LOCAL NEG CP: ROT22		

BHT,USARTL DATAMAP (VERS 3.10 - 24/02/82) 04/26/83 BELL HELICOPTER

Figure 43. Sectional pressure coefficient at 97% radius for Record 2806 (modified twist).

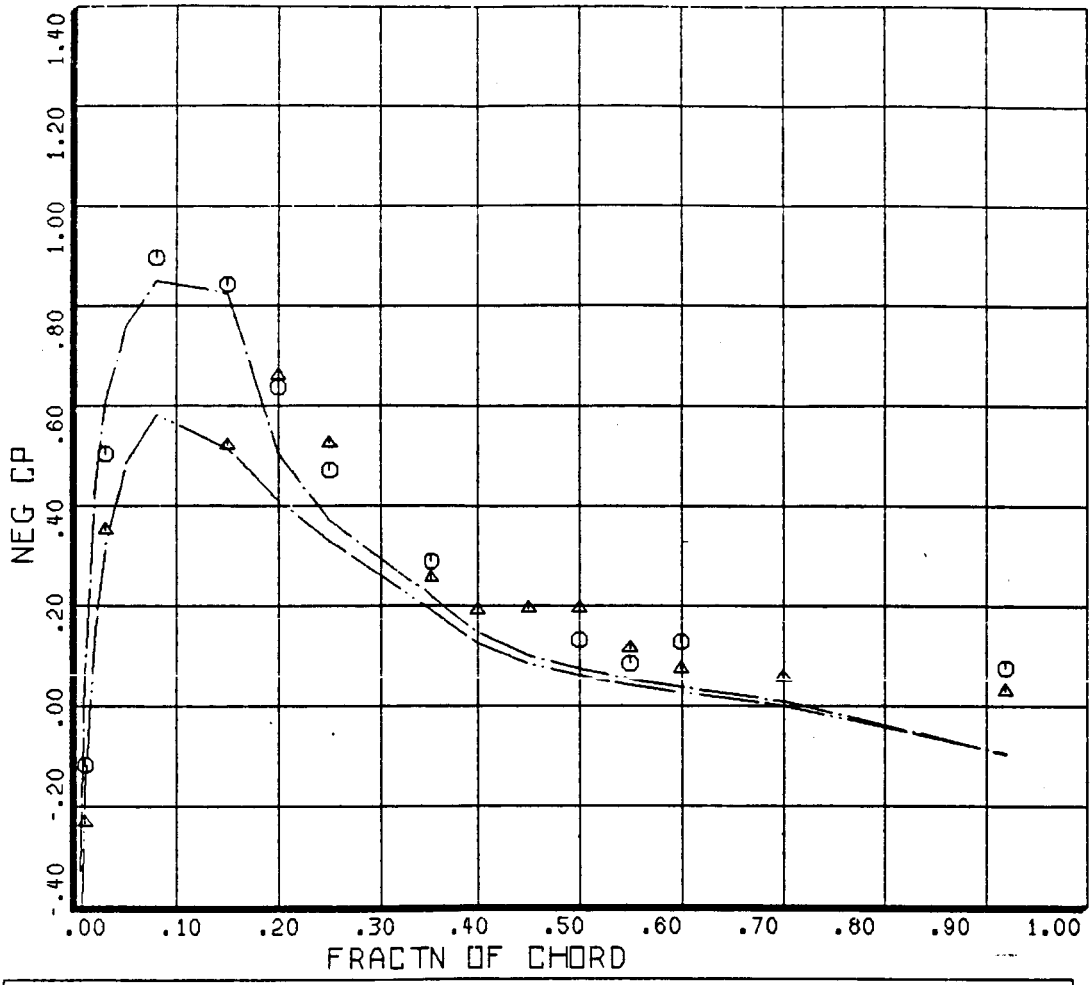

⏲ ⏲ ⏲ DERIVED PARAMETER:	COUNTER .99 BLADE STATIC	2806 R/RADIUS PRESSURE COEFF	GROSS WT LONG CG	SHIP MODEL AH-1G UPPER SURFACE
△ △ △ DERIVED PARAMETER:	COUNTER .99 BLADE STATIC	2806 R/RADIUS PRESSURE COEFF	GROSS WT LONG CG	SHIP MODEL AH-1G LOWER SURFACE
——— CYCLE AVERAGE:	COUNTER .99 LOCAL NEG CP:	273480 R/RADIUS ROT22	GROSS WT 8100 LONG CG	SHIP MODEL OLSAH1 UPPER SURFACE
——·——·—— CYCLE AVERAGE:	COUNTER .99 LOCAL NEG CP:	273480 R/RADIUS ROT22	GROSS WT 8100 LONG CG	SHIP MODEL OLSAH1 LOWER SURFACE

BHT.USARTL DATAMAP (VERS 3.10 - 24/02/82) 04/25/83 BELL HELICOPTER

Figure 44. Sectional pressure coefficient at 99% radius for Record 2806 (modified twist).

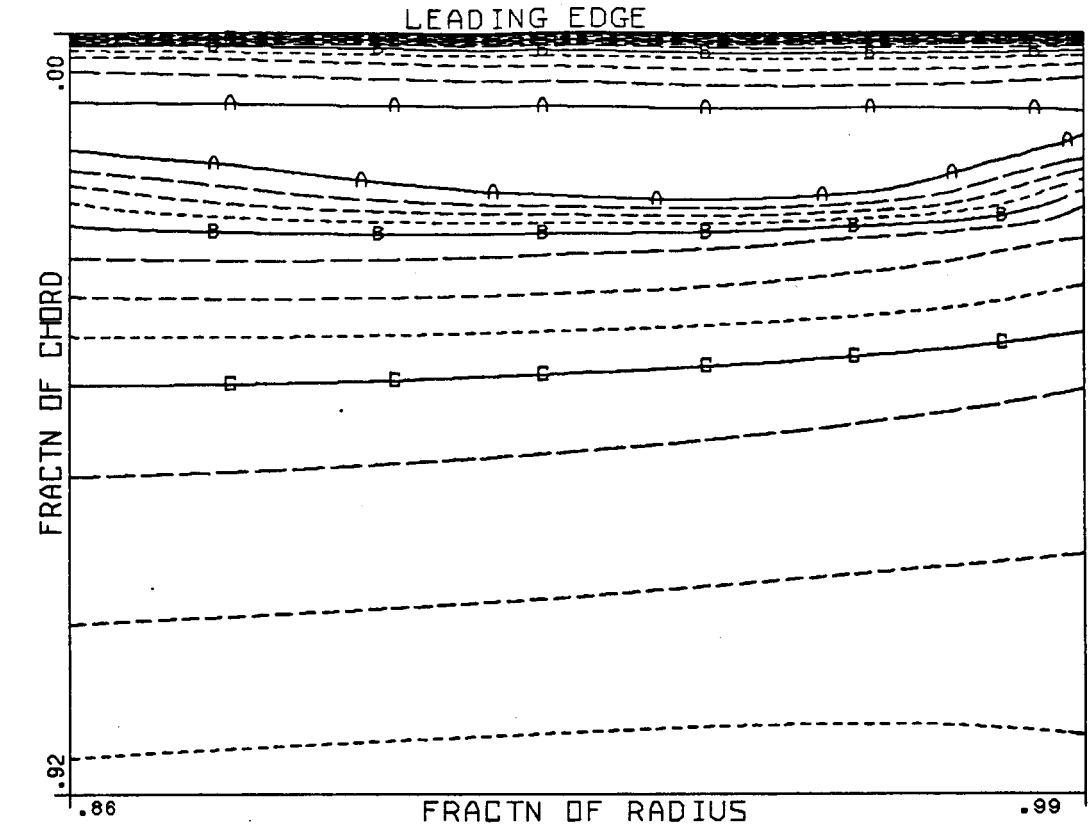

Figure 45. ROT22 blade tip pressure contours for Record 2806 (upper surface).

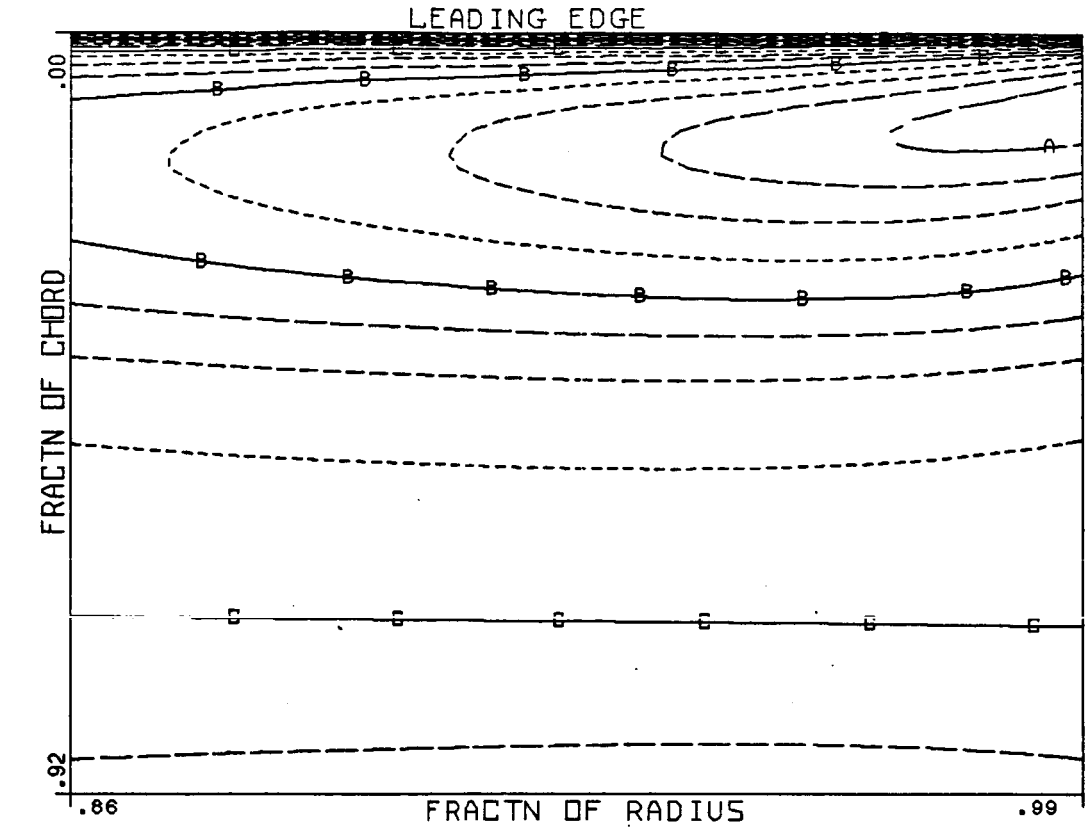

Figure 46. ROT22 blade tip pressure contours for Record 2806 (lower surface).

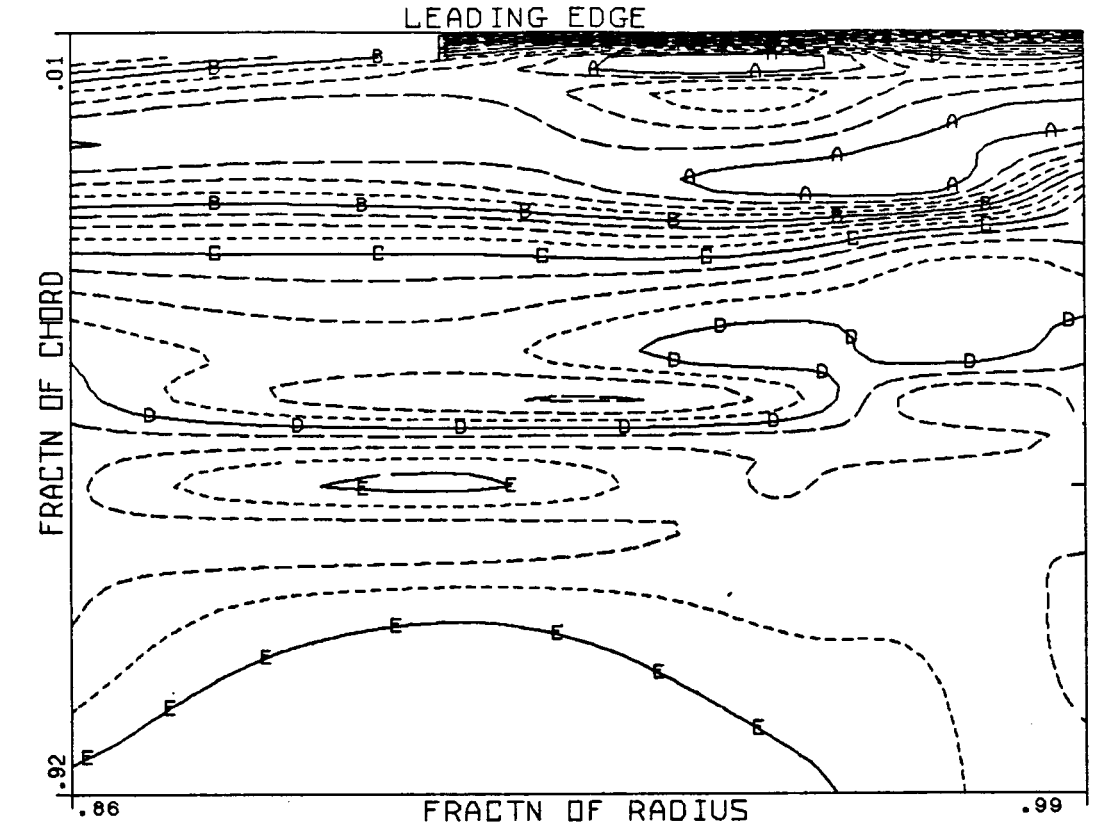

Figure 47. Flight test blade tip pressure contours for Record 2806 (upper surface).

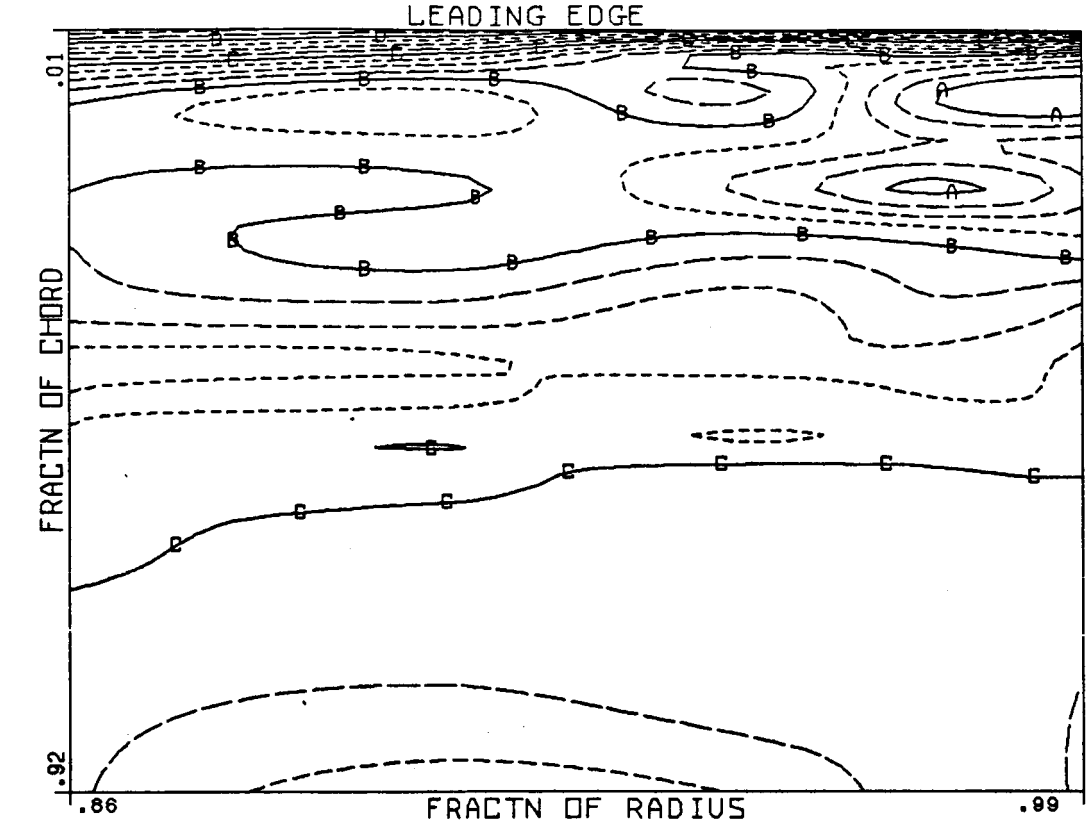

CYCLE AVERAGE: BLADE TIP ABSOLUTE PRESSURE, 180 DEG AZIMUTH CHANGE

COUNTER 2806 GROSS WT SHIP MODEL AH-1G
60.00 DEG LONG CG LOWER SURFACE

---------- CONTOUR LEVEL VAUES IN PSIA ----------

A 8.5
B 10.5
C 12.5
D 14.5

BHT,USARTL DATAMAP (VERS 3.10 - 24/02/82) 05/16/83 BELL HELICOPTER

Figure 48. Flight test blade tip pressure contours for Record 2806 (lower surface).

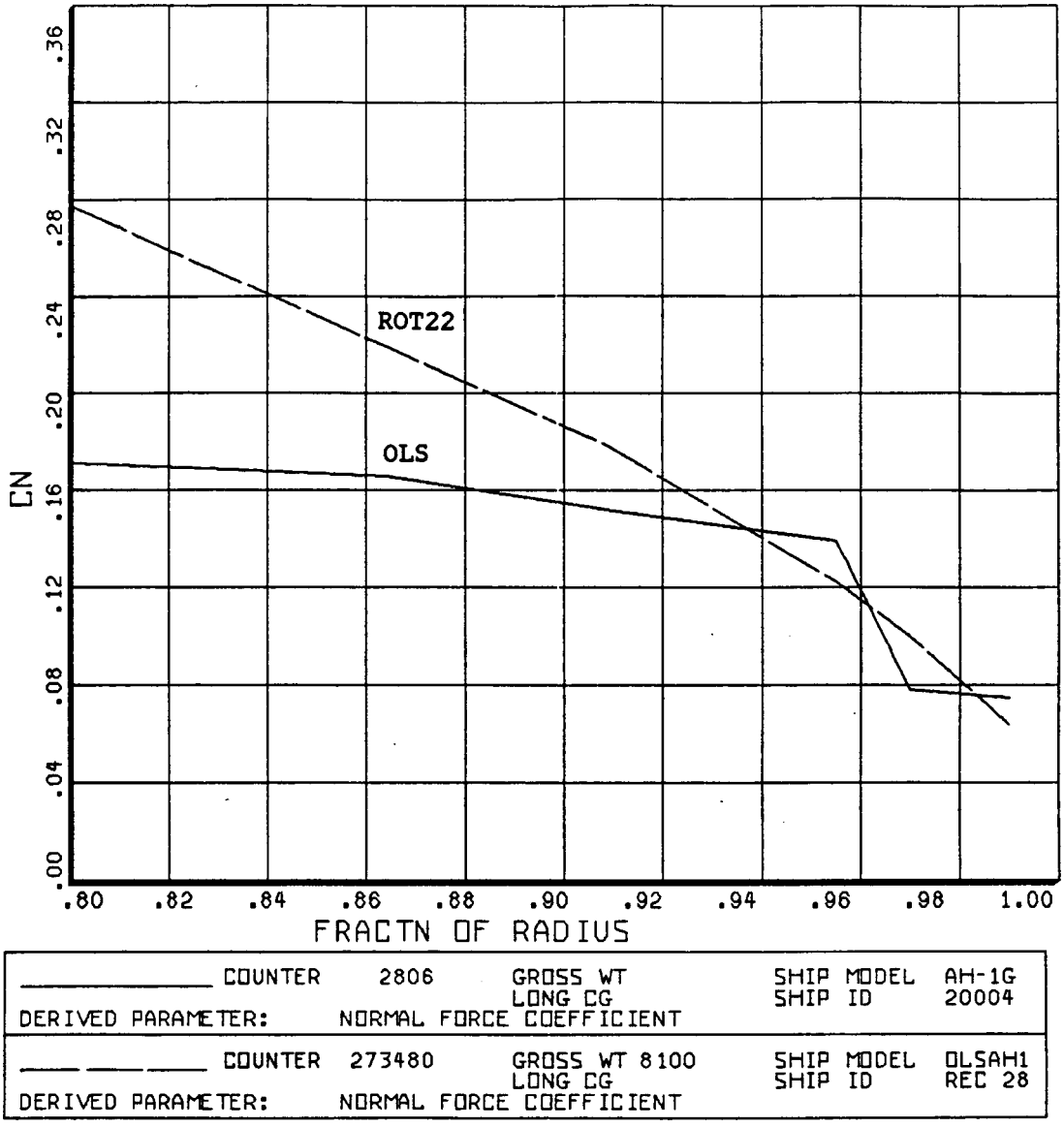

Figure 49. Normal force coefficient for Record 2806 (modified twist).

CONCLUSIONS

In addition to demonstrating the capability of the interface, the following conclusions are drawn from this study.

1. In all the cases studied, the location of the shock is well predicted. However, the negative pressure coefficients are underpredicted. This indicates an apparent thickening of the blade section. This disagreement appears to be a maximum at 86% radius and diminishes as the tip is approached. Since the instrumented AH-1G blades were built to close tolerance, this problem is not related to blade construction. It has been shown in References 5 and 6 that such increases in the negative pressure coefficients occur when the blade encounters a vortex. Also, the two-dimensional, unsteady transonic results of Reference 5 show that the increased suction on airfoils can last well after the vortex has swept past the blade. Figure 50 shows the planform view of a rigid wake trajectory for two flight conditions. The first one closely represents the flight conditions of Records 2872 and 2873. The second case represents the flight conditions of Record 2806. From both the figures, it may be noted that the blade region has just emerged from a vortex encounter within the preceding 15° azimuth. Consequently, the blade-vortex interaction may be the source of increased negative pressure coefficients on the blade. Further investigation is recommended before any final conclusion can be made.

2. Use of ROT22 program in concert with performance prediction programs provides a means of obtaining realistic pressure distribution and the location of shock in the tip regions of the blade.

3. The scatter in the measured pressure distribution, together with the linear interpolation/extrapolation scheme used in the DATAMAP program, makes

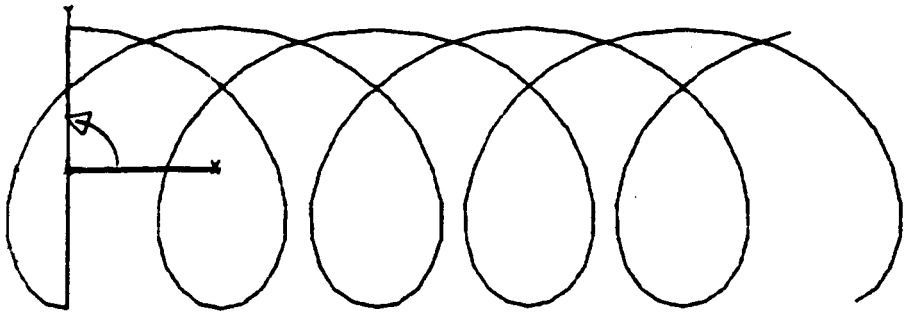

AH-1G OLS ROTOR V=150 KT

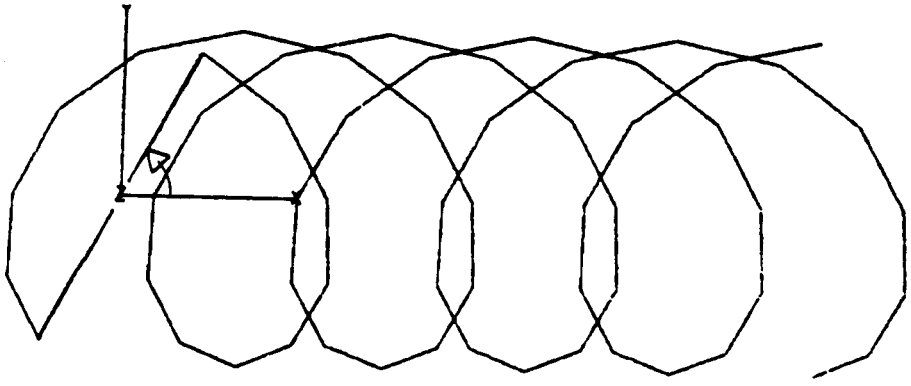

AH-1G OLS ROTOR V=123.7

Figure 50. Planform view of tip vortex trajectories for two flight conditions using rigid wake assumptions.

the normal force coefficient calculations highly unreliable. This problem can be alleviated by smoothing the measured pressure data (while retaining discontinuity due to shock) and also by providing an option to insert data points near the trailing edge of the blade when measurements are faulty in that region.

REFERENCES

1. R. Arieli and M. E. Tauber, "Analysis of the Quasi-Steady Flow About An Isolated Lifting Helicopter Rotor Blade," Stanford University, JIAA TR-20, August 1979.

2. R. B. Philbrick, "The Data from Aeromechanics Test and Analysis - Management and Analysis Package (DATAMAP)," USAAVRADCOM-TR-80-D30A, December 1980.

3. "OLS Blade Tip Aerodynamic Investigation," NASA Contract NAS2-10331, 1979.

4. Harris, Franklin D. et al., "Helicopter Performance Methodology at Bell Helicopter Textron," 35th Annual National Forum, American Helicopter Society, May 1979.

5. George, A. R. and Chang, S. B., "Noise Due to Transonic Blade-Vortex Interactions," 39th Annual Forum of the American Helicopter Society, May 9-11, 1983.

6. Tauber, M. E.; NASA CP2234, Rotorcraft Noise Workshop, NASA Langley, March 1982, pp. 357-373.

APPENDIX

User's Guide to Program ARSA05

Program ARSA05 is Bell's version of the original NASA-Ames ROT22 program. It is a 3-D transonic, full potential, nonconservative, quasi-steady, inviscid analysis program developed to predict the pressure and flow velocity on helicopter rotor blades. This version includes an interface to DATAMAP, a data management and analysis package, to provide extensive plotting capabilities.

FUNCTION

ARSA05 can be used to assess the effect of compressibility on various blade configurations and its implication on the aero-acoustic properties of the blade. The program can also be used to locate the high compressibility areas near the blade tip where transonic airfoils can be designed to minimize compressibility using two-dimensional design techniques (ADAM system). Using the DATAMAP[2] interface, the user can obtain surface Mach number and pressure contour plots. In addition, sectional pressure coefficients, pressure and Mach number plots can be obtained.

The user should take note of the following:

1. The analysis is quasi-steady and, hence, it does not account for the time history of the blade motion.

2. The analysis does not account for the blade flapping velocities or dynamic twist. However, the blade azimuth location, blade deflection due to flapping, geometric twist, cyclic and collective pitch, blade contour and tip path plane inclination, with respect to the flight path, can be accounted for.

3. The wake is not represented accurately in the program because of the complex transformations involved. Consequently, the induced velocities are in error. The error would probably be larger under hovering conditions. Some empirical technique may have to be used to get accurate inflow through the rotor. Though this is a certain limitation for performance prediction, it is not anticipated to be a serious handicap in assessing the effect of compressibility on different blades. This is particularly true for helicopters in high-speed flight for which the blade pitch angles are small in the advancing blade tip region.

FORMAT: All the odd-numbered cards are skipped. The format for all the even-numbered cards is 8F10.0 unless otherwise noted.

CARD 0: Title Card (format 20A4)

CARD 1: Comments

CARD 2: FNX, FNY, FNZ, PLTCP, PLTSEC, PLTSRF, FCONT, FPRINT

FNX No. of chordwise grids in the entire flow field (use 30; Max = 120)

FNY No. of y grids (+ up) in the entire flow field (use 4; Max = 16)

FNZ No. of z grids (+ spanwise out) in the flow field (use 8; Max = 32)

PLTCP controls CP plot routine, currently unavailable (Use 0.).

PLTSEC controls sectional characteristics computation for sectional plots (Use 1.).

PLTSRF controls surface characteristics computation for surface plots (Use 1.).

FCONT: This sets the switch for restart options.

0: Initial velocity potential, ϕ values are generated and final ϕ values are not saved (i.e., Tape 4 and Tape 7 are not used).

1: Initial ϕ values are generated (Tape 4 empty) and final ϕ values are saved on Tape 7 for future use.

2: Initial ϕ values are read in from Tape 4 from a previous run and the final ϕ values are written out on Tape 7.

3: Initial ϕ values are read in from Tape 4 but the final ϕ values are not saved (Tape 7 empty).

FPRINT controls printout of intermediate mesh size and final mesh size results.

0: All sectional printouts suppressed for intermediate mesh sizes.

$\neq$0: All sectional data printed.

CARD 3: Comments

CARD 4: FITMAX, FITMIN, CONV, P10, P20, P30, BETAO, FHALF

FITMAX: Max no. of iterations in the first grid defined by CARD 2. (Use 10 for rough grid, 20 for intermediate, and 30 for fine mesh.)

FITMIN: Min no. of iterations in the first grid (Use 1.).

CONV: Convergence criteria: (suggested 0.00003)

P10 Subsonic relaxation parameter 1.0<P10<2.0 (use 1.75)

P20 Subsonic relaxation parameter 0<P20<1 (Use 1.0)

P30 Circulation relaxation parameter P30>1 (Use 1.0)

BETAO Damping parameter 0<BETA)<0.25 (Use 0.15)

FHALF: Switch to grid halving.

=1. Halves the grid and need to provide Card 4a.

=0. Does not use another grid (no need for Card 4a).

CARD 4a: FITMAX, FITMIN, CONV, P10, P20, P30, BETAO
Used for successively finer grids.

CARD 5: Comments

CARD 6: KTA5, PSIDEG, ALPHAS, TEMPF, NDTF, INSTFL, NGRD, LDTF

KTA5: Forward flight speed, in knots

PSIDEG: Azimuth location, ψ in deg ($60° < \psi < 120°$)

ALPHAS: Shaft (or tip path plane) tilt in deg (+ aft)

TEMPF: Outside air temperature in °F

NDTF: DTF option
=0, no DATAMAP connection
≠0, write DTF to connect to DATAMAP

INSTFL: Instruction records option
=0, no instruction records included for DTF
≠0, include instruction records for DTF.
The last instruction record must be END and it must begin in column 1.

NGRD: Output grid option for DTF
=0, use the default grid (appropriate for OLS comparison)
≠0, user will input the grid for DATAMAP use

LDTF: File number for DTF. A positive value will write the DTF in internal format and a negative value will write the DTF in external format.

=0, program resets it to the default value of 14

CARD 7: Comments

CARD 8: TIPSPD, RAD, RROOT, CR, CPOFFB, WAKPRT

TIPSPD: R in ft/sec

RAD: Radius in inches

RROOT: Root radius in inches

CR: Reference chord for nondimensionalizing (in inches)

CPOFFB: Controls printout of CP beyond blade trailing edge 0: does not print beyond trailing edge
≠0: prints beyond T.E. (Use 1.0)

WAKPRT: Controls print out of wake calculations (Use 0.0)

CARD 9: Comments

CARD 10: GFACT1, XV1, YV1, THV11, THV12

CARD 11: Comments

CARD 12: GFACT2, YV2, ZV2, THV21, THV22

GFACT1 and GFACT2 control the use of two infinite vortex line filaments in the flow field.

XV1, YV1, THV11, and THV12 define the location and orientation of the first filament and similarly YV2, ZV2, THV21, and THV22 control the location and orientation of second filament in the flow field. It is recommended not to exercise these options.
Use GFACT1 = 0.0 and GFACT2 = 0.0.

CARD 13: Comments

CARD 14: KPLOTS: Determines what grid stations along the blade you want the C_p, Mach Number, U, V, and W to be printed out. Typically, the approximate blade root station is grid Sta #5

and tip Sta is #21. You can print any desired station by writing the number of that station on this card. For the DATAMAP option, the grid stations included here must bracket the DATAMAP radial grid (FORMAT 26I3).

If NDTF=0, omit cards 15 through 26.

If INSTFL=0, omit cards 15 and 16.

CARD 15: Comments

CARD 16: DATAMAP instruction records. There can be up to 56 of these cards. The last one must be an END card (beginning in Column 1) (FORMAT 18A4).

CARD 17: Comments

CARD 18: GWHT, HCG, PSTAIC

GWHT: Helicopter gross weight. Only used to label some DATAMAP plots.

HCG: Helicopter Center of Gravity. Only used to label some DATAMAP plots.

PSTAIC: Ambient air pressure. Used in CP to local Mach number calculations (lb/in **2).

CARD 19: Comments

CARD 20: MODNUM, SHPNUM (FORMAT A8, 2X, A8)

MODNUM: Helicopter Model Number (8 character field). Only used to label some DATAMAP plots.

SHPNUM: Helicopter Ship Number (8 character field). Only used to label some DATAMAP plots.

If NGRD=0, omit cards 21 through 26.

CARD 21: Comments

CARD 22: NRADUS, NCHRD (FORMAT 2I3)

The maximum allowed value of (2* NRADUS*NCHRD+1) is 510. The default values are NRADUS=8 and NCHRD=20.

NRADUS: Number of radial stations in the grid. If NRADUS=0, the radial stations are not redefined (the default OLS values are used). The maximum value is 21.

NCHRD: Number of chord values in the grid. If NCHRD=0, the chord values are not redefined (the default values are used). The maximum value is 21.

CARD 23: Comments

If NRADUS=0, omit card 24.

CARD 24: DTFRAD

DTFRAD: Radial values in fractions of the total radius (0 to 1). Input NRADUS values (7 per card). The default values are (.40, .60, .75, .864, .910, .955, .970, .990).

CARD 25: Comments

If NCHRD=0, omit card 26.

CARD 26: DTFCRD

DTFCRD: Chord values in fractions of the total local chord (0 to 1). Input NCHRD values (7 per card). The default values are (.005, .01, .02, .03, .05, .08, .15, .20, .25, .28, .32, .35, .37, .40, .45, .50, .55, .60, .70, .92).

CARD 27: Comments

CARD 28: FNC, PITCH, TAUP, XPO, BZ

FNC: No. of spanwise stations used to define blade.

PITCH: Blade pitch angle (cyclic + collective) in deg + nose up.

TAUP: Sweep of pitch axis w.r.t. ref. line, + aft.

XPO: Offset of pitch axis from ref line at Z=0 + toward T.E.

BZ: Mesh spacing functions use of 1 gives uniform spacing. 0< BZ <1.0. (Use 0.389 for close spacing near tip.)

CARD 29: Comments

CARD 30: ZZ, CHRD, THICK, XT, TWIST, XOFF, YOFF, FSEC (see Figure 50)

ZZ: Span location in inches at which the following information is supplied.

CHRD: Chord in inches at this ZZ.

THICK: Linear scale factor. Multiplies with thickness ratio of airfoil defined in cards 30d.

XT: Location of twist axis in (x/CHD) from L.E. typical value is 0.25.

TWIST: Geometric twist at this ZZ.

XOFF: X=Location of L.E. w.r.t. ref line (+ toward T.E.)

YOFF: Y=Location of L.E. w.r.t. ref line (+ upward).

FSEC: =0 => No new airfoil defined. Uses the same airfoil as the one at the previous ZZ.

=1 => Reads a new airfoil at this ZZ. At grid locations between this zz and the previous ZZ, a cubic spline routine interpolates the airfoil geometry.

If FSEC=1, provide cards 30a, b, c, and d.

CARD 30a: Comments

30b: YSYM, FNU, FNL

YSYM: 1.0 for symmetric airfoil (FNU=FNL)
0.0 for nonsymmetric airfoil

FNU: No. of upper surface airfoil geometry def locations.

FNL: No. of lower surface airfoil geometry def locations.

30c: Comments

30d: 1) XP, YP
Provide FNU pairs of x/c and y/c coords of upper surface of the airfoil, one pair per card.

If YSYM=1, then skip the remaining details of Card 30.

If YSYM=0, then provide the following cards.

2) Comment card

3) XP, YP
Provide FNL pairs of x/c and y/c coords of the lower surface of the airfoil, one pair per card.

CARD 31: Repeat CARD 29 thru CARD 30 until FNC number of spanwise stations are defined.

Sample input to ROT22 are provided in Tables 5 and 6 where the same blade geometry is provided in two different forms (see Figure 51). Of course, both of them will provide identical results. Sample input utilizing the DATAMAP interface is provided in Table 7.

TABLE 5. SAMPLE INPUT TO ARSA05

```
TEST BLADE WITH NACA 0012 A/F&COMPLEX GEOM.P.A.REF.
FNX          FNY          FNZ          FCONT
60.          8.           12.          0.
FITMAX       FITMIN       CONVO        FHALF
50.          1.           0.00003      1.
40.          1.           0.00001
FF.KNOTS     PSI.DEG      ALPHA.DEG    AINFFPS
100.0        90.0         -10.0        1117.0
TIPSP.FPS    RAD.IN       RROOT.IN     REFCHORD
700.0        200.0        50.0         10.00
KPLOTS
10 13 15 16 17 18 19 20 21
FNC          PITCHDEG     PA TILT      PA OFF
 6.          10.0         2.0          0.0
STN.ZZ       CHORD        TA/CHORD     TWIST        XOFF         YOFF         NEWSEC
50.0         10.0         0.25         5.0          -5.0         0.0          1.
YSYM         FNU          FNL
 1.0         44.          44.
NACA0012 UPPER SURFACE
   0.0          0.0
   0.00354      0.01033
   0.00743      0.01478
   0.01256      0.01898
   0.01888      0.02297
   0.02633      0.02677
   0.03489      0.03039
   0.04452      0.03382
   0.05519      0.03706
   0.06690      0.04012
   0.07961      0.04299
   0.09332      0.04566
   0.10800      0.04812
   0.12364      0.05037
   0.14024      0.05241
   0.15777      0.05421
   0.17623      0.05578
   0.19562      0.05712
   0.21591      0.05820
   0.23710      0.05904
   0.25919      0.05962
   0.28216      0.05994
   0.30601      0.06001
   0.33073      0.05981
   0.35632      0.05935
   0.38276      0.05863
   0.41006      0.05764
   0.43821      0.05639
   0.46719      0.05489
   0.49702      0.05313
   0.52768      0.05111
   0.55916      0.04884
   0.59147      0.04633
   0.62460      0.04356
   0.65854      0.04055
   0.69329      0.03729
   0.72884      0.03378
   0.76520      0.03000
   0.80236      0.02597
   0.84031      0.02166
   0.87905      0.01705
   0.91859      0.01214
   0.95890      0.00688
   1.00000      0.00126
ZZ           CHORD        XT           TWIST        XOFF         YOFF         NEWSEC
150.0        10.0         0.25         4.0          -5.0         0.0          0.0

176.0        10.0         0.25         3.2          -5.0         0.0          0.0

179.0        10.0         0.25         3.05         -5.0         0.0          0.0

190.0         8.0         0.25         2.5          -3.0         -1.0         0.0

200.0         6.0         0.25         2.0          -1.0         -2.0         0.0
```

TABLE 6. SAMPLE INPUT TO ARSA05

```
TEST BLADE WITH NACA 0012 A/F&COMPLEX GEOM
FNX          FNY          FNZ          FCONT
60.          8.           12.          0.
FITMAX       FITMIN       CONVO        FHALF
50.          1.           0.00003      1.
40.          1.           0.00001
FF,KNOTS     PSI,DEG      ALPHA,DEG    AINFFPS
100.0        90.0         -10.0        1117.0
TIPSP,FPS    RAD,IN       RROUT,IN     REFCHORD
700.0        200.0        50.0         10.00
KPLOTS
10 13 15 16 17 18 19 20 21
FNC          PITCHDEG     PA TILT      PA OFF
 6.          10.0         2.0          5.0
STN,ZZ       CHORD        TA/CHORD     TWIST        XOFF         YOFF         NEWSEC
50.0         10.0         0.25         5.0          0.0          0.0           1.
YSYM         FNU          FNL
 1.0         44.          44.
NACA0012 UPPER SURFACE
   0.0          0.0
   0.00354      0.01033
   0.00743      0.01476
   0.01256      0.01898
   0.01888      0.02297
   0.02633      0.02677
   0.03489      0.03039
   0.04452      0.03382
   0.05519      0.03706
   0.06690      0.04012
   0.07961      0.04299
   0.09332      0.04566
   0.10800      0.04812
   0.12364      0.05037
   0.14024      0.05241
   0.15777      0.05421
   0.17623      0.05578
   0.19562      0.05712
   0.21591      0.05820
   0.23710      0.05904
   0.25919      0.05962
   0.28216      0.05994
   0.30601      0.06001
   0.33073      0.05981
   0.35632      0.05935
   0.38276      0.05863
   0.41006      0.05764
   0.43821      0.05639
   0.46719      0.05489
   0.49702      0.05313
   0.52768      0.05111
   0.55916      0.04884
   0.59147      0.04633
   0.62460      0.04356
   0.65854      0.04055
   0.69329      0.03729
   0.72884      0.03378
   0.76520      0.03000
   0.80236      0.02597
   0.84031      0.02166
   0.87905      0.01705
   0.91859      0.01214
   0.95890      0.00688
   1.00000      0.00126
ZZ           CHORD        XT           TWIST        XOFF         YOFF          NEWSEC
150.0        10.0         0.25          4.0         0.0          0.0           0.0

176.0        10.0         0.25          3.2         0.0          0.0           0.0

179.0        10.0         0.25          3.05        0.0          0.0           0.0

190.0         8.0         0.25          2.5         2.0         -1.0           0.0

200.0         6.0         0.25          2.0         4.0         -2.0           0.0
```

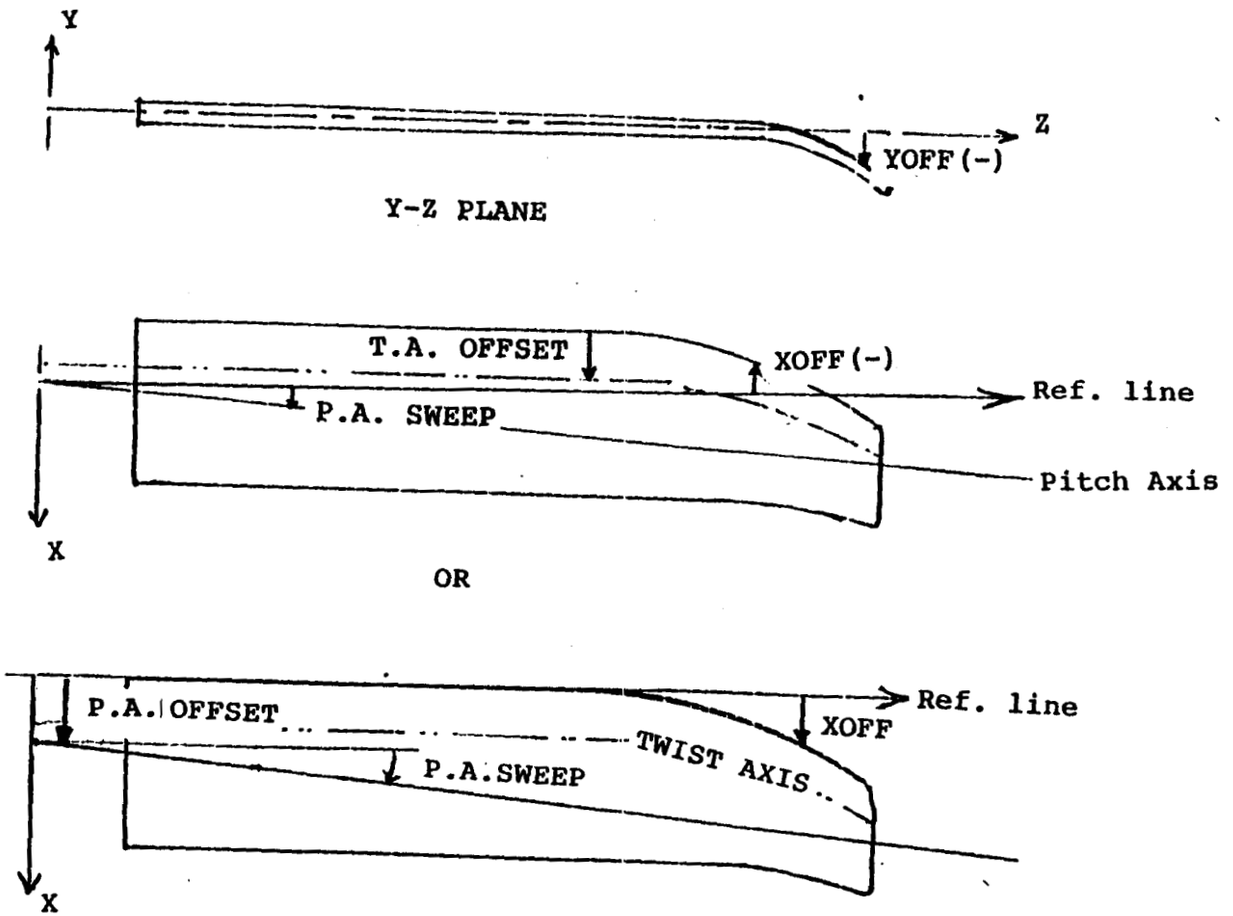

Figure 51. Blade geometry definition.

TABLE 7. SAMPLE INPUT TO ARSA05

```
 OLS AH-1G DATA CREATION WITH ROT22 FOR DATAMAP INPUT
 FNX        FNY        FNZ        PLTCP      PLTSEC     PLTSRF     FCONT      FPRINT
 3Ø.        4.          8.        Ø.         1.         1.         Ø.         -1.
 FITMAX     FITMIN     CONVØ      P1Ø        P2Ø        P3Ø        BETAØ       FHALF
 1Ø.        1.         Ø.ØØØØ1    1.6        1.Ø        1.Ø        Ø.15        1.Ø
 2Ø.        1.         Ø.ØØØØ1    1.725      1.Ø        1.Ø        Ø.15        1.Ø
 3Ø.        1.         Ø.ØØØØ1    1.8Ø       1.Ø        1.Ø        Ø.15
 KTAS       PSI,DEG    ALPHA,DEG  TEMF       NDTF       INSTFL     NGRD       LDTF
 15Ø.2       9Ø.Ø      -4.329     68.9       1.         1.Ø        Ø.Ø         14.
 TIPSPD     RADIUS     RROOT      CR         CPOFFB      WAKPRT
 694.Ø      264.Ø      4Ø.Ø       28.63       1.ØØ        Ø.Ø
 GFACT1     XV1        YV1        THV11      THV12
 Ø.Ø         Ø.25      Ø.25       1Ø.Ø       5.Ø
 GFACT2     XV2        YV2        THV21      THV22
 Ø.Ø        -Ø.5       12.1       Ø.Ø        Ø.Ø
 KPLOTS
 11 12 13 14 15 16 17 18 19 2Ø 21 22 23 24 25 26 27 28 29 3Ø 31 32
 DATAMAP INSTRUCTION RECORDS BEGIN
 REP ROT2872          PASSWRD TOM
 SPACE    2ØØØ        USERNAM K.R.SHENOY
 ITEMS
  NOFILT       CALIB        RATE      1ØØ
 ALL ITEMS
 COUNTERS
  RECORD 1Ø         ABSOLUT Ø
 ALL COUNTERS
END
  GW         HCG        PSTAT
8500.       Ø.Ø        11.98
MODEL NO   SHIP NO.
OLSAH1-G   REC 2872
 FNC         COLP       TAUP       XPØ        BZ
  8.         12.185     Ø.Ø        6.88       Ø.389
 STN,ZZ      CHRD       THICK      XT         TWIST      XOFF       YOFF       FSEC
 4Ø.Ø        28.63      1.Ø        Ø.24Ø3    -2.25       Ø.Ø        Ø.Ø        1.
 YSYM        FNU        FNL
 1.          48.        48.
  XP          YP        : STA 4Ø(REF CHORD IS 28.3 IN.)
 Ø.Ø         Ø.Ø
 Ø.ØØ453     Ø.Ø1163
 Ø.ØØ862     Ø.Ø1569
 Ø.Ø125Ø     Ø.Ø1857
 Ø.Ø1628     Ø.Ø2Ø87
 Ø.Ø2366     Ø.Ø2453
 Ø.Ø3Ø92     Ø.Ø2743
 Ø.Ø381Ø     Ø.Ø2986
 Ø.Ø4524     Ø.Ø3195
 Ø.Ø559Ø     Ø.Ø3463
 Ø.Ø6652     Ø.Ø3689
 Ø.Ø8Ø64     Ø.Ø3939
 Ø.Ø9121     Ø.Ø4Ø98
 Ø.1Ø177     Ø.Ø4235
 Ø.11231     Ø.Ø4353
 Ø.12285     Ø.Ø4455
 Ø.13339     Ø.Ø4543
 Ø.15Ø93     Ø.Ø466Ø
 Ø.17548     Ø.Ø4773
 Ø.2ØØØ1     Ø.Ø4836
```

TABLE 7. (Concluded)

Ø.214Ø2	Ø.Ø4851
Ø.221Ø2	Ø.Ø4855
Ø.22452	Ø.Ø4855
Ø.235Ø3	Ø.Ø4851
Ø.25253	Ø.Ø4832
Ø.28Ø53	Ø.Ø4767
Ø.3Ø152	Ø.Ø4696
Ø.3295Ø	Ø.Ø4572
Ø.35Ø48	Ø.Ø4461
Ø.38544	Ø.Ø4244
Ø.42Ø36	Ø.Ø4Ø15
Ø.45528	Ø.Ø3785
Ø.49Ø2Ø	Ø.Ø3556
Ø.52512	Ø.Ø3326
Ø.56ØØ3	Ø.Ø3Ø97
Ø.59495	Ø.Ø2867
Ø.62987	Ø.Ø2638
Ø.66479	Ø.Ø24Ø8
Ø.6997Ø	Ø.Ø2179
Ø.73462	Ø.Ø1949
Ø.76954	Ø.Ø172Ø
Ø.8Ø446	Ø.Ø149Ø
Ø.83938	Ø.Ø1261
Ø.8743Ø	Ø.Ø1Ø31
Ø.9Ø921	Ø.ØØ8Ø1
Ø.94413	Ø.ØØ572
Ø.979Ø5	Ø.ØØ342
1.ØØØØØ	Ø.ØØ2Ø5

STN,ZZ	CHRD	THICK	XT	TWIST	XOFF	YOFF	FSEC
8Ø.Ø	28.63	1.Ø	Ø.24Ø3	-4.11	Ø.Ø	Ø.Ø	Ø.
132.Ø	28.63	1.Ø	Ø.24Ø3	-6.4	Ø.Ø	Ø.Ø	SEC Ø.
198.Ø	28.63	1.Ø	Ø.24Ø3	-9.14	Ø.Ø	Ø.Ø	SEC Ø.
224.Ø	28.63	1.Ø	Ø.24Ø3	-1Ø.2	Ø.Ø	Ø.Ø	SEC Ø.
238.Ø	28.63	1.Ø	Ø.24Ø3	-1Ø.74	Ø.Ø	Ø.Ø	NGOP Ø.
251.Ø	28.63	1.Ø	Ø.24Ø3	-11.25	Ø.Ø	Ø.Ø	NGOP Ø.
264.Ø	28.63	1.Ø	Ø.24Ø3	-11.78	Ø.Ø	Ø.Ø	SEC Ø.

OUTPUT DESCRIPTION

The first section of the output describes the geometry of the blade. At each section Z, the spanwise location is printed out in both ZZ/CREF and in inches. The XSING and YSING correspond to the singular point near the leading edge of the blade about which a transformation is made. For practical purposes, the user can assume that the singular point is at the L.E. After all the sections are printed, ref. chord, sweep at the root of the blade (SWEEP1), sweep at the tip (SWEEP2), and the sweep of the singular line at infinity (SWEEP is set= SWEEP2/2) are printed.

Similarly, the dihedral angles are printed. The grid information and other transformation details follow. Finally, the section characteristics are printed out for the rough grid. The finer grid section characteristics are those of interest and they include freestream Mach No. at the section, azimuth location, shaft tilt angle, spanwise location (r/R), section c_l, c_d and $c_{ml/4c}$, C_{pcr} and the chord. Further, the x locations at the given section in inches, y/c at that x, local surface Mach number, C_p and U, V, W components of surface velocities are printed out. A graphical representation of the C_p values is provided along a distorted X scale. The location of the leading edge is also indicated. The information above the leading edge location corresponds to the lower surface and below, the leading edge location corresponds to the upper surface. Following this, a listing of sectional characteristics and their blade characteristics is printed. Finally, the DATAMAP file creation program details are printed.

User Tips

1. If there are sharp changes (kinks) in the planform, the interpolating cubic spline will exhibit instabilities unless the following steps are taken:

   i) Do not specify any geometry information at the kink.

ii) Define geometry on either side of the kink (r/R=±0.005). However, if the blade has just a single, straight sweep, one need not be concerned about the location of the point after the kink (near the tip).

iii) Define at least two points after each kink.

2. For a swept blade with smooth planform, define a number of stations to represent the blade as accurately as possible. However, if the airfoil definition changes from section to section, one may be limited by the number of stations at which the airfoil information is available. One may try to use the "thick" parameter to define transition sections.

3. The information on the blade surface is calculated at the computational grid points located evenly in the transformed plane. Consequently, the results are printed at nonuniform intervals in the physical plane.

4. The program uses a left-hand sign convention. As a result, x is in the chordwise direction, positive toward the TE; y is perpendicular to the chord and is positive upwards; z is in the spanwise direction, positive toward the tip.

1. Report No.	2. Government Accession No.	3. Recipient's Catalog No.
NASA CR- 177403		

4. Title and Subtitle	5. Report Date
Development of a ROT22 - DATAMAP Interface	April 1986
	6. Performing Organization Code

7. Author(s)	8. Performing Organization Report No.
K.R. Shenoy, T. Waak, J.T. Brieger	
	10. Work Unit No.

9. Performing Organization Name and Address	11. Contract or Grant No.
Bell Helicopter Textron Inc. Fort Worth, Texas	NAS2-10331
	13. Type of Report and Period Covered
12. Sponsoring Agency Name and Address	Contractor Report
National Aeronautics and Space Administration Washington, DC 20546	14. Sponsoring Agency Code 505-61-51

15. Supplementary Notes

Point of Contact: Technical Monitor, Michael E. Watts, MS 237-5
Ames Research Center, Moffett Field, Ca. 94035

16. Abstract

This report, prepared under Contract NAS2-10331 (Mod 10), outlines the development and validation of an interface between the three-dimensional transonic analysis program ROT22 and the Data from Aeromechanics Test and Analytics-Management and Analysis Package (DATAMAP). After development of the interface, the validation is carried out as follows. First, the DATAMAP program is used to analyze a portion of the Tip Aerodynamics and Acoustics Test(TAAT) data. Specifically, records 2872 and 2873 are analyzed at an azimuth of 90°, and record 2806 is analyzed at 60°. Trim conditions for these flight conditions are then calculated using the Bell performance prediction program ARAM45. Equivalent shaft, pitch, and twist angles are calculated from ARAM45 results and used as input to the ROT22 program. The interface uses the ROT22 results and creates DATAMAP information files from which the surface pressure contours and sectional pressure coefficients are plotted. Twist angles input to ROT22 program are then iteratively modified in the tip region until the computed pressure coefficients closely match the measurements. In all cases studied, the location of the shock is well predicted. However, the negative pressure coefficients were underpredicted. This could be accounted for by blade vortex interaction effects.

17. Key Words (Suggested by Author(s))	18. Distribution Statement
DATAMAP, ROT22, Numerical Predictions, Helicopters, Rotory Wing, Blade Pressures	Unclassified - Unlimited Subject Category 61

19. Security Classif. (of this report)	20. Security Classif. (of this page)	21. No. of Pages	22. Price*
Unclassified	Unclassified	104	

*For sale by the National Technical Information Service, Springfield, Virginia 22161